Dissertation zur Erlangung des Doktorgrades
der Fakultät für Chemie und Pharmazie
der Ludwig-Maximilians-Universität München

Dissecting the regulation of gene expression during steroid hormone signaling in *Drosophila* by Dynamic Transcriptome Analysis (DTA)

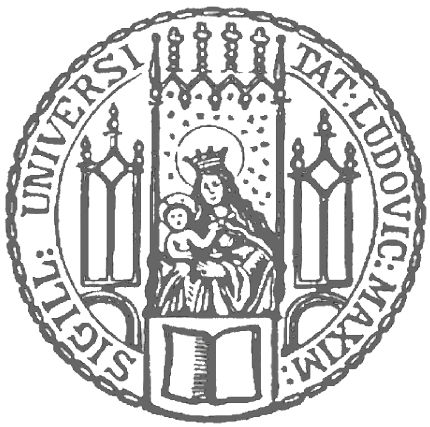

Katja Frühauf
aus
Pfullendorf, Deutschland

2015

Erklärung

Diese Dissertation wurde im Sinne von § 7 der Promotionsordnung vom 28. November 2011 von Frau Prof. Dr. Ulrike Gaul betreut.

Eidesstattliche Versicherung

Diese Dissertation wurde eigenständig und ohne unerlaubte Hilfe erarbeitet.

München, 20.01.2015

Katja Frühauf

Dissertation eingereicht am 20.01.2015

1. Gutachter: Prof. Dr. Ulrike Gaul
2. Gutachter: Prof. Dr. Klaus Förstemann

Mündliche Prüfung am 20.02.2015

Acknowledgments

Die Zeit der Promotion war für mich ein sehr intensiver, manchmal grenzwertiger, aber erfahrungsreicher und wichtiger Lebensabschnitt. Deshalb möchte ich mich bei den Menschen, die diese ermöglicht haben, die Zeit so interessant und bewegend gemacht haben, sowie mich auf diesem Weg begleitet und unterstützt haben, bedanken.

I would like to express my gratitude to you, Ulrike Gaul, for giving me the opportunity to work in your lab and for the trust you placed in me and my capabilities. I appreciate your personal support and effort to improve my skills towards perfection.

I am very grateful to Prof. Dr. Klaus Förstemann for reviewing this thesis and for his valuable experimental and scientific advices on microRNAs.

Moreover, I would like to thank all the other members of my thesis committee: Dr. Dietmar Martin, Prof. Dr. Nicolas Gompel, Prof. Dr. Karl-Klaus Conzelmann and Dr. Daniel Wilson for their support and time.

I am particularly grateful for the excellent bioinformatic assistance given by Björn Schwalb. Without your support and ideas this thesis wouldn´t have been possible.

I also would like to thank Fulvia Ferrazzi, Bettina Knapp and Steffen Sass for stimulating discussions and great work on data analysis. In this regard, I also want to thank Ulrich Unnerstall, and additionally for his fascination for details.

I am very grateful for the excellent scientific assistance given by Lars Dölken and Bernd Rädle for metabolic RNA labeling, as well as Stefan Krebs and Alexander Graf for next-generation sequencing.

I warmly thank all the present and former members of the Gaul group for a comfortable and supporting working atmosphere. I really appreciate that throughout the six years I was always happy to see and chat to you.

Hierbei möchte ich mich bei einigen persönlich bedanken:

Liebe Julia (Philippou-Massier), deine umsetzungsfreudige Arbeitsweise und technische Expertise war eine wertvolle Bereicherung für mich. Lieber Christophe (Jung), dir danke ich für deine grenzenlos optimistische Einstellung, analystische Expertise und für die wunderbare Zeit mit dir, die über den Dächern bzw. im Jazz Keller New Yorks begonnen hat.

Liebe Claudia (Ludwig) und Monika (Hanf), aller liebsten Dank für eure wertvolle experimentelle Unterstützung und dafür, dass ihr zusammen mit euch, Ruzica (Barisic) und Peter (Bandilla), dieses Labor perfekt ver- und entsorgt. Und auch dir, Sabine, möchte ich danken.

Liebe Susi (Rieder), ohne dich wären die ersten Jahre nur halb so effizient und halb so lustig gewesen. Ich bin sehr dankbar, dass wir uns auch in den privaten Höhen und Tiefen begleitet haben und die gemeinsame Zeit unvergesslich bleibt.

Genauso unvergessen bleibt auch die Zeit, die ich mit dir, Sofia (Axelrod), verbracht habe. Es war immer eine wunderbar erfrischende Abwechslung mit dir den Wald im Berghain oder die Schweine in der Oper aufleben zu lassen.

Bei einigen Leuten im Genzentrum möchte ich mich nicht nur für die exzellente Hilfestellung, sondern auch für die freundschaftlichen Beziehungen bedanken.
Romy (Böttcher), ohne deinen hot stuff wäre ein Teil dieser Arbeit nicht möglich gewesen und ohne deine herrlich fröhliche Art wäre vieles nicht so hyper, hyper gewesen.
Auch du Anja (Kiesel) hast mit deiner Fröhlichkeit und Begeisterung für den CASY dazu beigetragen, dass die S2 Zellen sich wohl fühlten und endlich das machten was ich wollte.
Genauso möchte ich auch noch einmal dir, Claudia, danken, dass du mich in der letzten doch sehr schweren Laborzeit sehr unterstützt hast.
Auch dir, Margaux (Michel) möchte ich danken, da es immer unglaublich wertvoll war einen weiteren RNA-Seq (Leid-)genossen zu haben.
Dir, Kerstin (Maier) danke ich für deine einzigartige Unterstützung im Andimetrix Raum und natürlich für das proof reading.
Auch dir Wolfgang (Mühlbacher) möchte ich danken, dass du in der allerschwersten Zeit noch für wesentliche Geistesblitze gesorgt hast.
Danke an euch, Simone (Boos), Martina (Oberhuber), Matthias (Siebert) und Stefan (Jordan) für die Zeit, die wir außerhalb des Genzentrums, meist auf der Tanzfäche, verbracht haben.

Ich möchte mich aus tiefstem Herzen bei all meinen Freunden und Bekannten bedanken, die die Zeit der Promotion mit unendlicher Unterstützung und Lebensfreude gefüllt haben.

Besonderen Dank an euch, Becky, Natalie, Marie, Petzi, Clare und Frederike, dass ihr alle auf eure ganz besondere Weise immer wieder mein Selbstvertrauen gestärkt habt und mit eurer Freundschaft diese Zeit so wunderbar erfüllt habt.

Liebe Julia (Graf), dir verdanke ich, dass ich in dir oft einen Spiegel meiner selbst gesehen habe und mich daher deine Gedanken und Ansichten ohne viel Worte bereichert haben.

Dir, Lisa (Marcinowksi), erst einmal vielen Dank, dass du diese Arbeit komplett gelesen hast und deine effiziente Art ein sehr wertvolles feedback für mich war. Viel mehr möchte ich dir aber dafür danken, dass du, wie schon so lange, immer für mich da warst, mich aufgebaut hast und auf deine eigene Art und Weise mit gelitten hast/musstest.

Bei meinen Geschwistern möchte ich mich bedanken, dass sie immer an meiner Seite sind. Besonders dir, Jessi, danke ich für deine kleinen Aufmerksamkeiten, die unendlich große Wirkung hatten. Das kleine Glück wurde ganz groß und hat Gesellschaft von der erleuchteten Fruchtfliege bekommen.

Bei euch, Mama und Papa möchte ich mich aus tiefstem Herzen bedanken. Danke, dass ihr mich in allem was ich tue so selbstverständlich unterstützt und immer hinter mir steht.

Etwas was mich persönlich durch all die Höhen und Tiefen dieser Zeit getragen hat, ist die Musik. Ihr verdanke ich auch das wertvollste, dass in dieser Zeit entstanden ist:

Die Beziehung mit dir, Michi. Mit dir an meiner Seite konnte ich immer wieder den Ausblick genießen, wenn ich mal wieder einen Umweg nehmen musste. Ich bin dir unendlich dankbar, dass du diese Arbeit mehrmals (!) gelesen und überarbeitet hast; sie mit deiner Meinung und Expertise wesentlich beeinflusst hast. Danke, dass du mich immer wieder und besonders in den letzten Monaten mit deiner Liebe aufgefangen und mir die nötige Kraft zum Durchhalten gegeben hast. You've got the love I need to see me through!

Abstract

The synthesis and decay of mRNA transcripts are key mechanisms for the regulation of gene expression in all organisms, from yeast to fly to human. However, a quantitative and global description of how transcriptional and post-transcriptional regulation is integrated to set and adjust gene expression levels is still missing.

In this work I used the genomic response to the steroid hormone ecdysone in the *Drosophila* S2 cell line as an experimental model to study the transcriptional and post-transcriptional regulation of gene expression dynamics. I combined highly quantitative time series data on mRNA expression levels, synthesis and decay rates, obtained by metabolic RNA labeling (Dynamic Transcriptome Analysis, DTA), with single-molecule microRNA expression profiling and phenotypic readouts of cell proliferation, cell cycle and cell morphology.

DTA measures the genomic response to ecdysone with high sensitivity and improved temporal resolution for early changes in gene expression and particularly for repressed genes. Overall, ecdysone signaling differentially regulates the mRNA expression levels, synthesis or decay rates of 2141 genes within the first 12 hours. The functional annotation of these genes correlates very well with the ecdysone induced phenotypic changes, namely exit from cell proliferation to enter differentiation. The first global assessment of decay regulation by ecdysone signaling shows that changes in decay rates are characterized by a less sustained progression compared to changes in synthesis rates, indicating that decay rates are controlled in a temporally more restricted (dynamic) fashion.

By complementing the DTA gathered gene expression data with k-means clustering of fold changes and kinetics of nascent and total mRNA expression levels as well as decay and turnover rates, we uncover that ecdysone signaling induces a rich and previously unknown diversity of gene expression dynamics. Specifically, we identified twenty distinct groups of potentially co-regulated genes, which exhibit unique combinations of effect type, strength and timing of changes in mRNA synthesis, decay rates and total expression level. Moreover, we observe a widespread, but not general coupling of mRNA synthesis and decay rates. Further investigation of these kinetically distinct gene clusters shows specific and reliable functional annotation enrichments and reveals the temporal order in which ecdysone signaling regulates the biological processes to direct the cell from its proliferating state into the differentiated state.

To gain first insights into the regulatory principles that underlie these patterns of coordinated gene activity we assessed the kinetics of transcription factors (TFs) and RNA-binding proteins (RBPs) and provide evidence that, in addition to the canonical regulators of the ecdysone cascade, the TFs foxo, Sox14 and schlank as well as the RBPs brat and lin-28 represent potential novel key regulators of ecdysone induced genes expression kinetics.

Based on mRNA decay rates we developed a novel approach for miRNA-mRNA network analysis that is superior to previous approaches and offers insights into the post-transcriptional regulation of the ecdysone response by miRNAs. Upon ecdysone treatment, we observe a rapid repression of miRNAs associated with the proliferative state and a progressive induction of miRNAs associated with the differentiated state. Strikingly, the largest fraction of the differentially regulated miRNAs and especially the early induced miRNAs (miR-282*, miR-276a*, miR-276a, miR-276b and miR-252) have not been implicated in ecdysone signaling or in the biological processes regulated by ecdysone, yet. Therefore, our dataset represents an excellent resource for studying the function of these miRNAs in ecdysone signaling, cell cycle, metabolism or differentiation/morphogenesis.

This work comprises a detailed dissection of ecdysone induced gene expression dynamics, their functional implications and underlying regulatory principles, and therefore, establishes ecdysone stimulation in *Drosophila* S2 cells as an experimental paradigm for studying mechanistic details of gene expression regulation.

Contents

Part I
Introduction

1 Mechanisms of gene regulation

Regulation of gene expression is the fundamental process governing both the development and adult homeostasis of all organisms. The elaborate regulation of gene expression occurs at multiple steps from DNA to RNA to protein (Figure 1), depends on spatial and temporal cues and is highly responsive to environmental perturbations. The accessibility of regulatory DNA sequences, such as promoters and enhancers, to trans-acting factors is jointly regulated by transcription factors (TFs) and the chromatin structure [114]. Cellular mRNA levels are determined by the interplay of tightly regulated processes for RNA production (transcription), processing (capping, splicing, polyadenylation, transport, localization) and degradation [160]. Translation of mRNA into protein can be controlled on a global or individual scale at multiple steps, with translation initiation being the most common [88]. Finally, the activity, location and degradation of proteins can be controlled by post-translational modifications including phosphorylation, methylation, acetylation, glycosylation or ubiquitination [158].

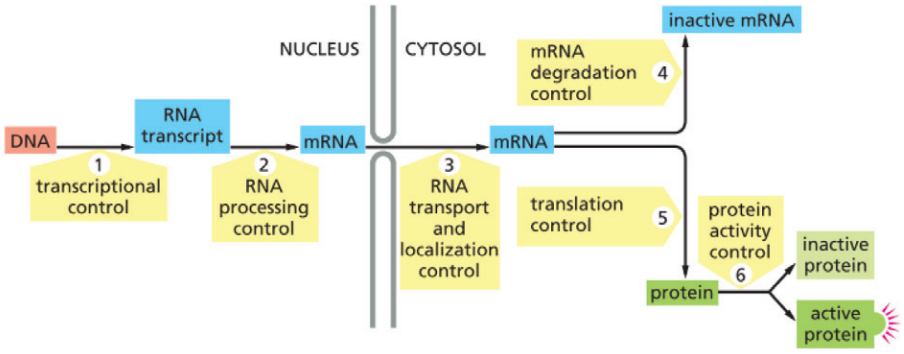

Figure 1: Eukaryotic gene expression can be controlled at several steps. Examples of regulation at each of the steps are known, although for most genes the main site of control is step 1: transcriptional control. Taken from [30].

1.1 Transcriptional mechansims

Transcriptional control of gene expression is determined by cis-regulatory elements (CREs) that are typically located in non-coding genomic regions. The accessibility of CREs is restricted by the local structure of chromatin, which is determined by nucleosome occupancy, positioning and epigenetic modifications such as post-translational modifications of histones [161, 203]. The accessibilty can be dynamically regulated by TFs that recruit chromatin remodeling or modifying enzymes to enhance the accessibility of CREs to TFs or the transcription machinery [126]. CREs can be subdivided into distinct classes according to their genomic location, trans-acting binding factors and function.
Gene distal elements (enhancers) are recognized by specific TFs and mainly control the spatio-temporal expression of genes. Enhancers can be located upstream, intronic, and downstream of the transcription unit and the distance to its regulated gene can vary from <500 bp up to 100 kb. Typically, enhancers contain binding sites for TFs of different signaling pathways to integrate multiple inputs of cellular signaling. Binding of specific TFs to enhancers can either activate or

repress the transcription of their target genes [114].
Gene proximal elements (core promoters) interact with the transcription machinery and control expression strength [101]. The core promoter is generally defined as the DNA region that is necessary for the initiation of transcription and is comprised of the transcription start site (TSS) and flanking sequence [101]. At the core promoter, RNA Polymerase II (Pol II) assembles together with general TFs (GTFs) into a pre-initiation complex (PIC). GTFs mediate promoter recognition, recruitment of Pol II, connect gene-specific factors to the PIC, interact with histones and promote DNA unwinding [182]. The PIC is required for transcription bubble formation, TSS scanning, and initial synthesis of the nascent transcript [116].
While the general composition and mechanism of the PIC is well studied, the gene class specific composition and the core promoter elements it binds to are not well characterized. Moreover, how the core promoter architecture and its surrounding features, such as nucleosomes, mechanistically control the plasticity of gene expression is largely unknown. Therefore, one challenging goal in the field of gene expression regulation is to understand how all regulatory input from trans-acting factors that bind to distal or proximal CREs is integrated at the core promoter resulting in a unified transcription rate.

1.2 Co-transcriptional and post-transcriptional mechanisms

1.2.1 mRNA life cycle

The mRNA life cycle consists of RNA production (transcription), processing (capping, splicing, polyadenylation, transport, localization), translation and degradation. The global and specific regulation of mRNA abundance is predominantly accomplished by alterations of synthesis and decay rates.
Transcription can be regarded as the most important regulatory step in the mRNA life cycle. It is not only catalyzing the synthesis of a transcript itself, but via co-transcriptional 5´ capping, splicing and 3´ end formation it also converts a pre-mRNA into an export, translation and decay competent mRNA. Pol II and associated TFs can also recruit various post-transcriptional regulators that are co-transcriptionally deposited onto the nascent mRNA [80]. Moreover, transcription controls the length of 5´ and 3´ untranslated regions (UTRs) through alternative TSS choice and alternative poly(A) site usage [168, 135]. The length of UTRs directly affects mRNA stability and/or translation efficiency, since longer UTRs typically contain more cis-regulatory elements, which can be targeted by RNA-binding proteins (RBPs) or microRNAs (miRNAs) [68, 64, 112, 188].
Eukaryotic mRNAs are equipped with two integral stability determinants – the 5´ 7-methylguanosine cap and the 3´ poly(A) tail. These two structures interact with the cytoplasmic proteins eIF4E and the poly(A)-binding protein (PABP), respectively, to protect the transcript from exonucleases and to enhance translation initiation [64]. Shortening (deadenylation) of the 3´ poly(A) tail by the Ccr4-Not complex is the first and often rate-limiting step in eukaryotic mRNA degradation [74]. Following deadenylation either the 5´ cap is removed by a process known as decapping and the uncapped mRNA subsequently degraded by the exonuclease Xrn1 or the unprotected 3´ end is attacked by a large complex of exonucleases known as the exosome [46, 123, 91]. In many cases, mRNA stability regulation is linked to changes in the poly(A) tail: activators protect or lengthen the tail, repressors shorten it. The latter is achieved by RBP or miRNA mediated recruitment of the Ccr4-Not complex and is a key mechanism to regulate the steady-state levels of mRNAs and, as a consequence, protein output [28].

1.2.2 miRNAs as post-transcriptional regulators

In 1993 the world of miRNAs was discovered by Ambros, Ruvkun and colleagues [125], who reported that the miRNAs lin-4 and let-7 control developmental timing in nematodes by modulating the

expression of other genes at the post-transcriptional level. Since then the miRNA field has grown tremendously becoming an integral component of gene expression regulation [96].

1.2.2.1 miRNA biogenesis miRNAs are small non-coding RNAs ∼20–24 nucleotides (nt) long, which post-transcriptionally repress the expression of target genes usually by binding to the 3´ UTR of mRNA. As a class, miRNAs constitute about 1%–2% of genes in worms, flies, and mammals [16]. Most miRNA genes are located as genomic clusters in intergenic regions and are transcribed as independent transcriptional units by Pol II. Other miRNAs (about 25-30%) are embedded within introns of coding genes and might be regulated by the promoter of their host gene [96]. miRNAs are transcribed as part of longer precursors (primary transcript; pri-miRNA) that fold on themselves to form hairpin structures (Figure 2). The hairpin structure is cleaved by the RNase III endonuclease Drosha and its double-stranded RNA-binding domain partner Pasha [127, 48] to yield the ∼60-70 nucleotide long pre-miRNA hairpin. The pre-miRNA is exported to the cytoplasm by Exportin 5 [108], where it is cleaved by a second RNase III endonuclease, Dicer (Dcr-1 in *Drosophila*) and its dsRBD partner Loquacious (Loqs) into a double-stranded miRNA-miRNA* duplex [134]. The mature miRNA strand is subsequently incorporated into the miRNA-induced silencing complex (miRISC), where it is bound to a member of the Ago protein family (Ago1 in *Drosophila*). The unincorporated strand (miRNA*) is degraded. However, in some cases miRNAs* can also be functional [140].

1.2.2.2 miRNA induced silencing of mRNA targets At the core of the miRISC lies the miRNA-loaded Ago protein and the scaffold protein GW182, which recruits additional silencing factors [59]. The miRNA guides target selection through canonical base pairing between the seed sequence of the miRNA (nucleotides 2–8 at its 5´ end) and its complementary seed match sequence in the target mRNA. The seed sequence contributes the majority of the binding energy and is typically located in the 3´ UTR of the mRNA [4, 77, 137]. However, it can also be located in the 5´ UTR or coding region of the mRNA [136, 60, 171, 85]. Upon binding miRISC represses the targets translation and/or stimulates its degradation. Translational repression can be modulated by interfering with eIF4E-cap recognition, 40S ribosomal subunit recruitment or by displacing PABP and inhibiting the circularization of the closed-loop structure necessary for translation [111, 59, 147]. The degradation of targets depends on the extent of sequence complementarity. Complete sequence complementarity leads to site-specific endonucleolytic cleavage by Ago (Ago2 in *Drosophila*) and subsequent degradation of the 5´ and 3´ ends by Xrn1 and the exosome [141]. However, most miRNAs bind with partial complementarity. In this case, miRISC interacts with the Ccr4-Not deadenylase complex and the Dcp1-Dcp2 decapping complex, to facilitate deadenylation and decapping, respectively [28, 50, 59, 152]. The remaining mRNA is subsequently degraded by Xrn1 and the exosome [94].
The relative importance and timing of translational inhibition versus mRNA degradation is a matter of current discussion. However, recent studies have shown that miRNA mediated transcript degradation explains ∼70-80% of the effect on protein levels [86].

1.2.2.3 miRNA function and their role in signaling pathways miRNAs are specific and essential post-transcriptional regulators in a wide range of biological processes. During both development and adulthood, miRNA function to coordinate cell growth, metabolism, fate, and morphology within changing environmental conditions [122, 97, 117, 183, 134]. In doing so, miRNAs ensure that the organism undergoes appropriate developmental and post-developmental transitions and confer biological robustness. The mechanistic concepts of miRNA functions depend on the specific biological context and include reinforcing transcriptional programs to sharpen transitions, entrench cellular identities, buffer fluctuations in gene expression or determine signal outcomes in the context of gene regulatory networks [54]. Within gene regulatory networks miRNAs can have

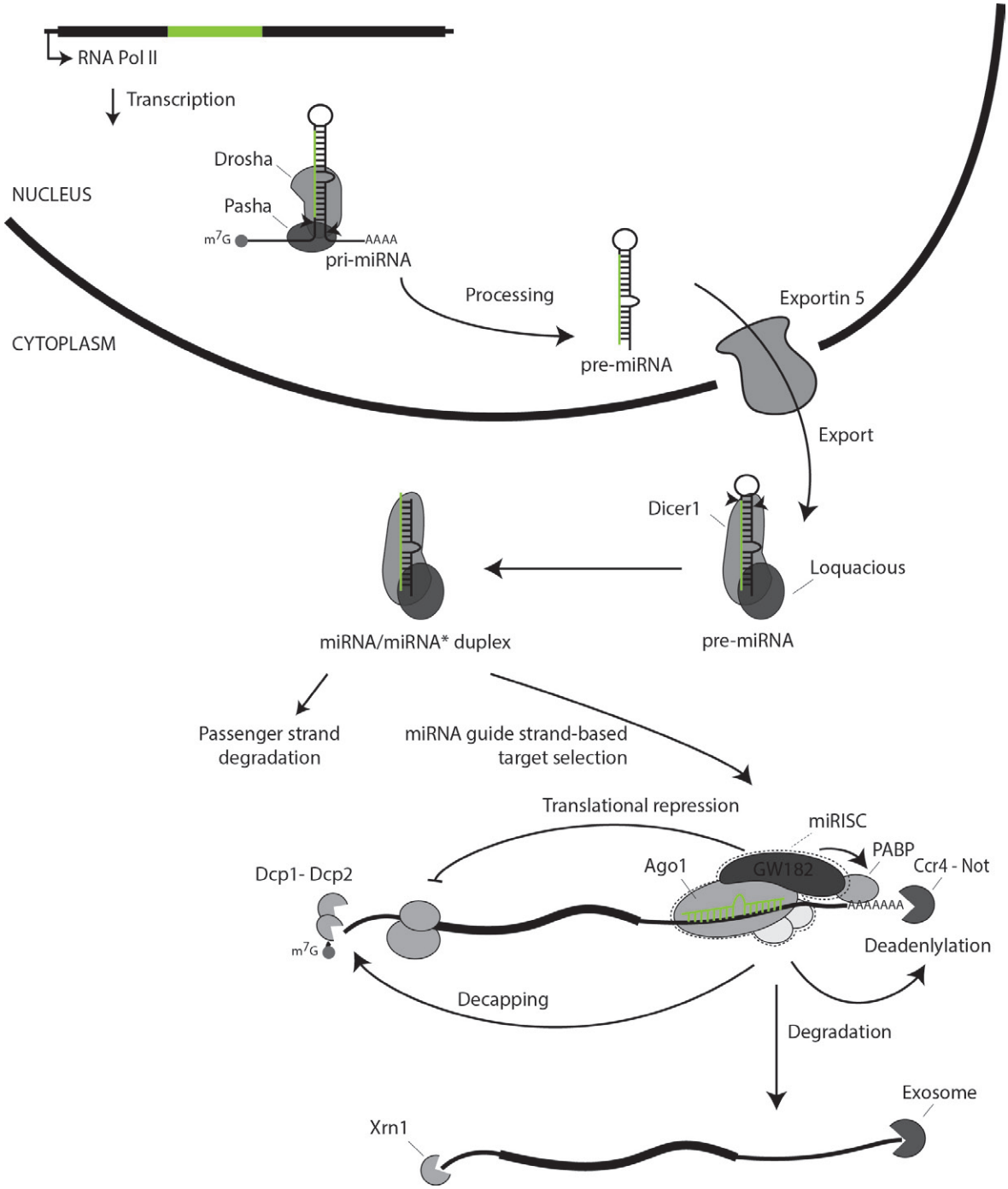

Figure 2: microRNA biogenesis and mode of action. The miRNA gene is transcribed by Pol II to generate a pri-miRNA. The pri-miRNA folds into a hair-pin structure, which is processed by the Drosha-Pasha microprocessor complex, and results in a pre-miRNA of around 60-70 nt. The pre-miRNA is exported to the cytoplasm by Exportin 5 and further processed by Dicer-1 and Loquacious to form the miRNA-miRNA duplex. The duplex is separated and one strand is selected as the mature miRNA, while the other strand is degraded. The mature miRNA strand is loaded into the miRISC complex and binds with its "seed sequence" to the complementary seed match sites within the 3′ UTR of mRNAs, resulting in translational inhibition and/or mRNA degradation. Adapted from [117].

quite different roles, from using to throw a developmental switch to buffering the consequences of noise in order to confer robustness [87].
Signaling pathways are ideal candidates for miRNA-mediated regulation owing to the sharp dose-sensitive activity of signaling pathways. Within these pathways miRNAs are crucial for tresholding against noise, default repression, context-dependent signaling, signal amplification or signaling pathway crosstalk [96, 54].
However, uncovering the specific function of individual miRNAs is challenging. miRNAs are frequently present as families of redundant genes and the degree of miRNA-mediated target down-regulation often tends to be quantitatively modest [96]. Therefore, a future challenge in the specific context of signaling pathways is to systematically identify miRNAs that affect and/or are regulated by cell signaling to unravel this gentle but essential layer of gene expression control.

1.2.2.4 Computational target prediction A crucial step in understanding miRNA function is to determine authentic miRNA targets. Computational biologists developed numerous prediction algorithms to capture the sequence and location characteristics of miRNA binding sites [2, 190]. Some of these characteristics are: (i) complementarity to the miRNA seed region, (ii) evolutionary conservation of the binding site, (iii) free energy of the miRNA-mRNA hetero-duplex, and (iv) mRNA sequence features outside the target site [106, 190]. However, neither individual nor combinations of these criteria are sufficient to predict all authentic targets without a serious number of false positives or false negatives. Since the development of the early algorithms, the importance of tolerating imperfect seed matches as well as extending the prediction to CDS became even more evident [79, 190].
The miRanda algorithm [22], used in this thesis, aligns a miRNA to the target 3´ UTR to identify highly complementary sequences. Seed pairing is weighed more strongly than pairing elsewhere, but seed G•U wobbles and mismatches are allowed. High-scoring targets are then filtered on a secondary criterion of heteroduplex free energy (ΔG).
Complementing computational predictions with expression profiles of miRNAs and mRNA targets along with experimental target identification is a fundamental approach to identify biological relevant miRNA targets.

2 The steroid hormone ecdysone

Steroid hormones regulate the development, maturation, reproduction, and metabolism of higher eukaryotes [12]. In vertebrates the process of maturation is primarily controlled by thyroid hormone and sex steroids, while in insects it is regulated by the steroid hormone 20-hydroxyecdysone (ecdysone). Although relatively little is known about how vertebrate hormones control maturation, molecular and genetic studies from the early 1950‘s onwards have provided a detailed understanding of the mechanisms by which ecdysone exerts its effects on insect development [31, 110].

2.1 Biological function of ecdysone

In *Drosophila*, the post-embryonic development progresses through three larval stages before the larva enters metamorphosis and finally emerges as an adult fly. The transitions between these stages are triggered by pulses of ecdysone (Figure 3a). Periodic pulses of α-ecdysone are released from the prothoracic glands and rapidly converted in peripheral tissues to its biologically active form, 20-hydroxyecdysone [165, 155]. There are two major pulses of ecdysone during metamorphosis. The first pulse occurs in the third instar larva triggering the initiation of (prepupal) morphogenesis. The second pulse is released 10-12 hours later triggering radical reorganization in body form: (i) histolysis of larval cells and tissues and (ii) differentiation and morphogenesis of adult cells and tissues.

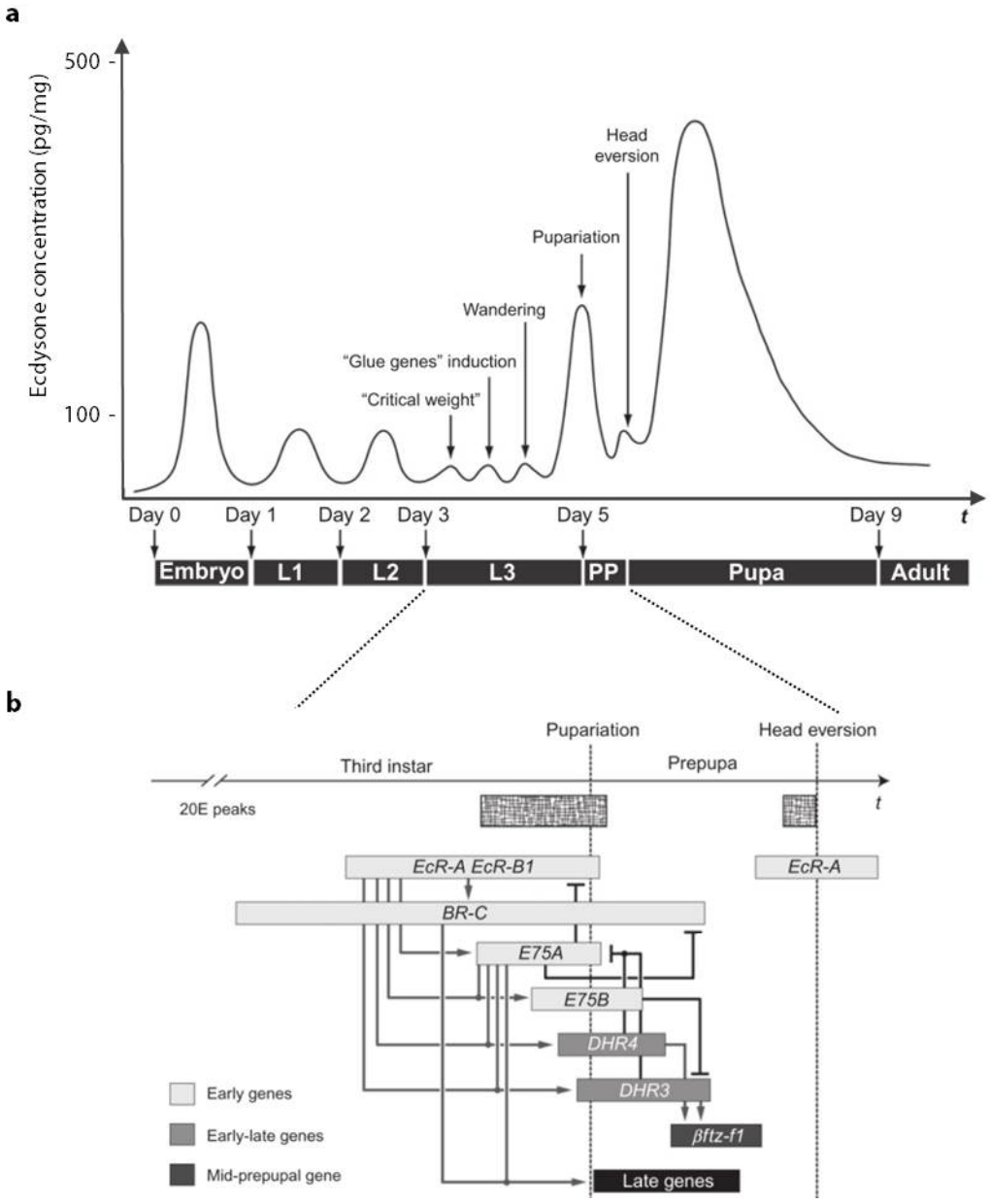

Figure 3: Ecdysone concentration and gene cascade during development. (a) Schematic representation of whole-body ecdysone concentrations during *Drosophila* development. Arrows indicate physiological and behavioral changes that are triggered by the respective ecdysone pulse. (b) Ecdysone induced gene cascade at the onset of metamorphosis. The expression of genes is shown in bars with different shades of gray representing different gene categories (see inset), and the length of the bars indicate the approximate duration of their expression. Positive and inhibitory interactions are shown. Ecdysone peaks are shown in dotted boxes at the top. L1/L2/L3, first/second/ third instar; PP, prepupa; E74A, Eip74EF; E75B, Eip75B; DHR4, Hr4; DHR3, Hr46. Adapted from [155].

The cellular processes controlled by ecdysone include cell death, cell proliferation, cell differentiation, tissue morphogenesis, metabolic and growth control, as well as changes in behavior and reproductive status [12, 155]. All these processes need to be adjusted in a cell and tissue specific manner multiple times during metamorphosis, implicating different levels of regulation. Consequently, a key question in the field is how a single hormone can have such a broad range of effects and how this diversity is regulated. The answer to these questions lies in the specific spatial (cell type) and temporal (developmental stage) regulation of ecdysone signaling.

2.2 Pathway components and its spatio-temporal regulation

Initial evidence for the ecdysone pathway was elucidated from an *ex vivo* culture system that used ecdysone regulated puffing patterns in salivary gland polytene chromosomes to reveal the underling gene expression hierarchy [8]. Chromosome puffs are DNA regions of active transcription, at which ecdysone signaling leads to recruitment of histone methyltransferases that methylate lysine 4 of histone 3, thereby loosening the nucleosomes in that area [175]. Four classes of puffs have been described: (i) intermolt puffs, which are active at the beginning of the response and thereafter regress, (ii) early puffs, which are induced within minutes, (iii) early-late puffs, appearing with a delay of two hours, and (iv) late puffs, which appear from three hours onwards [8]. This early conceptual framework is referred to as the Ashburner model. Ashburner postulated that the early puffs are direct targets of the ecdysone-bound receptor and that the corresponding early genes encode regulatory proteins that induce the late puffs. Ever since, decades of research have elucidated the molecular and regulatory mechanisms how these early (or primary) regulatory proteins coordinate the expression of late (or secondary) response genes, which ultimately direct the developmental changes.

Ecdysone receptor and DNA binding Ecdysone binds to a heterodimer of two nuclear receptors, the ecdysone receptor (EcR) and ultraspiracle (USP), which are orthologous of the vertebrate farnesoid X receptor (FXR) or liver X receptor (LXR), and RXR receptors, respectively [113, 110]. EcR comprises the ecdysone binding domain but is dependent on USP to facilitate its DNA- and ligand-binding activities [92]. EcR exists in three protein isoforms (A, B1 and B2), which arise through alternative promoter usage and differential splicing resulting in different amino-terminal domains but common DNA- and ligand-binding domains [113, 189]. EcR isoforms are expressed in a tissue- and stage-specific manner [110]. At the onset of metamorphosis isoform B1 dominates in larval tissues that will die during metamorphosis, while A dominates in the imaginal discs that undergo differentiation [189]. Isoform B2 might play a major role in the larval fat body and epidermis [38].
The EcR/USP heterodimer binds to specific promoter sequences called ecdysone response elements (EcREs) and interacts with transcriptional cofactors to regulate expression of ecdysone responsive genes. Recent research has elucidated the identity and mechanisms of several cofactors, such as chromatin remodelers, histone modifiers, histone chaperones and insulator-binding factors [13, 65, 11, 207, 109, 62, 169]. The selection of specific cofactors depends on DNA sequence or cellular context. Importantly, EcR/USP can function as repressors in the absence of ecdysone by recruiting co-repressor complexes. Upon ecdysone binding these repressors are displaced by recruited co-activators, resulting in the activation of a characteristic set of early target genes [66].

Ecdysone target genes At the larval-to-prepupal transition, the first pulse of ecdysone induces a small group of "early genes" including its own receptor (EcR) and the transcription factors Broad-Complex (Br), Eip74 and Eip75 (Figure 3b). The genomic loci encoding the "early genes" are extraordinary large (>60kb) and complex, with multiple overlapping transcription units driven by multiple nested ecdysone-inducible promoters, which respond to distinct ecdysone

concentrations [104, 93]. Br plays a pivotal role in the initiation and progression through metamorphosis and represents the most complex locus, which through differential initiation and splicing gives rise to 14 transcript isoforms. These isoforms are expressed in tissue and stage specific manner during metamorphosis and can be classified into four protein isoforms, distinguished by their zinc finger module (Z1 to Z4) [148].
All "early genes" are key regulators of the ecdysone cascade and induce the expression of a second series of genes such as Hr4 and Hr46, which shut off some "early genes" and activate "late genes". The latter are "effector genes", since they directly execute the developmental changes during larval-to-prepupal and prepupal-to-pupal transition. The second pulse of ecdysone during pupal development uses the same hierarchy of regulatory early genes but triggers a distinct set of late "effector genes" in order to remodel the body plan by regulating processes including cell death, cell proliferation, cell differentiation, energy metabolism and tissue morphogenesis [104, 93, 155].

In summary, at the core of ecdysone signaling lies the interaction of the ecdysone hormone with a heterodimer of EcR/USP to induce a cascade of primary (regulatory) and secondary (effector) genes. The final biological outcome depends on the specific spatio-temporal expression of ecdysone signaling components (Figure 4). The elaborate regulation of this spatio-temporal patterning involves multiple mechanisms including ecdysone concentration, the combination of specific protein isoforms and cofactors as well as other signaling pathways [104, 189, 155]. Signaling pathways such as insulin, TGFβ, or JAK/STAT interact with the ecdysone pathway components to further fine-tune the cell-type specific outcome [118].
Although multiple critical components of the tissue and stage specific regulation are identified, a global and detailed kinetic description of the underling regulatory network and its network motifs is missing. In regard to general mechanism of gene regulation, the control of transcription might not be sufficient to dynamically fine-tune ecdysone signaling and it is therefore likely complemented by post-transcriptional mechanisms, such as specific expression of miRNAs or RBPs (Figure 4).

2.3 Ecdysone regulated miRNAs

Multiple studies suggest a crucial role for miRNAs in the coordination of developmental transitions in insects [17, 177, 35]. Although changes in miRNA expression patterns coincide with the pulses of ecdysone, the direct relationship between ecdysone signaling as key trigger of all developmental transitions and miRNAs is largely unknown.
To date only a few miRNAs have an established role in ecdysone signaling or have even been identified as direct targets of EcR and Br (miRNAs of the let-7 locus, miR-14, and miR-8) [177, 193, 37, 100]. The miRNAs of the let-7 locus (let-7, miR-100 and miR-125) are thought to control developmental transitions [176, 177, 37]. miR-14 and its validated target EcR compose an auto-regulatory negative feedback loop [193]. miR-8 promotes insulin signaling and body growth and was shown to be transcriptionally repressed by ecdysone's early response genes, providing a link between the antagonistic signaling of insulin and ecdysone [95, 100].
Comprehensive insights into how ecdysone signaling is affected by and/or implements miRNAs as primary or secondary response genes are still missing. However, such knowledge would complement the transcriptional regulation of ecdysone signaling with one mechanism of post-transcriptional regulation.

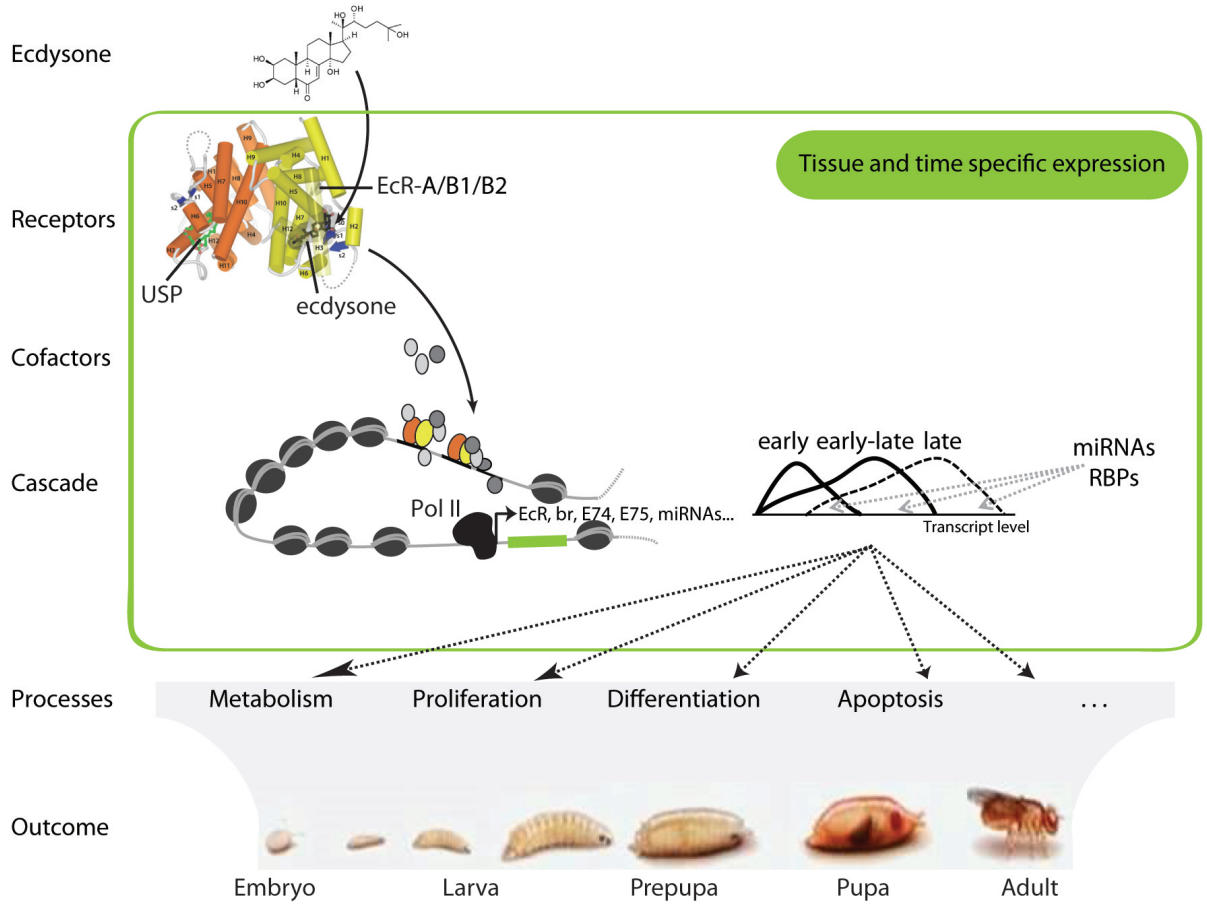

Figure 4: Spatio-temporal patterning of ecdysone signaling. Schematic representation of the ecdysone signaling cascade and affected cellular processes. Components within the boxed area (green) underlie tissue and time specific expression, including EcR isoforms, cofactors, target genes, miRNAs and RBPs. Structure of the EcR/USP heterodimer ligand-binding domain (*Heliothis virescens*) is taken from [89]. Ecdysone is shown in black within the ligand-binding pocket of the EcR.

3 Dynamic Transcriptome Analysis (DTA)

The cellular RNA abundance level is the consequence of two opposing mechanisms, namely nuclear synthesis and cytoplasmic decay. These individual contributions keep mRNA levels in a dynamic equilibrium and are highly responsive to environmental perturbations.

Until recently, RNA synthesis was measured by genomic run-on (GRO) [63], which required sarkosyl treatment, and decay was analyzed upon chemical blocking of transcription, e.g. by actinomycin-D treatment [170]. However, these methods are rather cell invasive and induce a cellular stress response, which on its own affects RNA stability [181]. Therefore, most gene expression studies are carried out using total cellular abundance RNA, accepting serious limitations: (i) the RNA abundance level has to be used as an approximation for changes in synthesis and (ii) the contribution of RNA degradation has to be neglected.

Metabolic RNA 4-thiouridine (4sU) labeling overcomes these limitations and determines changes in RNA synthesis and decay, as well as their impact on total cellular abundance level in a non-invasive manner within a single experiment. It has been known for several decades that exogenous thiol-containing nucleosides, such as 4sU, can be introduced into the eukaryotic nucleoside salvage pathway [142]. By introducing 4sU into this pathway, it is possible to label and selectively isolate newly synthesized (nascent) RNA since eukaryotic RNAs normally do not contain thiol-groups.

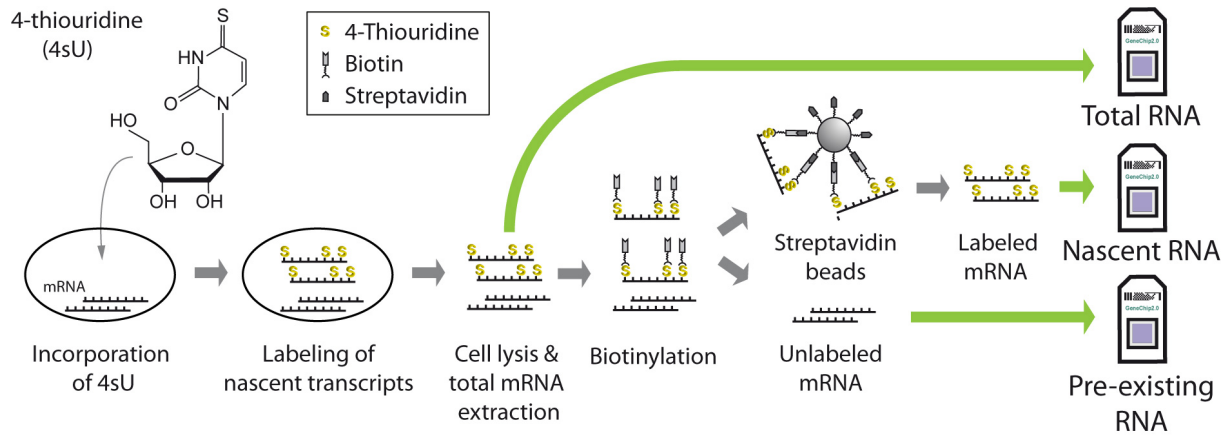

Figure 5: Schematic representation of metabolic 4sU RNA labeling. Eukaryotic cells take up 4sU from the culture medium in a concentration dependent manner and incorporate 4sU into nascent RNA, generating a pool of labeled RNA and pre-existing, unlabeled RNA. After cell lysis thiol-labeled nascent RNA is tagged with biotin and isolated by purification with streptavidin-coated magnetic beads. Adapted from [144].

4sU labeling is applicable to a large variety of cell types *(in vitro)* and organisms (*in vivo*) [105, 145, 51, 196, 138, 186, 67]. The experimental *in vitro* setup simply requires culturing cells in the presence of 4sU, which is taken up by eukaryotic cells in a concentration dependent manner, generating a pool of labeled RNA (Figure 5). After cell lysis, the thiol-labeled nascent RNA can be isolated by thiol-specific biotinylation and streptavidin purification [43]. If needed, the pre-existing (present prior to 4sU labeling) RNA can be recovered from the sample. Therefore, metabolic RNA labeling yields three types of RNA fractions: total cellular RNA, pre-existing unlabeled RNA and nascent labeled RNA. The quantification of these fractions can be accomplished by any gene expression profiling method.

4sU labeling has been shown to monitor gene expression dynamics with higher sensitivity and greater temporal resolution compared to conventional transcriptomics [51, 196, 144, 160, 186]. Moreover, labeling has minimal adverse side effects on gene expression, RNA decay, mRNA translation, protein stability, and cell viability [44, 105, 51, 144]. 4sU labeling was complemented with a customized novel statistical approach to estimate mRNA synthesis and decay rates on a genome-wide scale, assuming exponential decay (Dynamic Transcriptome Analysis, DTA) [172].

4sU labeling/DTA measures transcription with unprecedented sensitivity and temporal resolution and permits to dissect the contributions of RNA synthesis and decay to gene expression level.

4 Aims and scope of this thesis

The elaborate regulation of gene expression occurs at multiple steps from DNA to RNA to protein and is highly responsive to environmental perturbations. Although, regulation of transcription is the dominant step, rates of mRNA degradation and translation are regulated between genes as well [200, 160, 174, 128]. A quantitative and global description of how transcriptional and post-transcriptional regulation is integrated to set and adjust gene expression levels is still missing.

Microarray and next-generation sequencing techniques have revolutionized the way we can address this fundamental question of gene expression regulation. All aspects contributing to this regulation can be measured in a genome-wide and highly quantitative fashion, including discovery of accessible cis-regulatory elements by DNaseI Hypersensitivity Site-Sequencing (DHS-Seq), nucleosome positioning and occupancy profiling by MNase-Seq, identification of histone modification or protein binding profiles by ChIP-Chip/Seq as well as measurement of nascent and total abundance mRNA expression by DTA-RNA-Chip/Seq. The combination of all these experimental techniques with computational modeling enables investigating gene expression regulation at an unprecedented mechanistic level.

In this regard, the aims of my PhD thesis were:

1. Establishing ecdysone treatment of S2 cells as experimental paradigm for studying gene expression regulation

2. Using DTA and microRNA profiling to dissect the regulation of gene expression during ecdysone signaling

3. Establishing an improved DTA-RNA-Sequencing protocol for dissecting the *Drosophila* core promoter

Establishing ecdysone treatment of S2 cells as experimental paradigm for studying gene expression regulation

To correlate diverse genome-wide data sets, it is crucial to work within a consistent and reproducible experimental paradigm. Ideally, the paradigm should be easily perturbed to investigate the dynamics and plasticity of gene expression regulation.

Therefore, the first aim of my thesis was to establish and characterize such an experimental paradigm. Time series treatment of *Drosophila* Schneider 2 (S2) cells with the steroid hormone ecdysone represents a highly suitable and interesting paradigm: (i) Our S2 cell line represents a homogenous cell population, as it is derived from a single clone (K. Förstemann). We cultivate the cells under standardized condition in synthetic cell culture medium without serum. (ii) Binding of ecdysone to its nuclear receptor triggers a complex gene expression cascade that induces both transient and long-term expression changes in a wide range of functionally diverse genes, including TFs [155]. (iii) Despite much knowledge about the transcriptional players in ecdysone signaling, a comprehensive description of the regulatory mechanism involving TF activity, chromatin dynamics and post-transcriptional contributions has not been carried out.

In my thesis, I established the time series treatment of S2 cells comprising of a frequently sampled early interval (1-12 hours) and an extended interval up to 72 hours (Figure 6). I characterized the ecdysone induced phenotype using a cell analyzer, light microscopy and flow cytometry. I could reproducibly show that upon ecdysone treatment S2 cells cease proliferation and acquired a differentiated morphology, characterized by increase in cell size and granularity along with outgrowth of filopodia (Section 7.1, Figure 6).

Using DTA and microRNA profiling to dissect the regulation of gene expression during ecdysone signaling

The genomic response to ecdysone is one of the best studied transcriptional cascades in *Drosophila [129, 18, 66, 75]*. However, one common drawback of all studies is that they examined only RNA abundance levels. Therefore these studies suffered from imprecise measurements of transcription rate and were unable to discriminate whether changes in RNA abundance are due to alterations in RNA synthesis or decay. Metabolic RNA 4sU labeling, also known as Dynamic Transcriptome Analysis (DTA), was shown to be a direct readout of transcription, which allows genes expression profiling with superior sensitivity and improved temporal resolution compared to conventional transcriptomics [51, 144]. Moreover, it allows attributing changes in gene expression to alterations in synthesis or decay rates [160, 186, 58].

Therefore, the second aim of my thesis was the application of DTA to investigate the transcriptional and post-transcriptional regulation of gene expression dynamics during the ecdysone response. To this end, I established 4sU labeling coupled to microarrays for S2 cells and measured nascent and total mRNA levels during the early time interval (1-12 hours) of the ecdysone response (Section 7.2, Figure 6). We demonstrate that DTA monitors the genomic response to ecdysone with high sensitivity and great temporal resolution (Section 7.3), as well as that ecdysone induces major, progressively increasing and continuous changes in gene expression (Section 7.4). Functional annotation of ecdysone regulated genes explains the observed phenotypes very well and demonstrates how rapid the ecdysone cascade regulates a wide range of functionally diverse genes (Section 7.5). Furthermore, we estimated relative mRNA synthesis and decay rates and present the first global assessment of decay regulation by ecdysone signaling (Section 7.6). Overall, ecdysone signaling differentially regulates the mRNA expression level, synthesis or decay rate of 2141 genes (Figure 6). By complementing the DTA gathered gene expression data with k-means clustering of fold changes and kinetics in nascent and total mRNA expression levels as well as decay and turnover rates, we reveal that ecdysone induces a rich and previously unknown diversity of gene expression dynamics. Specifically, we identified twenty kinetically distinct groups of co-regulated genes, which exhibit unique combinations of effect type, strength and timing of changes in mRNA synthesis, decay rates and total expression level (Section 7.8). Notably, we observed a strong coupling of mRNA synthesis and decay rates. The functional annotation of these kinetic groups shows specific enrichments and indicates the temporal order in which ecdysone regulates biological processes to direct the cell from its proliferating state into the differentiated state (Section 7.9, Figure 6).

Moreover, to investigate the role of microRNAs in the ecdysone response, I quantified the expression of 184 microRNAs (miRNAs) in ecdysone stimulated S2 cells using a single-molecule counting technique (Section 7.11). Upon ecdysone treatment, we observed a rapid repression of some miRNAs and a progressive induction of other miRNAs (Figure 6). In addition to the known ecdysone responsive miRNAs, we identified 26 miRNAs that have no established function in ecdysone signaling or in the biological processes regulated by ecdysone in S2 cells. Therefore, our dataset represents an excellent resource for studying the function of these miRNAs in ecdysone signaling, cell cycle, metabolism or differentiation/morphogenesis. Finally, based on mRNA decay rates we established a novel approach for miRNA-mRNA network analysis to facilitate miRNA target identification (Sections 7.13) and gain first insights into the miRNA-mRNA network during the ecdysone response (Section 7.14, Figure 6).

Overall, our time series DTA analysis captures the complex gene expression dynamics of the ecdysone response and presents valuable insights into its elaborate transcriptional and post-transcriptional regulation.

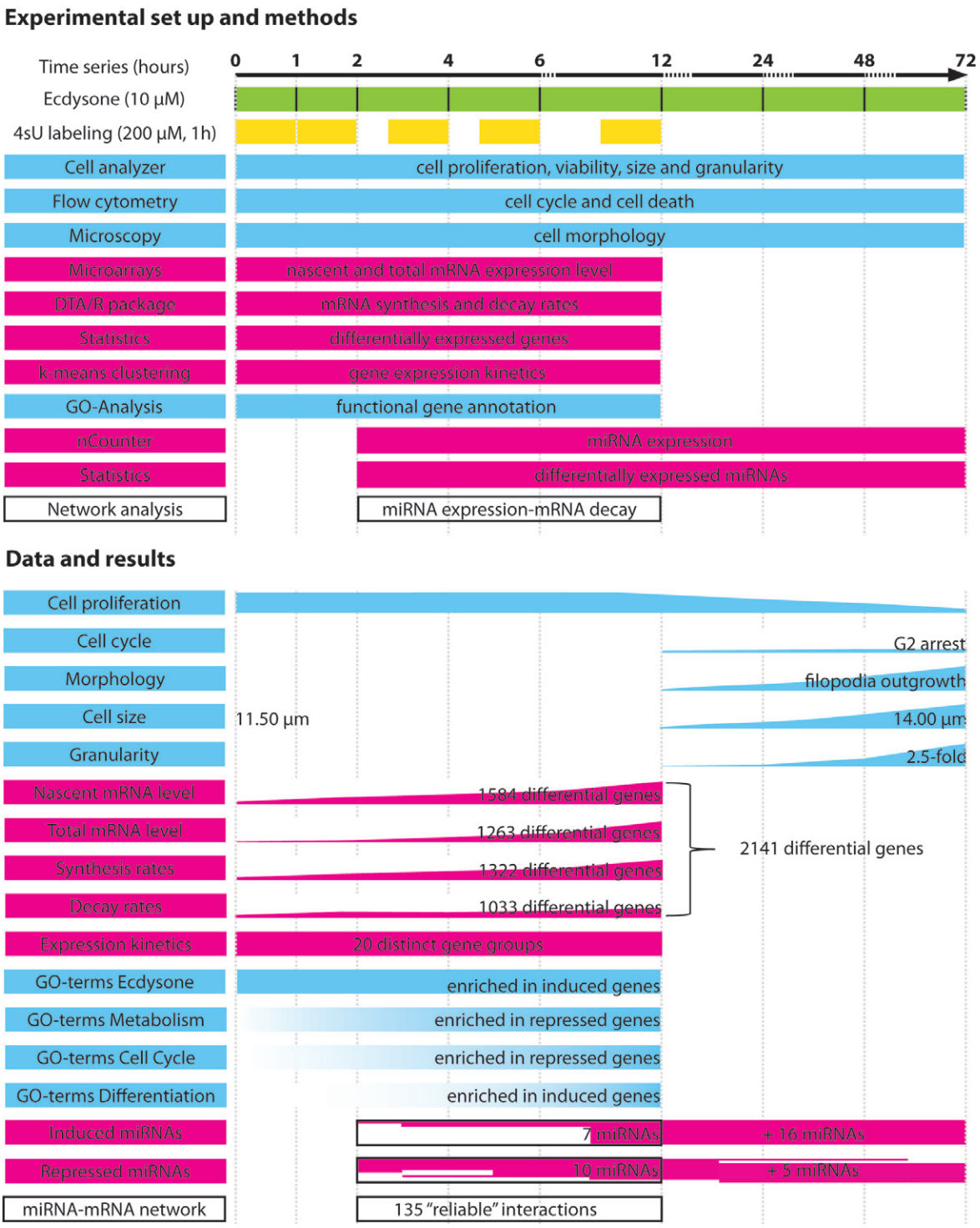

Figure 6: Overview on PhD thesis Aim 1 and 2. Experimental set up and methods panel (top) outlines the ecdysone time series treatment, 4sU labeling periods and methods used for phenotypic (blue) and transcriptome (pink) analyses. Data and results panel (bottom) illustrates the timing of identified phenotypic (blue) and genomic (pink) changes. For the phenotypic changes, bars correspond to fold changes compared to the beginning of the experiment. For differential genes, bars correlate to the number of significantly differentially regulated genes at each time point. GO term progression illustrates the temporal timing based on the comparison of GO term categories with cluster kinetics. For miRNAs the individual pink lines represent differential miRNAs according to the time point of >1.2-fold induction or repression.

Establishing an improved DTA-RNA-Sequencing protocol for dissecting the *Drosophila* core promoter

In an independent, collaborative project we used DTA to achieve a better quantitative understanding of gene expression as it is regulated by the core promoter, namely its sequence features and structural properties (Section 10). Since some of the features might operate in an activity dependent manner, we trigged different transcriptional programs, using ecdysone as developmental stimulus, insulin as metabolic stimulus and heat shock to induce a stress response. My main contribution to the project was the measurement of transcript steady state and nascent transcription rates using DTA-RNA-Sequencing (Section 10.3). To this end, I first adapted the DTA microarray protocol to next-generation sequencing and established a novel procedure for data normalization using artificial Spike-In transcripts (Section 10.1), as well as a novel strategy for rRNA depletion during sequencing library preparation employing rRNA specific oligos (Section 10.2).

In summary, my thesis made an important contribution to the laboratory's research interest in gene regulation. The established and characterized ecdysone paradigm will serve as a working model for diverse gene regulatory questions including the dynamic regulation of cis-regulatory elements and their TFs, as well as chromatin dynamics involving nucleosome positioning and chromatin modifications. Moreover, using this paradigm I generated highly quantitative genome-wide data sets on mRNA and miRNA expression dynamics during the ecdysone response. Our analysis provides novel insights into how cells coordinate distinct patterns of gene expression in order to adjust the transcriptome to environmental perturbations. These data furnish the laboratory with a comprehensive resource for further experimental and computational projects.

Part II
Material and Methods

5 Material

5.1 Cell line and culture

Name	Specification	Source (Catalog #)
Drosophila Schneider 2 (S2) cells	single clone derived from late *D. melanogaster* embryos	K. Förstemann
Express Five® SFM	protein-free, serum-free	Gibco (10486-025)
L-Glutamine	200 mM, add 90 ml per 1000 ml medium	Gibco (25030-081)
20-Hydroxyecdysone	10 mM stock in ethanol, store -20°C	Sigma-Aldrich (H5142)
Insulin	2 mM stock in water, store -20°C	Roche (11376497001)

Table 1: Cell culture, medium, supplements and treatments.

Name	Fill volume	Source (Catalog #)
75 cm^2 flasks	12 ml	Corning (430 641)
225 cm^2 flasks	25 ml	Corning (3001)
150 mm dish	20 ml	BD Falcon (353025)

Table 2: Cell culture consumables.

5.2 List of primers

All DNA primers were synthesized by Eurofins MWG Operon GmbH, Ebersberg, Germany.

ID	Name	Sequence (5´ > 3´)
kf43	RT_br_fw#2	AGGATGTCAACTTCATGGACC
kf44	RT_br_rev#2	GTGTGTGTCCTCTGCCTGCT
kf47	RT_EcR_fw	CAAAATGGCCGGAATGGCTGAT
kf48	RT_EcR_rev	AGCGCGTATTCGACGTTGTCCA
kf143	RT_CG30159_fw#1	CCACCGCAAAATCCTTGG
kf144	RT_CG30159_rev#1	AGCCTAACCAGCGACCAC
kf126	pri-miR-8_fw#2	GCGCCCCGGTTCAAAGTTA
kf127	pri-miR-8_rev#2	GCTGTGTGCTCAAGTGGGTT
kf117*	Rp49_fw	ATCGGTTACGGATCGAACA
kf121*	miR-8_fw	TAATACTGTCAGGTAAAGATGTC

Table 3: Primers used for RT-PCR. Primers were either designed with Primer 3 [115] or Primer-Blast [201]. (*) used with reverse primer miScript Universal Primer. br, broad; EcR, ecdysone receptor; rp49, Ribosomal protein L32.

ID	Name	Sequence (5´ > 3´)	Annealing
261	spike#2_fw3	**TAATACGACTCACTATAGGG**TGCTTTAACAAGAG GAAATTGTGT	53°C
262	spike#2_rev3	CCATCTTGTTTATAAAATCCTAATTACTC	53°C
278	spike#12_fw2	**TAATACGACTCACTATAGGG**GGCACAAGTTGCTG AAGTTGC	58°C
279	spike#12_rev2	TCTGCTGTAATCTCAGCTCC	58°C
263	spike#4_fw3	**TAATACGACTCACTATAGGG**TTTCGACGTTTTGA AGGAGGG	53°C
264	spike#4_rev3	GTACCCGGGAAAATCCTAGTTC	53°C
265	spike#5_fw3	**TAATACGACTCACTATAGGG**ACTGTCCTTTCATC CATAAGCGG	55°C
266	spike#5_rev3	CGCACGCCGAATGATGAAACG	55°C
267	spike#8_fw3	**TAATACGACTCACTATAGGG**GATGTCCTTGGACG GGGT	55°C
268	spike#8_rev3	GCTTTCGGAGCAAATCGCG	55°C
269	spike#9_fw3	**TAATACGACTCACTATAGGG**CCAGATTACTTCCA TTTCCGCC	55°C
270	spike#9_rev3	GGGTAAAACGCAAGCACCG	55°C

Table 4: PCR primers used for Spike-In amplification and *in vitro* transcription. Sequence in bold represents the T7 promoter.

5.3 Spike-In transcripts

Name	GC content	Length [nt]	Labeled
spike_2	0.33	983	4sU
spike_12	0.35	947	no 4sU
spike_4	0.42	1011	4sU
spike_5	0.44	1012	no 4sU
spike_8	0.50	1076	4sU
spike_9	0.51	1034	no 4sU

Table 5: Spike-In transcripts. Sequences can be found in Supplementary Table 6.

5.4 Antibodies and probes

Target	Host/Sequence (5´ > 3´)	Usage	Source (Catalog #)	Application
Actin	mouse	1:5000	Abcam	Western blotting
EcR	mouse	1:100	DSHB (Ag10.2)	Western blotting
Br-C	mouse	1:50	DSHB (25E9.D7)	Western blotting
α-Mouse-HRP	goat	1:2500	Abcam	Western blotting
let-7	CTACTATACAACCTA CTACCTCA	10 pmol	K. Förstemann	Northern blotting
2S rRNA	TACAACCCTCAACCA TATGTAGTCCAAGCA	10 pmol	K. Förstemann	Northern blotting

Table 6: Antibodies and probes.

5.5 Buffers and solutions

Name	Composition	Application
cOmplete Lysis-M EDTA-free	Commercial buffer, Roche (4719964001)	Cell lysis
Roti-Load 1	Commercial buffer, Roth (K929.1)	SDS-PAGE
Running buffer	30.3 g Tris, 144.1 g glycine, 10 g SDS in 1000 ml ddH_2O	SDS-PAGE
10x WB transfer buffer	14.5 g Tris, 72 g glycine in 1000 ml ddH_2O	Western blotting
1x WB transfer buffer	100 ml 10x WB transfer buffer, 200 ml methanol, 3 ml SDS 10%, 700 ml ddH_2O	Western blotting
WB blocking buffer	5% (w/v) milk powder in 1x PBS-T	Western blotting
1x PBS	2 mM KH_2PO_4, 4 mM Na_2HPO_4, 140 mM NaCl, 3 mM KCl, pH 7.4 (25°C)	Western blotting
1x PBS-T (0.1%)	100 ml PBS 10x, 1 ml Tween 20, 900 ml ddH_2O	Western blotting
Biotinylation buffer	100 mM Tris pH 7.4, 10 mM EDTA	DTA-protocol
Wash buffer	100 mM Tris pH 7.5, 10 mM EDTA, 1 M NaCl, 0.1% Tween 20	DTA-protocol

Table 7: Buffers and solutions.

5.6 Metabolic RNA labeling and RNA isolation

Name	Description	Source (Catalog #)
4-thiouridine	50 mM stock in PBS, store -20°C, thaw only once	Sigma-Aldrich (T4509)
peqGOLD TriFast	store at 4°C	Peqlab (30-2030)
15 ml PP-Tubes	tolerate up to 15000 g	Greiner Bio-One (188261)
EZ-Link HPDP-Biotin	1 mg/ml stock in DMF	Pierce (21341)
Screw cap micro tubes	1.5 and 2.0 ml	Sarstedt (72.692.005, 72.694.005)
Phase Lock Gel Heavy Tubes	2 ml	5 Prime (2900309)
Magnetic Stand		Miltenyi (130-042-303)
µMacs Streptavidin Kit		Miltenyi (130-074-101)
1,4-Dithio-DL-threitol (DTT)	1 M stock in RNase-free water, store -20°C	Sigma-Aldrich (43815-1G)
TURBO DNA-free Kit		Ambion (1907)
RNeasy MinElute		Qiagen (74204)
Agencourt RNAClean XP Beads		Beckman Coulter (A63987)
Round bottom 96 well plate		Greiner Bio-One (651161)
96 well magnetic stand		Ambion (AM10027)

Table 8: Consumables for metabolic RNA labeling.

5.7 mRNA and microRNA expression profiling

Name	Source (Catalog #)	Application
RQ1 RNase-Free DNase	Promega (M6101)	RT-PCR
Transcriptor First Strand cDNA Synthesis Kit	Roche (04897030001)	RT-PCR
SsoFast EvaGreen Supermix	Bio-Rad (172-5201)	RT-PCR
Bio-Rad CFX96 Real-Time System	Bio-Rad (185-5096)	RT-PCR
miRNeasy Mini Kit	Qiagen (217004)	microRNAs
miScript II RT Kit	Qiagen (218161)	RT-PCR
miScript SYBR Green PCR Kit	Qiagen (218073)	RT-PCR
nCounter Fly miRNA Expression Assay Kits	nanoString (GXA-FMIR-48)	microRNAs
GeneChip 3´ IVT Express Kit Assay	Affymetrix (901229)	Microarray
GeneChip Drosophila Genome 2.0	Affymetrix (900533)	Microarray
KOD Hot Start DNA Polymerase	Novagen (71086-3)	Spike-Ins
MEGAscript T7 Kit	Ambion (AM1334)	Spike-Ins
4-Thio-UTP	Jena-Bioscience (NU-1156S)	Spike-Ins
Ovation Human Blood RNA-Seq Multiplex System	NuGEN (0337, 0338)	Sequencing
BioruptorPlus	Diagenode (B01020001)	Sequencing
HiSeq 2500	Illumina	Sequencing

Table 9: Consumables and platforms for expression profiling.

5.8 Nucleic acid quantification

Name	Source (Catalog #)
Agilent RNA 6000 Nano Kit	Agilent (5067-1511)
Agilent DNA 7500 Kit	Agilent (5067-1506)
Qubit® dsDNA HS Assay Kit	Life technologies (Q32851)

Table 10: Consumables for nucleic acid quantification.

5.9 Staining for flow cytometry

Target	Source (Catalog #)	Usage
Vybrant DyeCycle Green Stain	Molecular Probes (V35004)	10 µM
SYTOX Red Dead Cell Stain	Molecular Probes (S34859)	5 nM

Table 11: Staining for flow cytometry.

6 Experimental methods

6.1 Cell based methods

6.1.1 Cell culture conditions

Drosophila Schneider 2 (S2) cells were cultured in synthetic, serum-free Express Five medium (Gibco) supplemented with 90 ml of 200 mM L-Glutamine (Gibco). Cells were thawed at passage 12 or 13 and cultivated until passage 18. During cultivation cells were grown at 25°C without CO_2 as semi-adherent monolayer in tissue culture flasks (Corning). Twice a week cells were split into fresh flasks by means of seeding 0.6 - 0.8 x 10^6 cells/ml.

6.1.2 Cell counting and phenotypic assessment

Cell counting was performed in duplicates using the Cell Counter and Analyzer System (CASY; Roche). Using CASY, cell viability and diameter were assessed to judge cellular health and monitor cellular phenotype upon experimental treatment. Cell morphology was monitored using a white field microscope.

6.1.3 Cell treatments

Cells were seeded 24 hours prior to cell treatment. On the next day, cell viability and monolayer confluence was assessed and if confluence was 80% cell treatment was started. For the ecdysone signaling project, cells were continuously treated with 10 µM ecdysone (Sigma-Aldrich) for 1-72 hours and samples were extracted after 1, 2, 4, 6, 12, 24, 48 and 72 hours (Figure 6). Untreated control cells were prepared for each time point, except for the DTA experiment, in which controls were prepared only for 1 hour and 12 hours. Stimulation time courses were carried out in two biological replicates. For the core promoter project cells were treated with 10 µM ecdysone (1, 1.5, 2, 4, 8 and 12 hours), 4 µM insulin (Roche; 1, 1.5, 2, 4 and 8 hours) or 37°C (0.5, 1, 1.5 and 2 hours). Untreated control cells were prepared at 1 and 1.5 hours.

6.1.4 Flow cytometry

For flow cytometry 1 x 10^6 cells were incubated with Vybrant DyeCycle Green Stain (Invitrogen) and SYTOX Red Dead Cell Stain (Invitrogen) according to manufacturer's protocol. For each sample data from 20000 cells was analyzed using a Becton Dickinson FACS Calibur. Cell cycle phases of living cells (negative cell death staining) were assigned by comparison to published S2 cell flow cytometry studies [23, 25] and quantitative results were extracted using FCS Express Version 3 software (De Novo Software).

6.2 Protein methods

6.2.1 Preparation of whole cell extracts for Western blot analysis

For preparation of whole cell extracts, 1.8 x 10^6 cells were seeded 24 hours before ecdysone treatment. After treatment 3 x 10^6 cells were harvested on cooled metal plates and collected by centrifugation (4°C, 1500 rpm, 5 min). Subsequent steps were performed at 4°C. Pellet was resuspended in 150 µl cell lysis buffer (cOmplete Lysis-M EDTA-free; Roche), incubated on ice for 10 min and centrifuged (4°C, 14000 rpm, 10 min). Next, protein concentration was determined using the Nanodrop® ND-1000 Spectrophotometer (Peqlab) and protein extracts were stored at -80°C.

6.2.2 SDS-Polyacrylamide gel electrophoresis (SDS-PAGE)

Protein extracts were thawed on ice. Then, 100 µg protein extract was mixed with modified Laemmli buffer (Roti-Load, Roth) along with 100 mM DTT and boiled at 95°C for 5 min. Electrophoretic separation of proteins was performed by SDS-PAGE using 10% acrylamide gels (acrylamide:bisacrylamide ratio = 37.5:1) in Bio-Rad gel systems filled with Running buffer (Table 7) for 20 min at 25 mA, then 90 min at 50 mA.

6.2.3 Western blotting

Separated proteins were transferred to a nitrocellulose membrane (Macherey-Nagel) using a semidry blotter (Bio-Rad) in the presence of WB transfer buffer (Table 7), (300 mA, 1 hour). Next, the membrane was blocked for 40 min with PBS-T + 5% milk powder and subsequently incubated with primary antibody at 4°C for 2 hours (Table 6). The membrane was washed three times with 1xPBS-T for 10 min and then incubated with secondary antibody, coupled to horseradish peroxidase (room temperature, 40 min). Washing steps were performed as before, except for the last wash, which was performed with PBS. Signals were detected using the Amersham ECL Prime Western Blotting Detection Reagent (GE Health Care) and imaged using ChemiDoc XRS+ system (Bio-Rad).

6.3 Methods for expression analysis of mRNAs

The recently reported approach for metabolic 4-thiouridine (4sU) RNA labeling [51], also known as Dynamic Transcriptome Analysis (DTA) [144], was applied to simultaneously analyze changes in RNA synthesis and decay rate, along with their impact on total cellular transcript levels.

6.3.1 Metabolic labeling of nascent RNA (DTA-protocol)

For all DTA experiments, 25 x 10^6 cells were seeded in 150 mm dishes and grown for 24 hours. On the next day, time course experiments comprising various cell treatments were carried out as described in Section 6.1.3. For metabolic RNA labeling 4-thiouridine (4sU; Sigma-Aldrich) was dissolved in sterile PBS at a stock concentration of 50 mM, stored in small aliquots at -20°C and thawed on ice before labeling. Nascent RNA was labeled using 200 µM 4sU, which was added to the cell culture medium for the last 60 min of each treatment time point. For the core promoter project labeling time was decreased to 30 min. To stop stimulation and RNA labeling cells were collected on cooled metal plates and 40 x 10^6 cells were pelleted by centrifugation (4°C, 1500 rpm, 5 min). Cell pellets were resuspended in 7 ml TriFast (Peqlab), incubated at room temperature for 5 min and transferred into 15 ml polypropylene tubes (VWR International). Cell lysates were stored at -80°C for further use.

6.3.2 Extraction of total cellular RNA (DTA-protocol)

Total cellular RNA was prepared by Phenol/Chloroform extraction following a modified protocol by Chomczynski et al. [41]. In brief, 0.2 ml chloroform per milliliter TriFast was added to the cell lysates, tubes were shaken vigorously for 15 sec and incubated at room temperature for 5 min. After centrifugation (4°C, 12000 g, 10 min), the upper (aqueous) phase was transferred into new polypropylene tubes. Equal volume of isopropanol was added; tubes inverted and RNA was precipitated at room temperature for 10 min followed by centrifugation (4°C, 12000 g, 10 min). Isopropanol was removed and pellet was washed in an equal volume of 75% ethanol and centrifuged as before. Ethanol was removed and the remaining ethanol was spun down twice and removed by firstly using a 200 µl pipette and then a 20 µl pipette. Next, 100 µl per 100 µg expected RNA yield RNase-free water was added and the pellet was carefully resuspended by pipetting. RNA quality

was assessed on a RNA 6000 Nano Chip (Agilent). The extracted total RNA was stored at -80°C for further use.

6.3.3 Biotinylation of 4sU labeled, nascent RNA (DTA-protocol)

To separate total RNA (T) into 4sU labeled (nascent) RNA (L) and unlabeled (pre-existing) RNA (U), 80 µg total RNA were incubated with EZ-Link Biotin-HPDP (Pierce). Biotin was dissolved in dimethylformamide (DMF) at a concentration of 1 mg/ml and stored in small aliquots at 4°C. 2 µl of biotin solution were used per 1 µg total RNA, together with Biotinylation buffer (1 µl / 1 µg RNA, Table 7) and RNase-free water (7 µl / 1 µg RNA). Biotinylation was carried out at room temperature on a rotating wheel for 2 hours, protected from light. Subsequently, unbound biotin and DMF were removed by chloroform extraction. First, an equal volume of chloroform was added and samples were shaken vigorously for 15 sec, incubated for 3 min at room temperature and centrifuged (room temperature, full speed, 5 min). Next, upper phase was transferred to 2 ml Phase Lock Gel Heavy Tubes (5 Prime) and a second extraction with 500 µl chloroform was performed. The upper phase was transferred into 1.5 ml tubes and total RNA was precipitated by addition of an equal volume of isopropanol and 1/10 volume of 5 M NaCl. RNA was pelleted by centrifugation (4°C, 20000 g, 20 min). RNA pellet was washed using an equal volume of 75% ethanol and pelleted by centrifugation (4°C, 20000 g, 10 min). Ethanol was removed immediately as described in Section 6.3.2 and the pellet was resuspended in 100 µl of RNase-free water by careful pipetting. The biotin labeled RNA was stored at -80°C or immediately used for isolation of labeled (nascent) RNA.

6.3.4 Isolation of labeled (nascent) RNA (DTA-protocol)

Biotinylated, 4sU labled RNA was heated to 65°C for 10 min to minimize secondary structures, immediately placed on ice for 5 min, and then captured by incubation with 100 µl streptavidin-coated magnetic beads (Miltenyi Biotec) on a rotating wheel for 15 min (4°C). Meanwhile, µMAC columns (Miltenyi Biotec) were equilibrated with 900 µl room temperature Wash buffer (Table 7). After 15 min, samples were applied twice to the same µMAC column. Next, columns were first washed 3x with 900 µl of 65°C Wash buffer, then 3x with room temperature Wash buffer. If the unlabeled (pre-existing) RNA had to be recovered, the flow-through of the sample together with the first wash was collected and RNA was precipitated with isopropanol as described in Section 6.3.3. Finally, labeled RNA was eluted into 700 µl RLT buffer (Qiagen) with 100 µl of 100 mM freshly prepared DTT (Table 8). A second elution step was performed 5 min later and RNA was recovered using the RNeasy MinElute Kit (Qiagen) according to manufacturer's cleanup protocol. RNA was eluted with 20 µl of RNase-free water, applied twice.

For the core promoter project the protocol was further optimized by substituting the MinElute Kit by Agencourt RNAClean XP Beads (Beckman Coulter). The RNA was recovered from the DTT eluate according to manufacturer's protocol for Large Volume Reactions. 15 µl of RNase-free water were used for elution.

6.3.5 RNA quantification and quality control

RNA concentration was measured using the Nanodrop® ND-1000 Spectrophotometer (Peqlab). Further, 1 µl of the eluted RNA was loaded on a RNA 6000 Nano Chip of the Agilent automated electrophoresis system to control RNA integrity and the characteristic molecular weight distribution of smallRNAs, 18S and 28S rRNA.

6.3.6 DNase treatment

Prior to preparing microarray or sequencing samples, DNase treatment was performed to exclude any DNA contamination in extracted total RNA. 10 µg of total RNA were subjected to TURBO DNase according to the manufacturer's protocol (Ambion). Nascent RNA, which is purified by its 4sU label, does not contain any significant DNA contamination, and therefore, no DNase treatment is needed.

6.3.7 Dot blot

In order to establish the 4sU labeling concentration and time for S2 cells, Dot blot analysis, which specifically detects 4sU labeled, biotinylated RNA, was performed as described previously [51]. Analysis was carried out in 10-fold dilutions (1 µg down to 1 ng) using a biotinylated control oligonucleotide of 81 nt length to quantify 4sU-incorporation (100 ng down to 0.1 ng).

6.3.8 Reverse transcription and real-time PCR

Real-time PCR (RT-PCR) was performed to prove the expression of a given gene in S2 cells or to monitor the activation of genes upon cell stimulation.
Gene specific 22-27 nt long primers were designed using the software Primer 3 (v. 0.4.0) [115] or Primer-Blast [201]. The specificity of the corresponding primer pairs was determined using a standard curve, and only primer pairs with a specific melting curve were used. A list of all RT-PCR primers used in this thesis is given in Table 3. Prior to reverse transcription, 400 ng total RNA or 100 ng nascent RNA were treated with DNase (Promega) at 37°C for 30 minutes. Reverse transcription into cDNA was carried using the First Strand cDNA Synthesis Kit (Roche) in the presence of a 2:1 ratio of random hexamer and oligo-dT primers, respectively. Approximately 60 ng of cDNA was used to set up 10 µl PCR reactions containing 5 µl 2x SSO-fast Evagreen Supermix (Bio-Rad) and 0.3 µl of both forward and reverse primer, 20 µM each. RT-PCR was performed on a Bio-Rad CFX96 Real-Time System (Bio-Rad) using a 30 sec denaturation step at 95°C, followed by 40 cycles of 5 sec at 95°C and 5 sec at 58°C. Finally, a melting curve was generated in 0.5°C increments for 5 sec from 65-95°C. To exclude any genomic DNA or general contaminations a -RT control (no reverse transcriptase during cDNA synthesis) and a water control (no cDNA template) were included in all RT-PCR runs. Threshold cycle (Ct) values were determined by application of the corresponding Bio-Rad CFX Manager software version 3.1 using the Ct determination mode "Single Threshold". Relative expression levels were calculated applying the $2^{-\Delta\Delta CT}$ method [131] with normalization of target gene expression levels to CG30159.

6.3.9 Microarray hybridization for DTA

Gene expression analysis by microarrays was carried out with 300 ng of total or nascent RNA using the GeneChip 3´ IVT labeling assay (Affymetrix). Samples were hybridized to the GeneChip Drosophila Genome 2.0 Array containing 18880 probe sets following the manufacturer's instructions (Affymetrix). All GeneChips were processed in the Affymetrix facility at the Gene Center LMU Munich, Großhadern.

6.3.10 Data processing, quality control, normalization and filtering

Data were analyzed by B. Schwalb (Max Planck Institute for Biophysical Chemistry, Göttingen) using the open source R/Bioconductor software [70, 49]. Microarray processing, quality control, baseline normalization across microarrays as well as probe intensity calculation were performed using GeneChip Robust Multiarray Averaging (GC-RMA) [198]. Probe sets were annotated based on the Affymetrix annotation file Drosophila_2.na32.annot (June 10, 2011), along with manual

re-annotation or exclusion of probe sets, which were observed to be wrongly annotated or hit multiple genes. The detection limit for expressed probe sets was defined as: probe set intensity value greater than $\log_2(3)$ in any of the measured microarrays. After quantile normalization of the biological replicates, all probe set values were further normalized by median centering on 506 *stable* genes. The list of *stable* genes was compiled by intersecting two datasets: (i) genes constantly expressed throughout *D. melanogaster* development [39, 76] compiled by U. Unnerstall (AG Gaul, Gene Center), and (ii) most stable genes throughout the performed ecdysone stimulation. The latter selection was based upon ranks, since they are more stable than fold changes. Expression values of the total and labeled RNA data were ranked for each time point and rank gains were calculated relative to the ranks in the untreated sample. Genes exhibiting a rank gain below 500 during ecdysone treatment were considered as *stable*. The median centering on *stable* genes was done separately for total and labeled RNA.
We decided not to average intensity values of probe sets targeting the same gene, considering that in some cases different transcript isoforms might be targeted. As 95.5% of the regulated probe sets targeted unique transcripts, I will, in this thesis, equivalently use the word "gene" when I refer to "probe set".

6.3.11 Estimation of relative mRNA synthesis and decay rates

The R/Bioconductor package Dynamic Transcriptome Analysis (*DTA*) [173] was used to estimate relative mRNA synthesis and decay rates. For detailed description of the model and parameter estimation refer to [144]. In brief, during a 4-thiouridine (4sU) labeling period t, 4sU is integrated into the nascent RNA, generating a pool of labeled RNA. Therefore, the total mRNA level (C) of a given gene g in a sample r consists of the pre-existing, unlabeled RNA fraction (B) and the nascent, labeled RNA fraction (A).

$$C_{gr}(t) = A_{gr}(t) + B_{gr}(t) \tag{1}$$

The *DTA* model assumes an unperturbed steady-state, where RNA synthesis and decay determine the equilibrium mRNA level. To that end the synthesis rate μ_g and decay rate λ_g of a gene g are assumed to be constant during the 4sU labeling time, if averaged over a cell cycle period. This steady-state assumption is valid because we measure a large, unsynchronized population of cells. The same argument holds true for temporal fluctuations in transcription. Consequently, *DTA* estimates the cell cycle and population average of mRNA synthesis and decay rates during the 4sU labeling period t. The assumption of constant rates during labeling allows for changes in synthesis and decay rates between distinct time points in a time series experiment. In order to calculate decay rates the model assumes that the pre-existing, unlabeled RNA fraction (B) follows an exponential decay law given by

$$B_{gr} = C_{gr} \times e^{-t(\alpha+\lambda_g)} \tag{2}$$

or equivalently with (1),

$$\frac{A_{gr}}{C_{gr}} = 1 - e^{-t(\alpha+\lambda_g)} \tag{3}$$

The parameter α is known as the dilution rate and considers that the increase in total mRNA amount of all cells is proportional to the increase in cell number during the labeling time. The increase in cell number depends on the cell cycle length, which is the time in which the cell number doubles. This time was measured to be 24 hours. The unknown decay rate can be inferred by solving equation (3) for λ_g. However, the described assumptions and equations reflect an idealized situation, that does not account for experimental bias such as 4sU labelling efficiency (labeling bias), RNA extraction

efficiencies, amplification steps and scanner calibrations. Consequently, a set of parameters is defined to relate the mRNA fractions $A_g(t)$ and $C_g(t)$ to the measured levels of total RNA $T_g(t)$ and labeled RNA $L_g(t)$. The parameter estimation was done as described in [144]. The final equation for calculation of decay and synthesis rates is given by

$$\frac{L_{gr}}{T_{gr}} = l_{gr}\frac{a_r}{c_r}\left[1 - e^{-t(\alpha+\lambda_{gr})}\right] \tag{4}$$

and considers the estimated labeling bias l_{gr} as well as the ratio of a_{gr} and c_{gr}, which account for multiple experimental bias introduced during sample and microarray preparation. $\frac{a_r}{c_r}$ has been determined in previous experiments to be 0.08.
Using equation (4) the decay rate can be deduced from

$$\lambda_{gr} = -\propto - \frac{1}{t_r} log\left[1 - \frac{\frac{c_r}{l_{gr}a_r}L_{gr}(t_r)}{T_{gr}(t_r)}\right] \tag{5}$$

The synthesis rate can be calculated from

$$\mu_{gr} = \frac{\frac{c_r}{l_{gr}a_r}L_{gr}(t_r)(\alpha+\lambda_{gr})}{\left[e^{\propto t_r} - e^{-\lambda_{gr}t_r}\right]} \tag{6}$$

Note: Using our experimental setup *DTA* cannot estimate absolute rates, but reliably reports relative rates as shown in [144]. Furthermore, the synthesis rate is not given in mRNA molecules produced per cell cycle period, as we did not have an estimate of how many copies of a transcript exist in *Drosophila* S2 cells. Since our data did not suffer from any labeling bias (data not shown) rates could be calculated without bias correction.

6.3.12 Differential expression analysis

6.3.12.1 Single time point analysis Significantly differentially expressed probe sets were identified using the R/Bioconductor package *LIMMA* [184]. *LIMMA* was applied to all measured and calculated values: (i) total RNA expression, (ii) labeled RNA expression, (iii) synthesis rate and (iv) decay rate. We considered a probe set "significantly differentially expressed", if the calculated expression value fold or rate fold of the treated versus the untreated group differed by a factor of at least $\log_2(1.5)$ along with a p-value smaller than 1% in the respective two-group comparison.

6.3.12.2 Time series analysis Differential expression analysis across the treatment time series was carried out by B. Knapp, ICB Helmholtz Zentrum, München.
For the time series analysis total RNA and labeled RNA expression values of untreated (mock) and ecdysone treatment at the individual time points 1, 2, 4, 6, and 12 hours were extracted from the DTA text file output (*total_expression_table*; *labeled_expression_table*). Next, the fold change $\log_2$(sample/mock) was calculated, where sample corresponds to the data given for each replicate at each time point. For mock, the median of the 1hour and 12hours time points and their respective replicates was used. To identify probe sets differentially regulated over the time series, the R/Bioconductor package Bayesian Estimation of Temporal Regulation (*betr*) [7] was applied. In short, in *betr* a probability is computed for each probe set denoting whether it is differentially expressed or not. The algorithm fits two models to the data, one assuming that the probe set is differentially expressed across time points, and one assuming no differential expression. The latter model is a random effects model that takes correlations between time points into account and thus, allows an increased sensitivity in comparison to an analysis based on individual time points. Probe sets were considered as being differentially expressed, if they exhibited a replicate's averaged probability equal to 1.

6.3.13 Gene Ontology (GO) analysis

6.3.13.1 *topGO* Gene Ontology (GO) enrichment analysis in the categories Biological Process (BP), Molecular Function (MF) and Cellular Component (CC) were performed using the R/Bioconductor package *topGO* [1]. Annotation terms were derived from the R/Bioconductor package *drosophila2.db* [33]. Enrichment was tested for the union of all differentially regulated probe sets (single time point and time series), but also separately for up- and down-regulated probe sets. *topGO* was applied in three different modes: (i) classical mode using a Fisher test in which each GO category was tested independently, (ii) *elim* algorithm which scores parent nodes according to the significance of their children, and (iii) *weight01* algorithm which uses *elim* and additionally a weighting scheme for the nodes. The latter algorithm was used to sort the enriched GO categories according to their p-value.

6.3.13.2 Cytoscape plugin ClueGO The ClueGO v2.1.1 plugin [24] for the open source software Cytoscape V3 [45] was used to analyze and visualize the GO network. Functional annotations were retrieved through Cytoscape from Gene Ontology "Biological Process" and KEGG database [103]. Gene lists submitted to ClueGO: (i) genes with induced/repressed expression in total or labeled RNA, (ii) genes with induced/repressed synthesis rate and (iii) genes with induced/repressed decay rate. Enrichment was tested using a two-sided hypergeometric test and Bonferroni correction. Enriched GO terms (hierarchy level 3-8, without IEA) had to contain at least six genes and the associated genes needed to represent at least 8% of all genes of that term. GO terms were grouped when they overlapped in at least 50% of their genes using Kappa Score 0.5 and initial Group Size 4. After a gene list was tested for overrepresented terms, all genes associated with terms unrelated to either cell cycle (Figure 5), metabolism (Figure 6) or differentiation/morphogenesis (Figure 7) were excluded and enrichment analysis was repeated. For visualization only the most representative terms and genes were chosen.

6.3.14 k-means clustering

In order to group probe sets according to similar expression or rate kinetics across the time series k-means clustering was applied.

6.3.14.1 Individual k-means clustering Data sets of total and labeled RNA, as well as synthesis and decay rate were separately clustered considering all probe sets, which were defined as significantly differentially regulated at any time point in all data sets (Section 6.3.12). All $\log_2$ expression values or rates of a gene at a given time point were converted to z-scores and subjected to k-means clustering. Clustering was initiated on stable cluster centers for the optimal number of clusters. Both parameters were determined by hundred fold iteration, until stable centers were found and optimal separation of the clusters achieved.

6.3.14.2 Combined k-means clustering All significantly differentially regulated genes (Section 6.3.12) were subjected to k-means clustering using all data sets to group genes according to their similarity in all evaluated parameters: (i) z-score kinetics in total RNA, labeled RNA and decay rate and (ii) $\log_2$ fold change at a given time point in total RNA, labeled RNA or decay rate. Further, the turnover of a gene, being defined as "synthesis rate x decay rate", was included instead of the synthesis rate. Final clustering was initiated on the stable cluster centers for the optimal cluster numbers, as described above.

6.3.15 Cluster characterization

6.3.15.1 Description of cluster timing, strength, effect type and coupling of synthesis and decay rates The characterization of timing was based upon mean fold change progression of total RNA or labeled RNA, and described in five time windows: early (1, 2 hours), early until late (1-12 hours), middle (4, 6 hours), middle until late (4-12 hours) and late (12 hours). The effect strength was defined as the maximum mean fold change in total RNA expression: $<$1.5-fold, $\geq$1.5-fold, $\geq$2-fold or $\geq$4-fold. Effect type, i.e. increase or decrease of gene expression or rate was discretized based on mean fold changes $\geq$1.5-fold by color coding in red and blue, respectively. Coupling of synthesis and decay rates was assessed by Pearson correlation of mean fold changes: strong ($r \geq 0.75$), moderate ($r \geq 0.50$), poor ($r \geq 0.25$) and no coupling ($r < 0.25$).

6.3.15.2 UTR sequence analysis For all clusters genomic 5´ UTR and 3´ UTR coordinates were obtained from flybase-r5.22. Average UTR length of each cluster was compared to average UTR length of all clusters. Difference was called significant, if the cluster average differed by at least 25% with a p-value smaller than 1% in the respective two-group comparison (Wilcoxon Rank Sum test).

6.3.15.3 Enrichment analyses The functional annotation enrichment of each cluster was calculated using a Fisher's exact test against all genes present on the Affymetrix *Drosophila* Genome 2.0 array. Annotation terms were derived from the R/Bioconductor package *drosophila2.db* [33] and an optimized functional prediction resource [199]. Enrichment was called significant, if it achieved a p-value smaller than 1%. The degree of over-representation defined as the number of expected genes versus the number of observed genes was calculated for significantly enriched terms. RNA binding protein (RBP) enrichment of each cluster was calculated using a Fisher‘s exact test using a published data set of Pumilio targets (embryo) [71] and unpublished data from G. Meister for Brat targets (embryo). Enrichment was called significant, if it achieved a p-value smaller than 1%. Degree of over-representation was calculated for significantly enriched terms. For the random enrichment analysis, all significantly differentially regulated genes were randomly assigned to 20 clusters of the size equal to the original 20 clusters (Section 6.3.14) and enrichment analyses were performed as described above. The random assignment and analysis was repeated 50 times and the occurrence of each enriched GO term or RBP target was documented. Occurrence of $\leq$5 was called reliable.

6.4 Methods for expression analysis of microRNAs

6.4.1 microRNA purification

For all microRNA (miRNA) experiments 1.8 x 10^6 cells were seeded 24 hours before ecdysone treatment. After treatment 2.5 x 10^6 cells were harvested and total RNA containing the small RNA fraction was extracted using the miRNeasy Mini Kit (Qiagen) according to manufacturer's protocol.

6.4.2 Northern blotting

Northern blotting using 15 µg RNA was carried out by R. Böttcher (AG Förstemann, Gene Center) and was performed as described in [61]. 2S rRNA was used as positive control. All probes are listed in Table 6.

6.4.3 RT-PCR

The relative quantification of mature microRNAs was carried out using primers designed by K. Förstemann (Table 3). miRNA tailing and reverse transcription of 200 ng RNA was performed using miScript II reverse transcription kit (Qiagen) according to the manufacturer's instruction. PCR

amplification was executed on a Bio-Rad CFX96 Real-Time System (Bio-Rad) using Qiagen miScript RT-PCR kit according to the manufacturer's instruction. The 15 sec denaturation step at 95°C was followed by 40 cycles of 15 sec at 95°C, 30 sec at 55°C and 30 sec at 72°C. Finally, a melting curve was generated in 0.5°C increments for 5 sec from 65-95°C. Threshold cycle (Ct) values were determined by application of the corresponding Bio-Rad CFX Manager software version 3.1 using the Ct determination mode Single Threshold. Relative expression levels were calculated applying the $2^{-\Delta\Delta CT}$ method [131] with normalization of target miRNA expression levels to rp49. Relative quantification of pri-miRNAs was performed as for mRNAs (Section 6.3.8). Primers were designed to target a preferably unstructured region next to the mature miRNA stem loop.

6.4.4 nCounter

In order to simultaneously measure the differential expression of 184 microRNAs, the digital multiplexed nanoString nCounter Fly miRNA expression assay (nanoString Technologies) was performed with 100 ng total RNA extracted from two biological replicates. Sample hybridization and nCounter analysis was conducted by the nCounter Core Facility, Heidelberg.

6.4.5 nCounter data analysis

Raw data were transformed to log scale and normalized based on the average counts of the internal positive spike controls to account for platform associated sources of variation. The detection limit was set to two standard deviations above the average count of the lower 33% of the data. Next, a global normalization between the biological replicates was applied calculating a scaling factor based on the top 40 expressed miRNAs. Data were further normalized by a scaling factor calculated from the average of six invariant miRNAs. The invariant miRNAs were selected using the R/Bioconductor package *NanoStringNorm* [195]. Differentially expressed candidate miRNAs were identified applying the *betr* package (Section 6.3.12) with minor modifications. First, two time intervals were used for the time series analysis (i) 2-12 hours and (ii) 2-72 hours. For mock the mean of the 2-24 hours time points was used. Second, the significance level α was set to 0.1. miRNAs were considered to be significantly differentially expressed, if they exhibited a replicate's averaged score of at least 0.99. The lists of differentially expressed candidate miRNAs were manually refined to exclude putative false positives or include obvious false-negatives. miRNAs with inconsistent and minor fold changes ($<$ 1.2-fold) were excluded, whereas miRNAs with strong ($\geq$1.5-fold), but not monotonic fold changes were included.
Note: An improved normalization strategy would be to use Spike-In RNA oligos of the negative controls C, D and E, which then control for RNA extraction efficiency and sample input [98].

6.4.6 miRNA target predictions

The target predictions from microRNA.org are based on the miRanda algorithm [56] and are further scored for likelihood of mRNA down regulation using mirSVR [22]. All fruit fly pre-computed target site predictions were downloaded from microRNA.org (August 2010 release) and combined to one target graph (good and non-good mirSVR score, conserved and non-conserved miRNAs). In addition, miRanda was run in its default setting to predict targets for dme-mir-282-3p. All predicted miRNA-mRNA target pairs containing differentially regulated miRNAs and mRNAs were extracted for further use.

6.4.7 miRNA-mRNA network analysis

miRNA-mRNA network analysis was carried out by B. Knapp and S. Sass, ICB Helmholtz Zentrum, München.

To identify potential miRNA mediated down-regulation of mRNA expression a simple matching criterion, based on discrete expression and decay rate fold change patterns, was applied. First, for significantly regulated genes a discrete decay rate pattern was generated at the time points 2, 4, 6 and 12 hours. The fold change (FC) in decay rate after treatment was discretized to $+1$ and -1 for FC>0 or <0, respectively. Furthermore, the expression pattern of differentially regulated miRNAs was discretized just as well. Next, discrete expression and decay rate patterns of miRNAs and mRNAs were correlated for all predicted microRNA-mRNA target pairs (Section 6.4.6) over the entire time series or using one time shift: miRNA pattern at 2-4-6 hours was allowed to match an mRNA decay rate pattern at 4-6-12 hours. A miRNA-mRNA pair was called "valid", if the expression pattern of an induced or repressed miRNA matched to the increased or decreased decay rate pattern of its target, respectively. Finally, we used the total mRNA expression data to filter for miRNA-mRNA interactions, in which mRNA expression levels are significantly changed ($\geq$1.5-fold, p-value$<$0.01). We classified these interactions as "reliable".

In addition, miRNA-mRNA pairs were correlated by the miRNA expression pattern and discrete mRNA total RNA expression pattern. In this case "valid" pairs had to be positively correlated and for "reliable" pairs the mRNA decay rate had to be significantly regulated ($\geq$1.5-fold, p-value$<$0.01). Networks of miRNAs and their targets were visualized using Cytoscape V3 [45].

6.5 Methods for optimizing the *D. melanogaster* DTA-RNA-Seq protocol

6.5.1 Spike-In controls

Artificial RNA spike-in controls were established as a novel method for normalization against various experimental biases including variations in RNA input amount, purification efficiency or PCR amplification biases due to variable GC-content. 1 µl of the ERCC RNA Spike-In Mix (Ambion) was reverse transcribed using the First Strand cDNA Synthesis Kit (Roche) with oligo-dT primers. Specific PCR primers were designed to amplify six Spike-In sequences characterized by: (i) approximate length of 1000 nt, (ii) almost equal number of thymine/uridines and (iii) either 30%, 40% or 50% GC content (Table 5). GC contents were represented by two sequences. The 5´ end of the forward primer included the T7 promoter sequence to facilitate *in vitro* transcription (IVT) from the PCR product. All experimental procedures were conducted under RNase-free conditions. PCR amplification was performed using the KOD Hot Start DNA Polymerase (Novagen) on a Bio-Rad DNAEngine Thermo Cycler (Bio-Rad). After an initial denaturation step at 95°C for 2 min , 30 cycles of 95°C for 20 sec, primer annealing step for 3 sec and 72°C for 70 sec were performed. Annealing temperature was adjusted for each Spike-In sequence (Table 4). After the final extension step at 72°C for 10 sec, PCR products were purified using the QIAquick PCR Purification Kit (Qiagen). Size and purity of PCR products was assessed by gel electrophoresis. If PCR products showed contaminations with smaller fragments, the desired PCR fragment was isolated by gel extraction using the QIAquick Gel Extraction Kit (Qiagen). Final fragments were sent for sequence verification to Eurofins MWG Operon. Finally, *in vitro* transcription of 500 ng PCR product was performed for 4 hours using the MEGAscript T7 Kit (Ambion) according to manufacturer's protocol. For each GC content one Spike-In was transcribed in the presence of 1:1 ratio UTP to 4-Thio-UTP (Jena Bioscience). Final products were purified using the Agencourt RNAClean XP Beads (Beckman Coulter) following the manufacturer's protocol and eluted in 100 µl RNase-free water. Transcript integrity and size was assessed on a RNA 6000 Nano Chip (Agilent). All six Spike-Ins were pooled in equal numbers (1.44×10^6 molecules) to generate a stock mix and 8 µl of this mix was spiked in the cell lysate prior to total RNA isolation (Section 6.3.2).

6.5.2 Depletion of ribosomal RNA (primer design)

Depletion of ribosomal RNA (rRNA) was achieved by *D. melanogaster* rRNA specific primers coupled to the Insert Dependent Adaptor Cleavage (InDA-C) method (NuGEN).
The rRNA specific primers were designed by NuGEN based on two resources: Firstly, we extracted all rRNA sequences from the Flybase genome release dmel_r5.53_FB2013_05, resulting in 160 transcripts. Secondly, we provided sequencing results from our own previous experiments, in which 70% of all reads mapped to rRNA. 17-25 nt long primers were placed approximately every 70-300 nt along the transcript with emphasis on the most prominently expressed rRNAs. After the design, primers were aligned to the genome (NCBI Blast) to identify possible off target effects. Finally, a total of 124 primers were synthesized by Metabion. Before use, all primers were pooled and the concentration adjusted to 125 nM each.
After this work was completed NuGEN released a commercial library preparation kit containing *D. melanogaster* rRNA specific InDA-C primers (Ovation Drosophila RNA-Seq System 1-16).

6.5.3 Next-generation sequencing

The Ovation Human Blood RNA-Seq Library Systems 1-8 and 9-16 (NuGEN) was used for strand specific RNA-Sequencing library generation. 250 ng total or labeled RNA were first converted into double stranded cDNA according to manufacturer's protocol (NuGEN) and fragmented by sonification using the BiorupterPlus (Diagenode). 15 cycles time on 30 sec, time off 30 sec, "low" setting, followed by 10 cycles using the same settings after 10 min cool down. Next, library preparation was continued as described by the manufacturer, except that component SS5 was replaced by the *D. melanogaster* specific InDA-C primer mix (Section 6.5.2). Libraries were amplified using 15 PCR cycles. Final libraries were quantified using the Qubit dsDNA HS Assay Kit (Invitrogen). In addition, molarity and fragment distribution was analyzed on a Bioanalyzer DNA 7500 Chip (Agilent). Libraries were pooled and 50 bp paired-end sequencing was performed on an Illumina HiSeq 2500 sequencer. Sequencing was continued until 40 x 10^6 fragment reads could be mapped to the genome (without rRNA reads). Next-generation sequencing was performed by the LAFUGA sequencing facility at the Gene Center LMU Munich, Großhadern.

6.5.4 Processing of sequencing data

Sequencing raw data were processed using Galaxy [72, 26, 73]. First, FASTQ files were demultiplexed to obtain reverse and forward reads for each sample. Then reads were trimmed from the 3´ end using a Phred score cutoff of <30 and read pairs shorter than 30 bp were discarded. Furthermore, the first 5 bases from the 5´ end were removed. Reads were then mapped to all rRNA sequences (extracted from the *D. melanogaster* genome build 5.53, September 2013) using Bowtie version 1.0 [120] using its default parameter settings except allowing for ambiguous mapping of reads (parameter $m = -1$). Next, read pairs that did not map to rRNA sequences were extracted and mapped to the *D. melanogaster* genome (build 5.53) using Tophat version 2.0 [107] using the following parameter settings: Anchor length 5, minimum intron length 40, maximum number of alignments allowed 1, minimum length of read segment 15 and gene annotation model file of build 5.53. Mapped reads were counted using the tool HTseq-count version 1.0 [5] in its setting "intersection_nonempty".

Part III

Dissecting the regulation of gene expression during steroid hormone signaling in *Drosophila*

7 Results

7.1 Ecdysone induced cell cycle exit and differentiation in S2 cells

Time series treatment of *Drosophila* Schneider 2 (S2) cells with the steroid hormone ecdysone represents a highly suitable and interesting paradigm to study gene expression regulation. Ecdysone induces major changes in cell physiology, the cells cease proliferation and subsequently differentiate. In order to characterize the ecdysone induced phenotype in a quantitative manner, I measured four phenotypic features (i) cell proliferation, (ii) cell cycle phase, (iii) cell death and viability, along with (iv) cell size and granularity. Additionally, I monitored the cell morphology. S2 cells were treated with 10 µM ecdysone [32, 40] for 1-72 hours and each feature was evaluated in biological replicates (Methods Section 6.1, Figure 6).

Cell proliferation was determined by the increase in total cell count for untreated and ecdysone treated cells. Using our standard cultivation conditions (Methods Section 1), untreated S2 cells undergo cell division every 24 hours. Upon ecdysone treatment the proliferation rate of S2 cells slightly decreases after 12 hours and ceases from 24 hours onwards (Figure 7a). To examine this phenotype in greater detail, I fluorescently labeled cellular DNA content and determined the fraction of cells in different cell cycle phases using flow cytometry. I assigned the cell cycle phases by comparing the obtained DNA content histograms to published cell cycle analyses of S2 cells [82, 23, 25]. As one follows the progression of cell cycle phases during ecdysone treatment the proportion of cells in the G1 phase decreases from 12 hours onwards down to 4% after 48 and 72 hours (Figure 7b). Hence, the cells are unable to complete mitosis by cell division and exit cell cycle in the G2/M phase. This result explains the observed decrease in cell proliferation.

Since exit from cell cycle can either be explained by cell death or differentiation, I quantified the occurrence of cell death in the population using flow cytometry. During ecdysone treatment the percentage of cells with positive cell death staining does not substantially increase (Figure 7c). Moreover, throughout the treatment the cells are characterized by high viability (Figure 7d). Furthermore, the microscopic inspection of the cell population does not display extensive cell death, which would become visible by the accumulation of cell debris in the culture medium.

Interestingly, the visual inspection of cells revealed a pronounced change in morphology. Untreated S2 cells are round and mostly uniform in size (diameter 11.50 µm), while ecdysone treated cells change in shape and size: from round to spindle forms with long thin filopodia-like processes along with increased cell diameter and large intracellular vesicles (Figure 7e). The increase in cell diameter can be measured at an early stage of ecdysone treatment (12 hours) and results in a significant 25% increase by the end of the experiment (Student's t-test, p-value <0.001; Figure 7f). The emergence of intracellular vesicles can be monitored by the side-scattered light (SSC), which is emitted during flow cytometry and is proportional to cell granularity. After ecdysone treatment the cell granularity continuously increases from 12 hours onwards and is significantly different from untreated cells after 48 hours (Student's t-test, p-value <0.01; not shown) and 72 hours (p-value <0.001; Figure 7g).

Taken together, ecdysone abrogates S2 cell proliferation by arresting the cell cycle in the G2/M phase. Furthermore, it induces pronounced changes in S2 cell morphology, including increase in size and granularity as well as outgrowth of filopodia-like processes. The first phenotypic changes can be observed from 12 hours onwards and become pronounced effects after 48 hours (Figure 6).

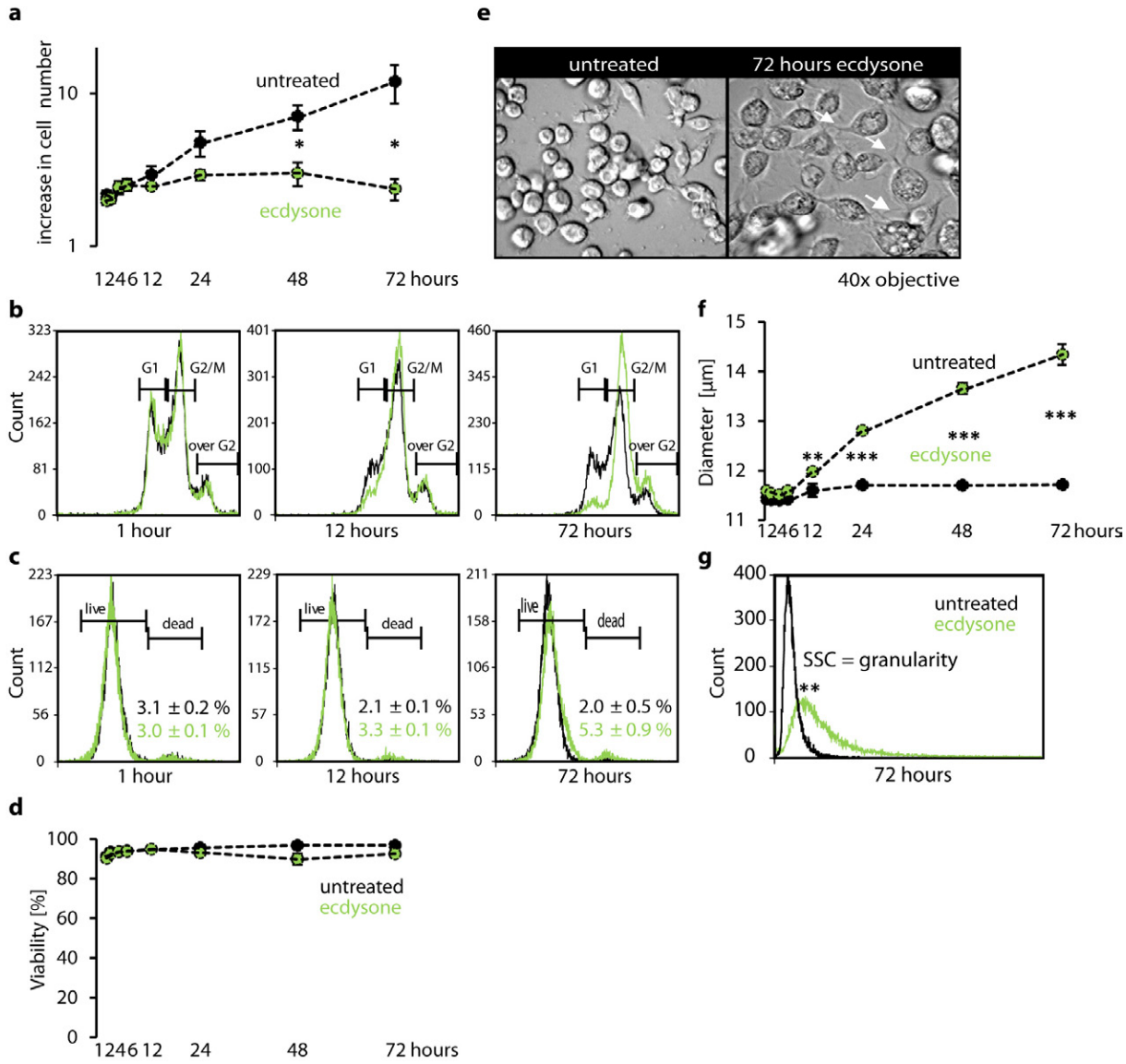

Figure 7: Ecdysone treated S2 cells exit the cell cycle and differentiate. S2 cells were treated with 10 µM ecdysone or left untreated for 72 hours and phenotypic features were characterized at eight time points (Methods Section 6.1). (a) Ecdysone abrogates S2 cell proliferation. Shown is the fold increase in cell number of untreated (black) and treated (green) cells compared to the seeded cell number (-24 hours; mean±SEM; four biological replicates). Y-axis is in logarithmic scale. (b) S2 cells do not undergo cell division and accumulate in the G2/M phase. Cell cycle progression was monitored by flow cytometry using a cell membrane permeable DNA dye. Each panel depicts a representative flow cytometry histogram of untreated (black) and treated (green) cells at the indicated time points. S2 cells have 4N DNA content ([82]; personal communication P. Becker). (c) Ecdysone treatment does not induce cell death. Cell death was quantified using a DNA stain that only permeates compromised cell membranes. Each panel depicts a representative flow cytometry histogram of untreated (black) and treated (green) cells at the indicated time points. Numbers represent percentage of cells with positive cell death stain (mean±SEM, two biological replicates). (d) S2 cells show high viability throughout the ecdysone treatment. Cell viability was assessed using CASY Cell Counter and Analyzer System. Panel illustrates percent viable cells (mean±SEM, two biological replicates). (e) S2 cells acquire a differentiated morphology, characterized by increased size and outgrowth of filopodia (white arrows). Micrographs were taken using a 40x objective. Depicted are S2 cells at the beginning of the experiment (left) and after 72 hours of ecdysone treatment (right). (f) S2 cell size increases. Cell diameter was assessed using CASY Cell Counter and Analyzer System. Panel depicts population mean diameter [µm] (mean±SEM, four biological replicates). (g) S2 cell granularity increases. Shown is a representative flow cytometry histogram of the side-scattered light (SSC), which is proportional to internal complexity (cell granularity). Student's t-test (*) p-value <0.05, (**) <0.01 and (***) <0.001.

7.2 Establishing 4sU labeling and the transcriptional time scale of ecdysone signaling in S2 cells

Having characterized the ecdysone induced phenotype, I next established non-invasive 4sU labeling conditions for *Drosophila* S2 cells and determined the transcriptional time scale downstream of the ecdysone signaling cascade. To this end, I adapted the 4sU labeling protocol [51] for S2 cells (Methods Sections 6.3.1-6.3.4). I quantified the incorporation of 4sU into nascent RNA using Dot blot analysis (Methods Section 6.3.7), which specifically detects 4sU labeled, biotinylated RNA. 4sU is efficiently incorporated into nascent RNA in a concentration and time dependent manner (Figure 8a). Since 200 µM 4sU for 1 hour yields sufficient nascent RNA in a relatively short labeling time (compared to the cell cycle length of 24 hours), we decided to use this as our labeling condition. Next, we asked whether 4sU labeling perturbs gene expression and hybridized expression microarrays (Affymetrix) with total RNA of wild-type S2 cells and 4sU exposed cells (Methods Section 6.3.9). Our labeling condition does not induce any significant changes in gene expression (Figure 8b).
To investigate the temporal scale of ecdysone signaling, I measured nascent mRNA and protein levels of ecdysone receptor (EcR) and the transcription factor broad (br), as representatives for early (primary) ecdysone target genes (Methods Sections 6.3.8, 6.2). Nascent mRNA expression revealed that transcription of EcR and br are rapidly and strongly induced and peak at 2 and 4 hours, respectively (Figure 8c). At 12 hours, transcription has almost returned to initial levels. The respective protein levels were analyzed by Western blot for an extended time period (1-72 hours), to account for the time lag between transcription and translation. As EcR and Br are both expressed in multiple isoforms, I used antibodies targeting common protein domains [189, 55]. EcR and Br levels are strongly induced from 2-24 hours and regress thereafter (Figure 8d). Furthermore, we observed two interesting phenomena. First, protein levels of EcR are lower at 48 hours compared to 72 hours. Second, Br is expressed in different isoforms upon ecdysone stimulation. This has been observed in *in vivo* studies as well [55].
These results demonstrate that the early transcriptional cascade of ecdysone signaling is induced within the first twelve hours. Moreover, the protein kinetics of EcR and Br indicate that transcription of their target genes, the early-late and late genes, might already be affected during this interval, as well.

7.3 DTA monitors the transcriptional response to ecdysone with high sensitivity and improved temporal resolution

To dissect ecdysone induced gene expression kinetics with high temporal resolution in a genome-wide fashion, I applied Dynamic Transcriptome Analysis (DTA) [144]. Specifically, I performed a time series of ecdysone treatment and 4sU nascent RNA labeling in S2 cells, comprising frequently sampled early time points (1, 2, 4, 6 and 12 hours), (Figure 6; Methods Sections 6.1.3, 6.3.1-6.3.6). Expression profiling of nascent and total mRNA was carried out using microarrays (Affymetrix; Methods Section 6.3.9). We identified 1788 genes as being significantly differentially expressed upon ecdysone treatment in the nascent or total mRNA fractions at any time point (fold change >1.5, p-value <0.01; Methods Sections 6.3.10, 6.3.12; Supplementary Table 1). Considering the entire time series, the number of genes identified in nascent or total mRNA was rather similar, 1437 and 1153, respectively. However, we find differences in the temporal resolution of nascent and total RNA expression profiling.
When comparing the number of significantly differentially expressed genes after 1 hour, expression profiling in nascent RNA identifies four times more genes compared to total RNA (Figure 9a). This effect is particularly pronounced for repressed genes. To assess this effect more globally, I quantified induced and repressed genes at each time point and classified them according to the mRNA fraction they were identified in. Especially at early time points most genes are identified in the "only nascent mRNA" fraction. Again, this is particularly pronounced for repressed genes ($>80\%$; Figure 9b). The

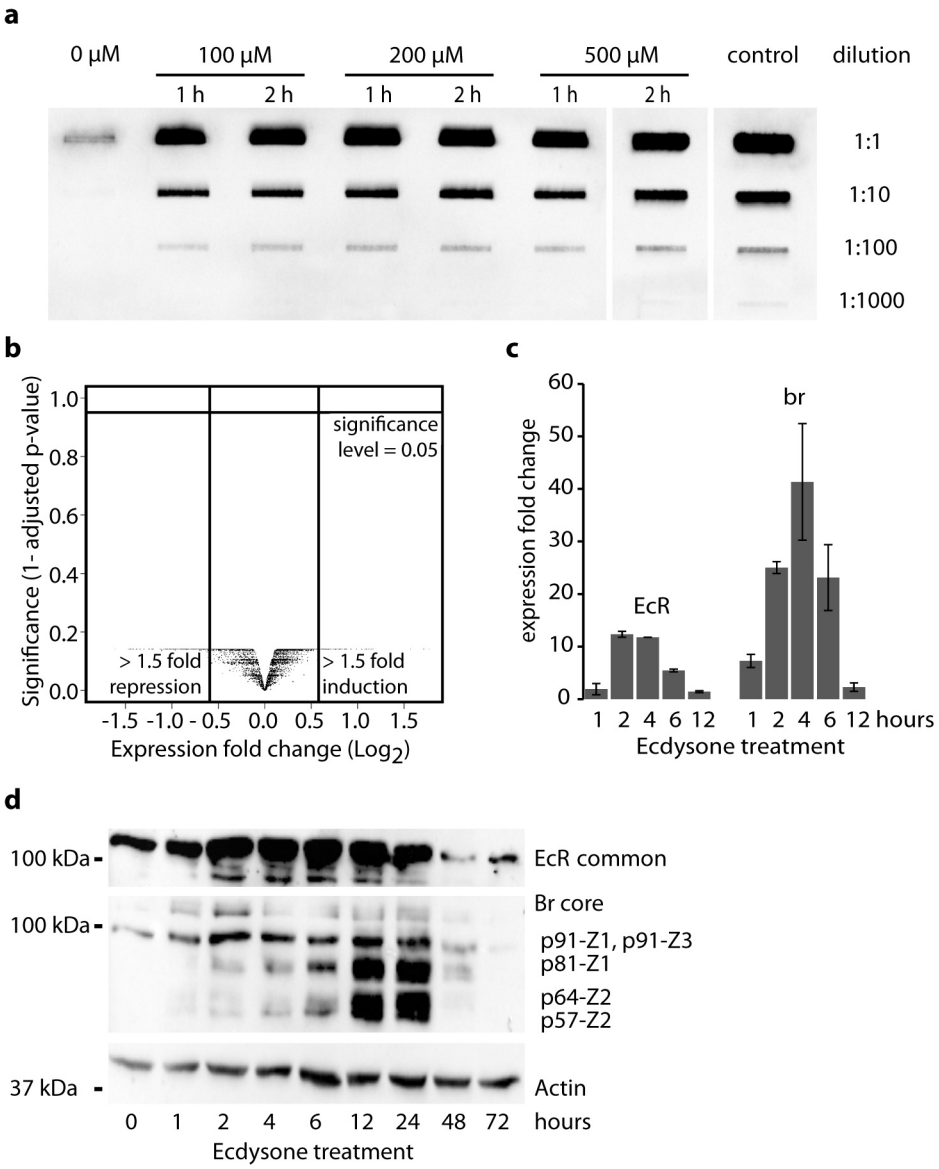

Figure 8: Establishing 4sU labeling and the transcriptional time scale of ecdysone signaling in S2 cells. (a) Concentration and time dependent incorporation of 4-thiouridine (4sU) into nascent RNA. S2 cells were cultured in the presence of 0, 100, 200 and 500 µM 4sU for 1 and 2 hours. Following isolation of total RNA and thiol-specific biotinylation, Dot blot analysis was carried out in 10-fold dilutions (1 µg down to 1 ng) (Methods Section 6.3.7). A biotinylated oligonucleotide (control) was used to quantify 4sU-incorporation (100 ng down to 0.1 ng). (b) Gene expression is unaffected by 4sU labeling (200 µM, 1 hour). Volcano plot shows the mean fold change (x-axis) in gene expression of 4sU exposed cells compared to unexposed cells. Each dot corresponds to one gene. Y-axis represents the multiple testing adjusted p-value (Benjamini–Hochberg). The inner vertical and horizontal lines represent the defined cutoff for fold change and p-value ($>\log_2(1.5)$; adjusted p-value <0.05). (c) Transcriptional kinetics of early ecdysone target genes. Nascent mRNA expression was analyzed by RT-PCR (Methods Section 6.3.8). Histograms represent normalized fold change of EcR and br expression relative to untreated cells (mean±SEM, two biological replicates). EcR and br expression was normalized against housekeeping gene CG30159. (d) EcR and Br protein levels show characteristic induction patterns. Monoclonal antibodies directed against the common EcR and Br-core (α-Br core) domains were used to probe equivalent Western blots. Br isoforms are shown on the right [55]. Actin was used as protein loading control. 4sU, 4-thiouridine; EcR, ecdysone receptor gene and protein; br/Br, broad gene/protein.

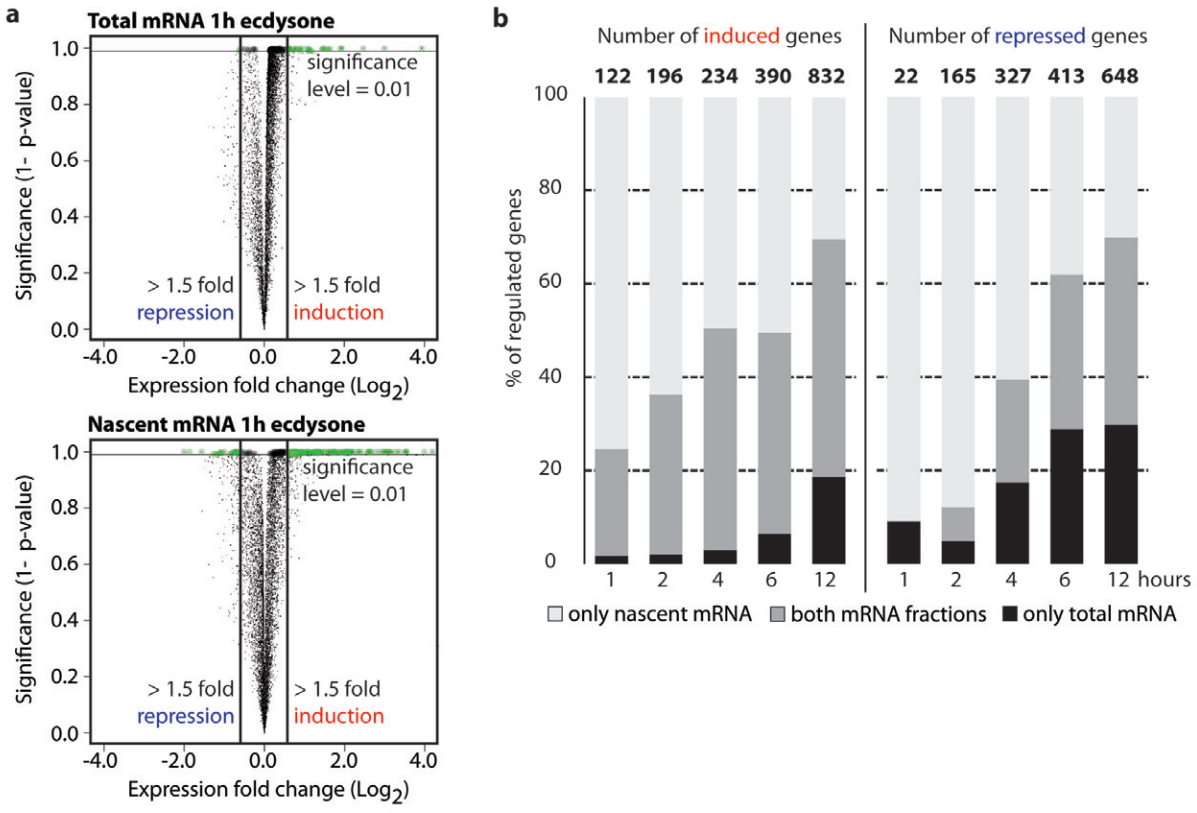

Figure 9: DTA monitors the transcriptional response to ecdysone with high sensitivity and improved temporal resolution. (a) Expression profiling using nascent RNA exhibits higher sensitivity compared to total RNA. Volcano plot shows the mean fold change (x-axis) in gene expression after 1 hour of ecdysone treatment compared to untreated cells for total (top) and nascent (bottom) mRNA. Each dot corresponds to one gene. Significantly differentially expressed genes are colored in green (fold change $>\log_2(1.5)$; Student's t-test p-value <0.01; two biological replicates). (b) Distribution of differentially expressed genes between mRNA fractions. Numbers on top denote the total number of genes induced (left) or repressed (right) at each time point. Histograms illustrate the percentage of genes identified as regulated in the corresponding mRNA fraction: only nascent mRNA (light grey), only total mRNA (black) or both fractions (dark grey).

overlap, genes identified in both fractions, increases with time. Nevertheless, the exclusive fractions, "only nascent mRNA" and "only total mRNA", persist throughout the time course.
Genes in the "only nascent mRNA" fraction can be explained by higher sensitivity of nascent RNA profiling. Genes in the "only total mRNA" fraction can be explained by two considerations: Firstly, the distance between 4sU labeling intervals at later time points was rather long and the nascent mRNA fraction cannot identify changes in transcription, which occur between these intervals. Secondly, while nascent RNA is dependent on RNA synthesis, total RNA levels are influenced by both RNA synthesis and decay. Therefore, changes in gene expression as a result of altered RNA decay can be identified only in the total RNA fraction.
In conclusion, gene expression profiling of the ecdysone response using nascent RNA shows a higher sensitivity and therefore improved temporal resolution compared to total RNA profiling.

7.4 Ecdysone induces major, progressively increasing and mostly sustained changes in gene expression

Binding of ecdysone to its nuclear receptor triggers a complex gene expression cascade. First, a small set of early regulators is induced or repressed, which in turn affects other regulatory genes to finally induce or repress late effector genes. This particular signaling pathway architecture amplifies

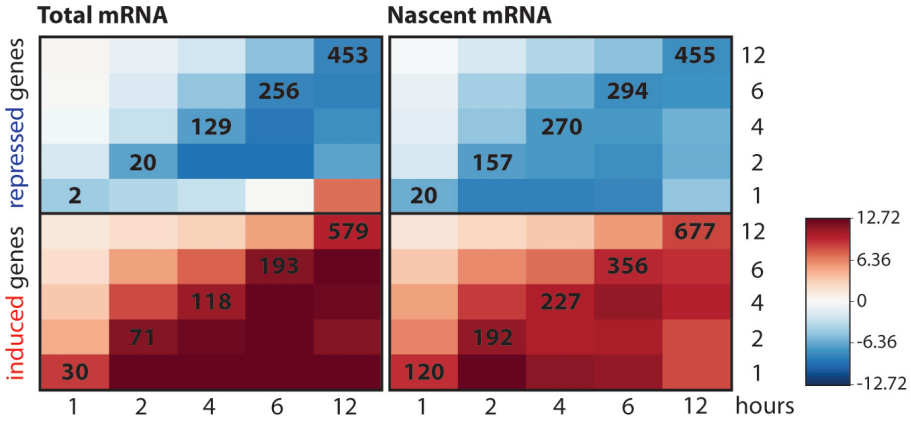

Figure 10: Ecdysone induces major, progressively increasing and mostly sustained changes in gene expression. The heat map is based on t-values, which are calculated with t-statistics and denote if the mean total (left) or nascent (right) mRNA expression value of a gene is significantly induced (red) or repressed (blue) by ecdysone treatment. Each row and column corresponds to one time point. All rectangles in one row represent mean t-values of the same group of genes, which were significantly differentially expressed at the indicated time point (number in bold), (fold change $>\log_2(1.5)$; Student´s t-test p-value < 0.01; two biological replicates). As one horizontally follows the progression of a gene group over time, darker color indicates that these genes become more significantly induced or repressed. Less significant induction or repression is indicated by lighter color. Color scale denotes the range of t-values. 95% of the data is shown.

the signal to induce both rapid and long-term expression changes in a wide array of functionally diverse genes [89]. Our time series DTA data reflects this architecture. The number of induced and repressed genes progressively increases from early to late time points (Figure 10; numbers in bold) and represent a major proportion of the expressed genes (28%, data not shown). Moreover, changes in gene expression observed at one time point are mostly sustained over the entire time series (Figure 10).
One drawback of our analysis is that we applied a stringent cutoff to define differential fold changes. Thereby, we neglect all genes that show only minor but consistent changes. To identify these genes we additionally used the Bayesian algorithm for Estimation of Temporal Regulation (*betr*) [7]. *betr* identified 110 and 147 additional genes in nascent and total mRNA, respectively (Supplementary Table 1). These genes are included in the subsequent data analysis.

7.5 Functional annotation of ecdysone regulated genes explains observed phenotypic changes

From our phenotypic analysis we know that after one day of ecdysone treatment S2 cells start to cease proliferation and subsequently undergo major morphological changes (Figure 6; Section 7.1). Given that ecdysone induces major changes in the transcriptome within the first 12 hours (Section 7.4), we wondered if these early changes already comprise genes that might affect the later phenotype. Therefore, we tested induced and repressed genes for enrichment in functional annotation terms of "Biological Process", "Cellular Component" and "Molecular Function" based on Gene Ontology [9] using *topGO* [1] (Methods Section 6.3.13.1) and the Cytoscape plugin ClueGO (Methods Section 6.3.13.2). The latter allows for both GO and KEGG [103] term enrichment analysis and visualization [24]. Functional annotation of the differentially regulated genes explains the ecdysonse induced progression of S2 cells from the proliferative to the differentiated state very well (Supplementary Tables 2 and 3).
As expected, induced genes are enriched for terms related to ecdysone signaling, e.g. "steroid hormone receptor activity" or "steroid hormone mediated signaling pathway". The genes in these categories

include key regulators of the early ecdysone cascade (EcR, br, Hr39, Eip74EF and Eip75B). Notably, many enriched terms are related to cell death, e.g. "ecdysone-mediated induction of salivary gland cell autophagic cell death". However, our phenotypic analysis demonstrates that ecdysone does not induce cell death in S2 cells (Section 7.1). Furthermore, the key cell death regulators, reaper, grim and hid are not induced or even expressed. Hence, the GO term enrichment of cell death terms is mainly due to the well-established general function of ecdysone regulated genes in cell death pathways during *Drosophila* development [99, 32, 124, 40] and therefore, equivalent to activation of ecdysone signaling.

The decline in proliferation rate is the first phenotypic change we observe upon ecdysone treatment and due to a cell cycle arrest in the G2/M phase (Figure 6; Section 7.1). This cell cycle arrest is reflected by repressed genes, which are enriched for multiple GO annotation terms related to DNA replication, cell cycle and proliferation (Figure 11), e.g "DNA replication initiation", "mitotic spindle organization" and "centrosome separation". Strikingly, the GO analysis of repressed genes also reveals a strong enrichment for multiple terms related to energy and biomolecule production, suggesting a metabolic rearrangement as the cell leaves the proliferating state to enter a resting, differentiated state, e.g. "Glycolysis", "Citrate cycle" or "Cellular amino acid metabolic process" (Figure 12). The late observed extensive remodeling of cell size and shape (Figure 6; Section 7.1) is reflected by induced genes, which are enriched for multiple terms related to morphogenesis and differentiation terms (Figure 13). Furthermore, most significantly enriched "Cellular Component" terms are "Plasma membrane" and "Cytoskeleton".

The great variety of enriched functional annotation terms demonstrates how rapid the ecdysone cascade regulates a wide range of functionally diverse genes. Moreover, within this early time interval (1-12 hours) ecdysone regulates not only the regulatory key players of the ecdysone cascade, but also genes that presage phenotypic changes observed much later.

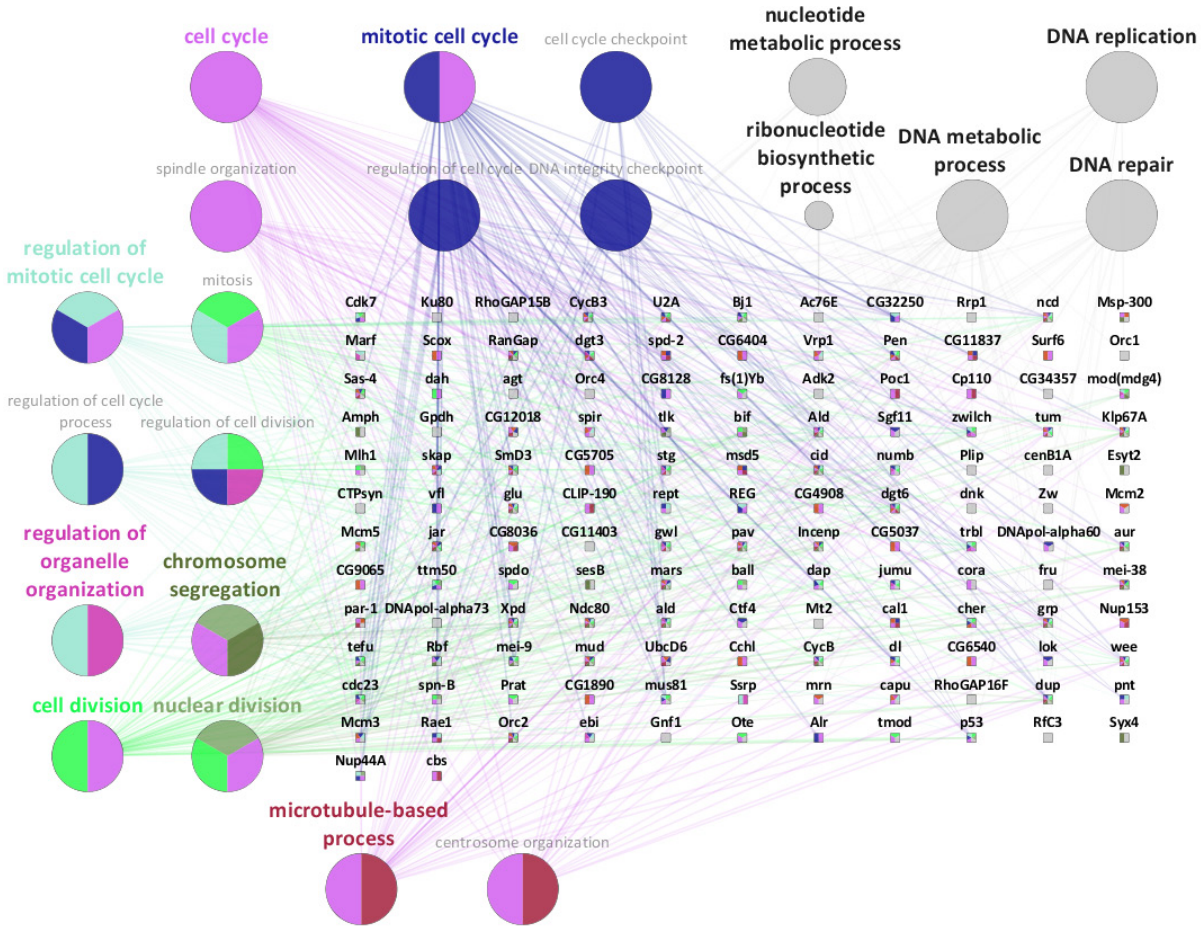

Figure 11: Ecdysone represses genes involved in cell cycle, mitosis and DNA replication. Network of GO terms "Biological Process" and their corresponding genes was created using the ClueGO plugin for Cytoscape [24]. All repressed genes were tested for functional enrichment as described in Methods Section 6.3.13.2. Significantly enriched GO terms had to contain >6 genes and associated genes had to represent >8% of all genes of that term. Terms were combined to a GO group, if they overlapped in >50% of their genes. For visualization the most representative cell cycle related terms were chosen. GO terms are shown as circles and genes as squares. Circle color indicates GO terms that compose a GO group, for which the most significant term is printed in color. Grey color represents ungrouped GO terms. Square color denotes the GO group a gene belongs to. Circle size corresponds to significance (Two-sided Hypergeometric test; Bonferroni correction, p-value <0.05). Larger diameter indicates smaller p-value. All terms are listed in Supplementary Table 3.

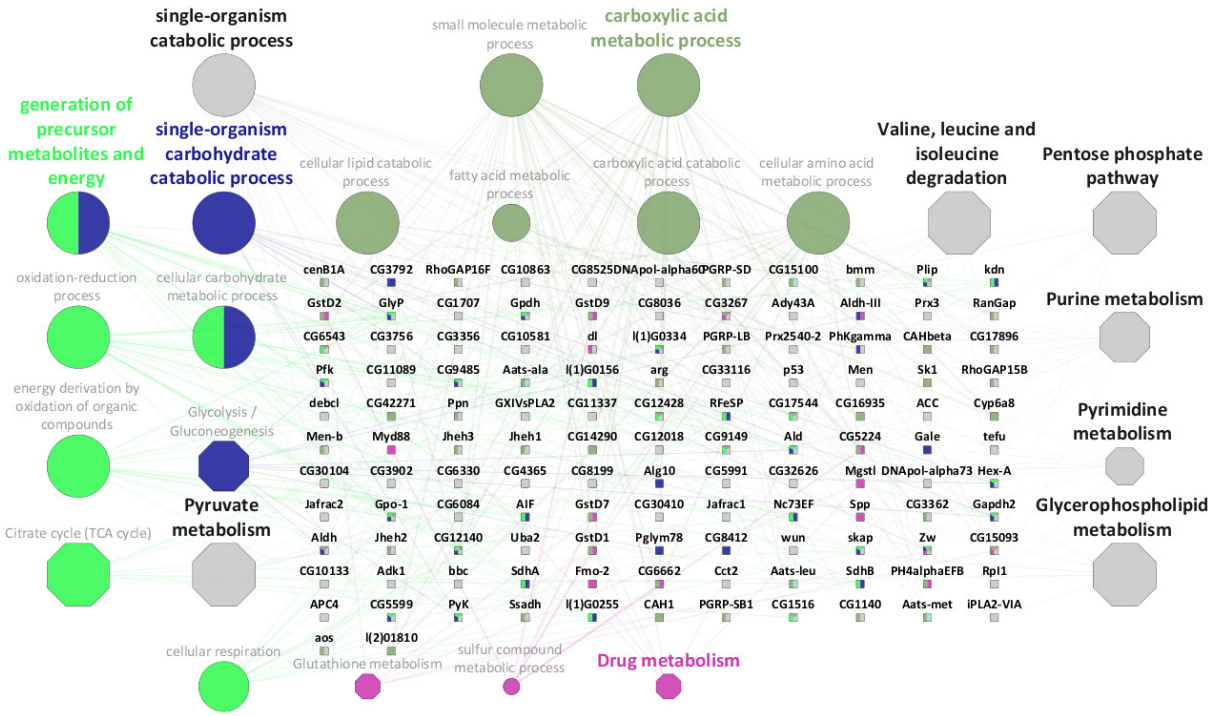

Figure 12: Ecdysone affects energy and biomolecule production. All repressed genes were tested for functional enrichment as described in Methods Section 6.3.13.2. Legend as in Figure 11, but KEGG terms (octagons) were included and the most representative terms related to metabolism are visualized. All terms are listed in Supplementary Table 3.

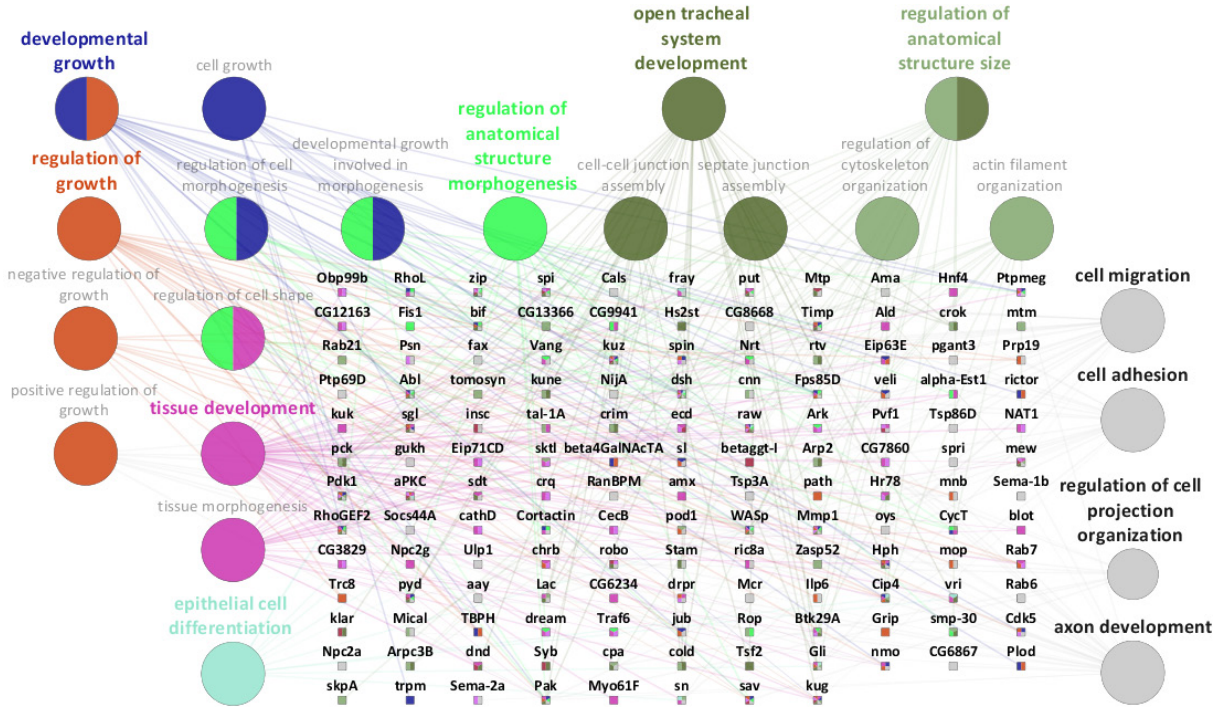

Figure 13: Ecdysone induces genes involved in morphogenesis and differentiation. All induced genes were tested for functional enrichment as described in Methods Section 6.3.13.2. Legend as in Figure 11, except the most representative terms related to morphogenesis and differentiation are visualized. All terms are listed in Supplementary Table 3.

7.6 First global assessment of ecdysone regulated synthesis and decay rates suggests different regulatory principles

Next, we used the measured nascent and total mRNA expression level to estimate relative mRNA synthesis and decay rates (Methods Section 6.3.11). Our study represents the first global assessment of synthesis and decay regulation by ecdysone signaling. Ecdysone regulates synthesis and decay rates of a large fraction of genes, 1322 and 1033, respectively (fold change >1.5, p-value <0.01). Although the number of genes with regulated synthesis and decay rates is similar, we find distinct characteristics in their regulation. For the synthesis rates the number of genes with increased and decreased rates progressively increases over time (Figure 14a). Moreover, the genes exhibit a mostly sustained change over multiple time points, similar to nascent mRNA (compare Figure 14a and Figure 10). In contrast, as suggested by the less sustained progression of mean t-values, decay rates are controlled in a temporally more restricted fashion (Figure 14a).
Besides these kinetic differences, genes with altered synthesis and decay rates differ in their biological annotation. Although for both rates the total number of differential genes is similar, genes with regulated synthesis rates show more enriched functional annotation terms compared to genes with regulated decay rates (66% more; Methods Section 6.3.13.2; Supplemental Table 4). Similar to the differential genes of nascent mRNA, genes with increased synthesis rates are enriched in terms related to development and morphogenesis, while genes with decreased synthesis rates reflect metabolic or cell cycle related processes (Figure 14b). The few terms that are enriched in genes with increased and decreased decay rates are in either case involved in regulation of metabolic processes (Figure 14c). Generally, these analyses suggest that synthesis and decay rate regulation by ecdysone is governed by different principles.

Figure 14 ***(facing page)*****:** First global assessment of ecdysone regulated synthesis and decay rates suggests different regulatory principles. (a) Changes in synthesis and decay rates differ in their continuity. Heat map is based on t-values, which are calculated in the t-statistics and denote if the mean synthesis (left) or decay (right) rate of a gene is significantly increased (red) or decreased (blue) by ecdysone treatment. Each row and column corresponds to one time point. All rectangles in one row represent mean t-values of the same group of genes, which exhibited significantly differential rates at the indicated time point (number in bold),(fold change log2(1.5); Student's t-test p-value < 0.01; two biological replicates). As one horizontally follows the progression of a gene group over time, darker color indicates that these rates become more significantly increased or decreased. Less significant increase or decrease is indicated by lighter color. 95% of the data is shown. Color scale denotes the range of t-values. (b) Genes with altered synthesis rate are enriched in the same categories as differential genes in nascent mRNA. Pie diagrams represent all GO groups and terms enriched in genes with increased (left) and decreased (right) synthesis rates (Methods Section 6.3.13.2). Colored pie sections represent GO groups, which are named by the most significantly enriched term. Pie section size correlates with the number of terms included in the GO group. Grey sections represent ungrouped terms or KEGG terms. (c) Genes with altered decay rate are enriched in few GO term groups. Histogram presents the enriched terms, the number of associated genes and the percentage that these genes represent compared to all genes associated with the term. Enriched terms that did not group are not shown. Complete lists of enriched terms in Supplemental Table 4. (*) p-value <0.05, (**) p-value <0.01 (Two-sided Hypergeometric test; Bonferroni correction).

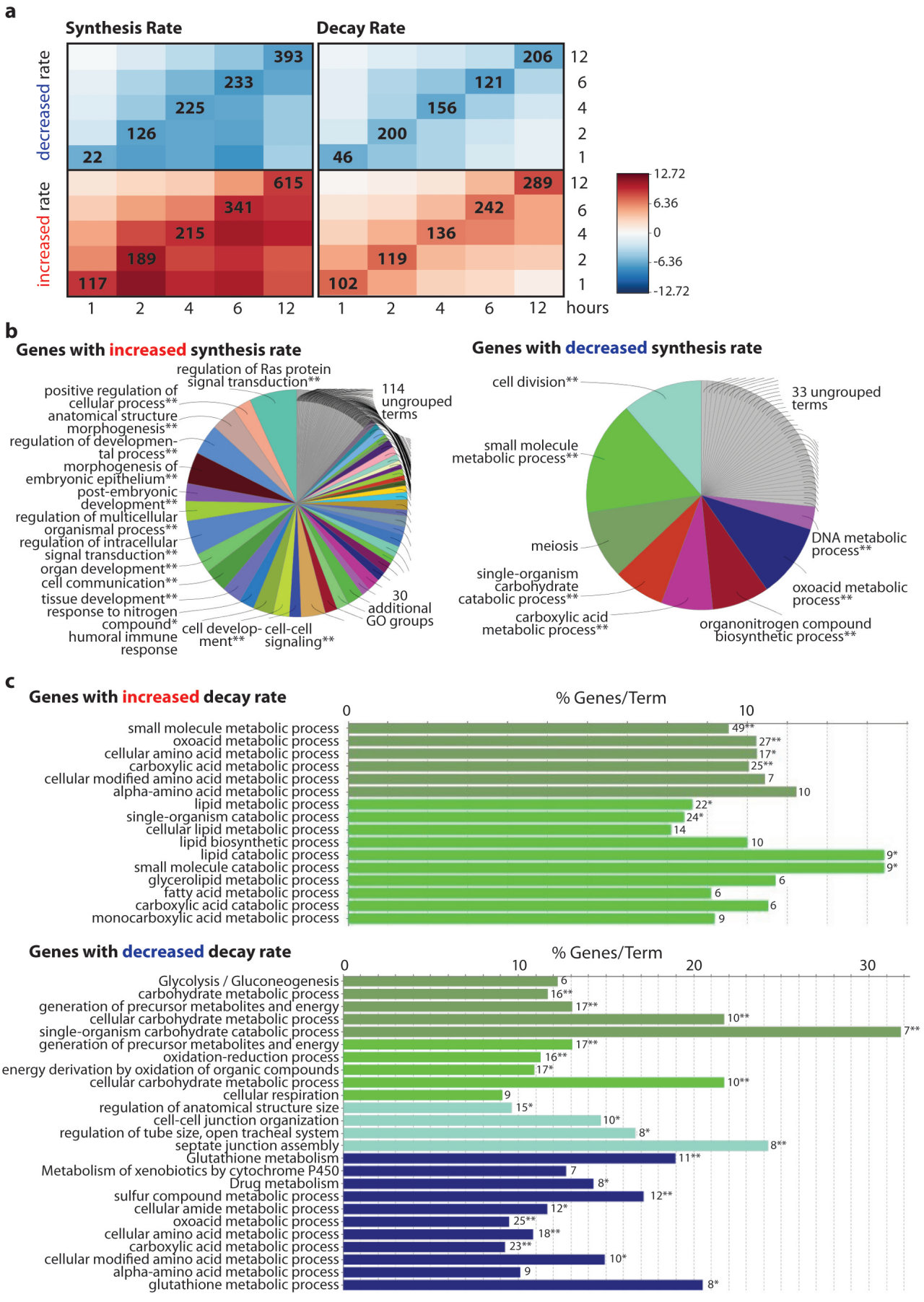
a
Synthesis Rate
Decay Rate
decreased rate
increased rate
393
233
225
126
22
206
121
156
200
46
615
341
215
189
117
289
242
136
119
102
12
6
4
2
1
12.72
6.36
0
-6.36
-12.72
1 2 4 6 12 1 2 4 6 12 hours
b
Genes with increased synthesis rate
regulation of Ras protein signal transduction**
positive regulation of cellular process**
anatomical structure morphogenesis**
regulation of developmental process**
morphogenesis of embryonic epithelium**
post-embryonic development**
regulation of multicellular organismal process**
regulation of intracellular signal transduction**
organ development**
cell communication**
tissue development**
response to nitrogen compound*
humoral immune response
cell development**
cell-cell signaling**
30 additional GO groups
114 ungrouped terms
Genes with decreased synthesis rate
cell division**
small molecule metabolic process**
meiosis
single-organism carbohydrate catabolic process**
carboxylic acid metabolic process**
organonitrogen compound biosynthetic process**
oxoacid metabolic process**
DNA metabolic process**
33 ungrouped terms
c
Genes with increased decay rate
% Genes/Term
0 10
small molecule metabolic process 49**
oxoacid metabolic process 27**
cellular amino acid metabolic process 17*
carboxylic acid metabolic process 25**
cellular modified amino acid metabolic process 7
alpha-amino acid metabolic process 10
lipid metabolic process 22*
single-organism catabolic process 24*
cellular lipid metabolic process 14
lipid biosynthetic process 10
lipid catabolic process 9*
small molecule catabolic process 9*
glycerolipid metabolic process 6
fatty acid metabolic process 6
carboxylic acid catabolic process 6
monocarboxylic acid metabolic process 9
Genes with decreased decay rate
% Genes/Term
0 10 20 30
Glycolysis / Gluconeogenesis 6
carbohydrate metabolic process 16**
generation of precursor metabolites and energy 17**
cellular carbohydrate metabolic process 10**
single-organism carbohydrate catabolic process 7**
generation of precursor metabolites and energy 17**
oxidation-reduction process 16**
energy derivation by oxidation of organic compounds 17*
cellular carbohydrate metabolic process 10**
cellular respiration 9
regulation of anatomical structure size 15*
cell-cell junction organization 10*
regulation of tube size, open tracheal system 8*
septate junction assembly 8**
Glutathione metabolism 11**
Metabolism of xenobiotics by cytochrome P450 7
Drug metabolism 8*
sulfur compound metabolic process 12**
cellular amide metabolic process 12*
oxoacid metabolic process 25**
cellular amino acid metabolic process 18**
carboxylic acid metabolic process 23**
cellular modified amino acid metabolic process 10*
alpha-amino acid metabolic process 9
glutathione metabolic process 8*

7.7 Ecdysone induces multiple distinct temporal patterns of transcription, decay rates and total expression level

The organization of the ecdysone cascade – early, early-late and late genes – suggests that some genes exhibit similar kinetics over time. Using a clustering approach on z-score normalized expression or rate values, we indeed identified groups of genes exhibiting such time-dependent patterns in nascent mRNA expression, total mRNA expression, synthesis rates and decay rates (Methods Section 6.3.14.1).

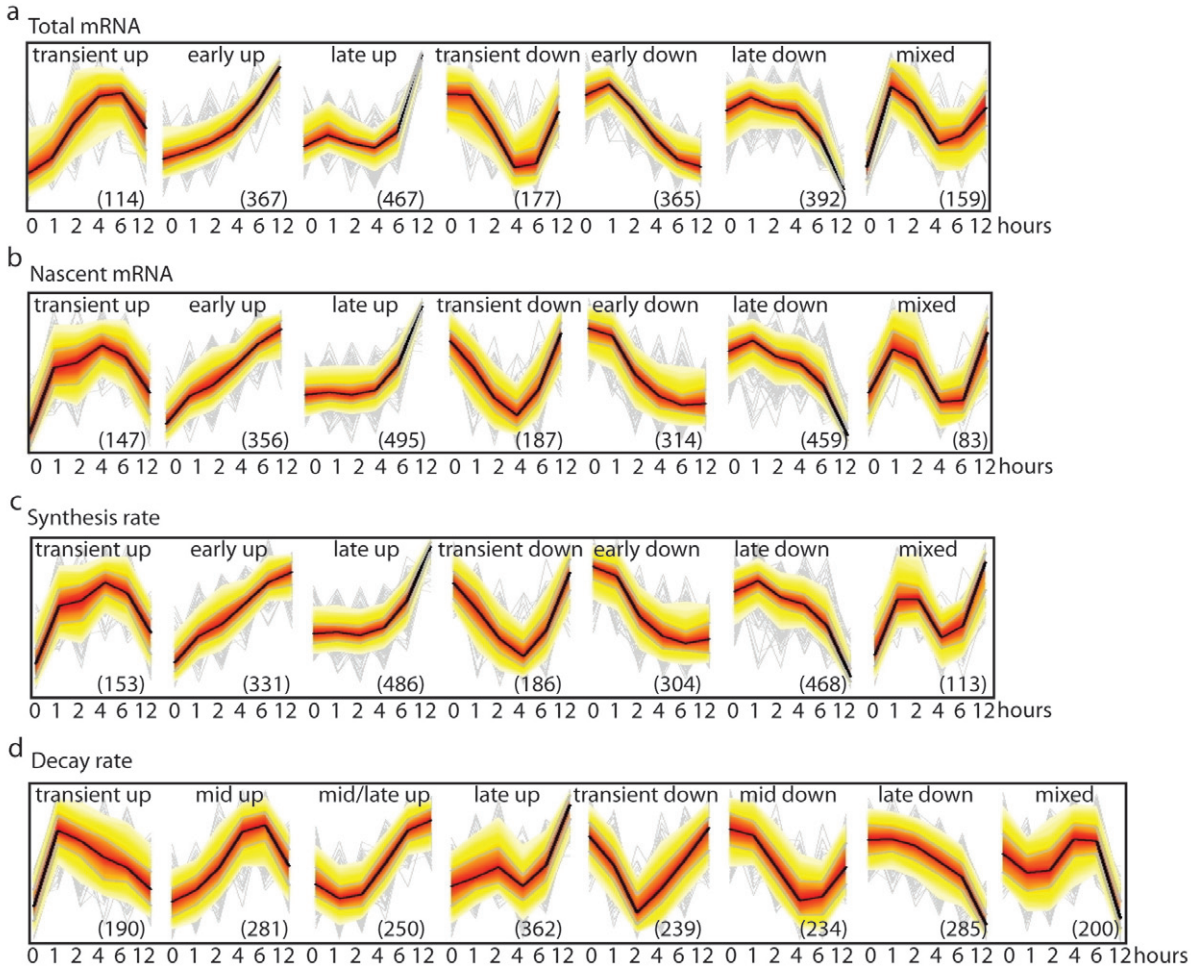

Figure 15: Ecdysone induces multiple distinct temporal patterns of transcription, decay rates and total expression level. Each panel presents a group of genes exhibiting a similar time-dependent pattern in (a) total mRNA, (b) nascent mRNA, (c) synthesis rate and (d) decay rate. Total and nascent mRNA expression values as well as estimated synthesis and decay rates of all differentially regulated genes were transformed to z-scores. Next, k-means clustering on z-scores was initiated on stable cluster centers using an optimized number of clusters (Methods Section 6.3.14.1). Number of genes in each cluster is indicated in the respective panel (bottom right). Individual cluster descriptions (top) are based on the kinetic pattern of the median z-score (black curve). Y-axis shows z-scores indicating the relative expression or rate. Colored shading represents the central 95% region; red denotes 50% of the data. Grey curves correspond to individual gene profiles.

The seven kinetics in the data sets of nascent and total mRNA expression as well as synthesis rates could be described by three induced, three repressed patterns and one showing a mixed progression over time (Figure 15a-c). Two of the induced kinetics are characterized by early induction, while one is transient and the other constant. The third pattern describes genes with later induction

(6-12 hours). The kinetics of repressed genes follow similar patterns: early but transient repression, early and constantly increasing repression and late repression. Notably, the kinetics of genes in nascent mRNA precede the kinetics of total mRNA (e.g. compare "transient down" clusters). The eight kinetics of genes with differential decay rates reflect the early transiently induced/repressed as well as the late induced/repressed patterns (Figure 15d). However, the middle time points are best described by four kinetics. This agrees well with the observed more dynamic regulation of decay rates (Section 7.6).
The functional GO/KEGG annotation enrichment analysis of each cluster does not assign specific annotations to individual clusters. Generally, clusters with induced patterns show enrichment of terms related to development and morphogenesis, while clusters with repressed patterns are involved in cell cycle and metabolism (data not shown). As the individual clusters are not enriched for specic biological processes, we wondered if we could further subdivide these cluster kinetics using a more complex clustering approach that reveals the kinetics of individual biological processes.

7.8 DTA reveals a rich and previously unknown diversity of gene expression dynamics downstream of ecdysone signaling and uncovers principles of transcriptional and post-transcriptional regulation

Upon ecdysone stimulation the gene expression dynamic of an ecdysone responsive gene is determined by the time dependent changes in mRNA synthesis and/or decay rate that lead to changes in the total expression level. Therefore, the most comprehensive approach to describe genome-wide gene expression dynamics is to simultaneously consider a gene's synthesis rate, decay rate and total expression level, and then identify all genes with similar gene expression dynamic.
To this end, we applied a more complex clustering approach that is able to find groups of genes based on similar time-dependent changes in all of those parameters (Methods Section 6.3.14.2). Specifically, we used k-means clustering to segregate differentially regulated genes in groups based on similar fold changes in (i) nascent mRNA expression (synthesis rate), (ii) total mRNA expression, (iii) decay rate and (iv) turnover. To include the time-dependency we used the z-score kinetics of genes in nascent mRNA expression, total mRNA expression and decay rates (Section 7.7) as additional parameters for the clustering. Since nascent mRNA expression and synthesis rate are rather equal in their information content (Pearson correlation of 1; data not shown), we used the measured nascent mRNA and not the estimated synthesis rate for the clustering. The parameter "turnover", defined as "synthesis rate x decay rate", was included, since it contains additional information content and is expected to be different for genes with similar synthesis or decay rates.
Combined clustering on these parameters separated all differentially regulated genes into twenty kinetically distinct groups. To visualize the kinetics of these gene groups, we plotted the fold change of individual genes in a cluster at each time point in a two dimensional space comparing nascent mRNA against total mRNA (Figure 16a) and decay rates against synthesis rates (Figure 16b). This visualization demonstrates a rich and previously unknown diversity of ecdysone induced gene expression dynamics. The temporal progression of changes in nascent and total mRNA expression demonstrates that immediately after ecdysone treatment the first genes start to exhibit differential expression, primarily in nascent mRNA (Figure 16a; Clusters 2, 3, 12 ,13). Over time and particularly after 12 hours, all clusters show changes in nascent and total mRNA emphasizing ecdysone's impact on the total transcriptome. When we compared decay and synthesis rates, we observed that more clusters start to diverge within the first two hours and that this divergence increased even more over time (Figure 16b).
To better understand the distinctiveness of the cluster kinetics, we calculated the mean expression or rate fold change at individual time points for each cluster. These mean fold changes then defined coordinates for a trajectory of each cluster (trajectory start: 1 hour; end: 12 hours; Figure 16c,d). Strikingly, each cluster is characterized by a unique combination of effect strength (fold change) and

type, i.e. increase or decrease in expression or rate. Furthermore, even if clusters exhibit similar increase or decrease in expression or rate, the timing for these changes is different (e.g. Figure 16c Clusters 3 and 9). Those unique combinations explain the distinctiveness in expression dynamics. For instance, the early and persistently strong expression fold changes in Cluster 12, in contrast to the strong, but late fold changes in Cluster 9, or the more transient increase in nascent mRNA in Cluster 2 (Figure 16c), (individual cluster trajectories in Supplementary Figure 1).

Importantly, our clustering approach uncovers principles of transcriptional and post-transcriptional regulation that govern these expression dynamics. First, we are able to discriminate, if a change in total expression level is due to changes in synthesis or decay rates. For instance, Clusters 17 and 20 exhibit both an increased total mRNA expression at 12 hours (Figure 16c, Figure 17a). However, the increased total mRNA expression in Cluster 17 is the result of combined effects of increased synthesis and decreased decay rates, while in Cluster 20 it is only due to increased synthesis rates (Figure 16d, Figure 17a). Similarly, the decreased total expression level of Cluster 7 is a result of increased decay rates only (Figure 16c,d).

Second, most clusters are characterized by a correlated (coupled) change in synthesis and decay rates, i.e. transcriptionally induced genes show increased decay rates and transcriptionally repressed genes show decreased decay rates. Ten of the twenty clusters exhibit a strong coupling of synthesis and decay rate (896 genes; e.g. Figure 16d Clusters 5 and 9), and six clusters show moderate coupling (642 genes, e.g. Figure 16d Clusters 3 and 11). In contrast, four clusters exhibit pronounced uncoupled progression (497 genes; e.g. Figure 16d Clusters 7 and 17). This result demonstrates that coupling of transcript synthesis and decay is a predominant regulatory principle of ecdysone induced expression kinetics. However, since we find uncoupled kinetics as well, the underlying coupling mechanisms seem to be complex and not of general nature.

Overall, our combined clustering approach of nascent transcription, total mRNA expression, decay rates and turnover reveals a rich and previously unknown diversity of ecdysone induced gene expression dynamics. All clusters are characterized by a unique combination of effect strength, type and timing, as well as extent of coupling between synthesis and decay rates (Figure 17b; Methods Section 6.3.15.1). Therefore, these kinetic clusters represent potentially co-regulated genes and describe how gene expression dynamics of subsets of genes are coordinated upon ecdysone stimulation.

Figure 16 ***(facing page)*****:** DTA reveals a rich diversity of gene expression dynamics downstream of ecdysone signaling and uncovers principles of transcriptional and post-transcriptional regulation. All differentially regulated genes (2141) were assigned by k-means clustering into twenty distinct groups (Methods Section 6.3.14.2). (a) Temporal progression of changes in nascent and total mRNA expression. Each diagram corresponds to one time point and compares the ecdysone induced log2 fold change for nascent (x-axis) and total (y-axis) mRNA expression. Each dot represents one gene, which is colored according to its affiliation with one of the twenty clusters. Ellipses show the 75% regions of highest density within each cluster, assuming Gaussian distribution. The inner horizontal and vertical gridlines indicate a linear two-fold, four-fold or eight-fold induction (red) or repression (blue). Cluster legend is given in the lower right. Number in brackets denotes the number of genes. (b)Temporal progression of changes in decay and synthesis rate. Diagrams as in (a), but log2 fold changes for decay (x-axis) and synthesis (y-axis)rate are shown. For (c) and (d) fold changes of genes in a cluster were averaged (mean) at each time point to delineate a trajectory for each cluster. Each dot along the trajectory represents the mean fold change at one time point (1 hour to trajectory end at 12 hours). Color code as above. (c) Cluster kinetics for nascent and total mRNA. (d) Cluster kinetics for decay and synthesis rate. Individual cluster trajectories are given in Supplementary Figure 1.

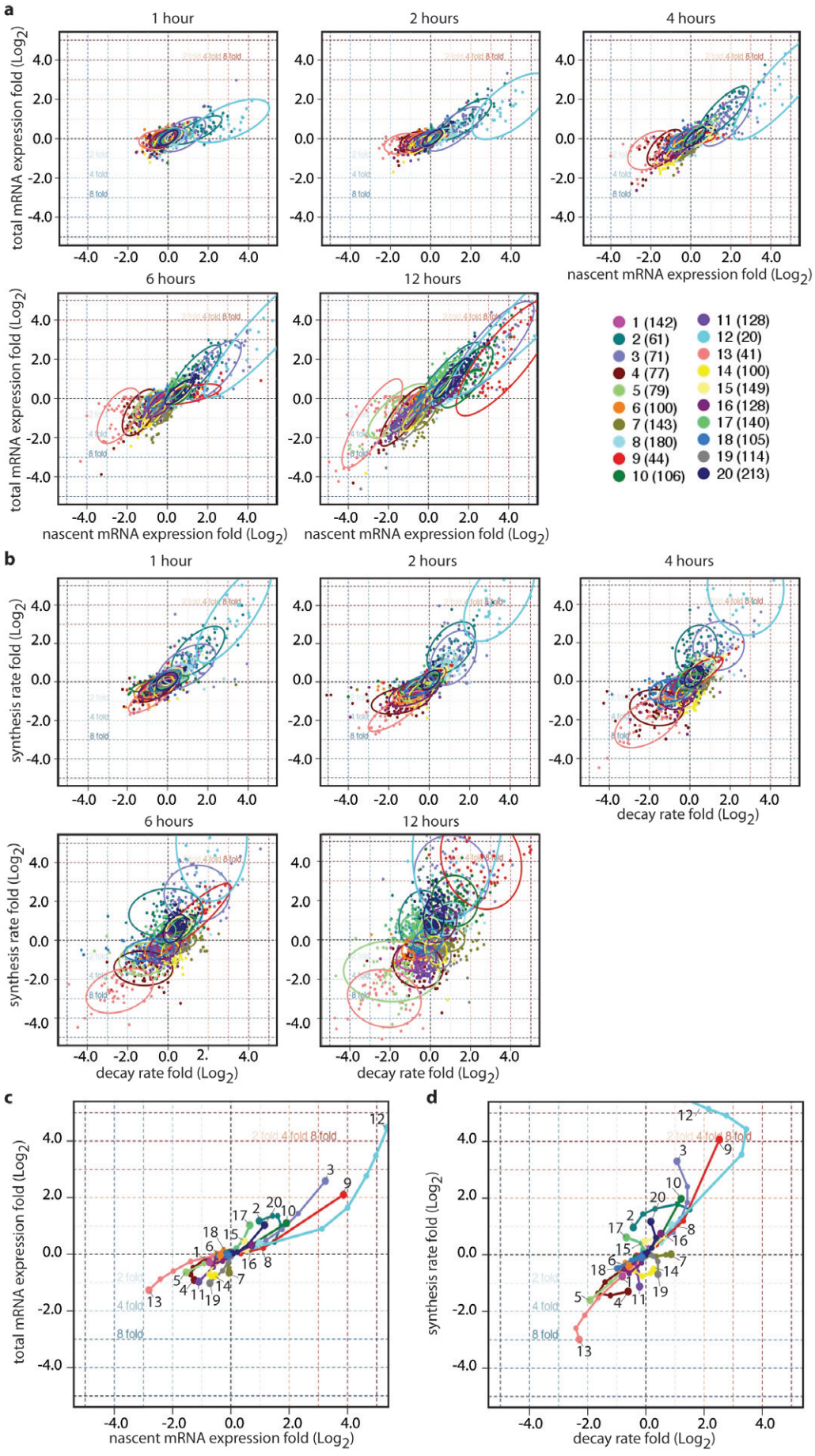
a
1 hour
2 hours
4 hours
6 hours
12 hours
total mRNA expression fold (Log2)
nascent mRNA expression fold (Log2)
2 fold
4 fold
8 fold
1 (142)
2 (61)
3 (71)
4 (77)
5 (79)
6 (100)
7 (143)
8 (180)
9 (44)
10 (106)
11 (128)
12 (20)
13 (41)
14 (100)
15 (149)
16 (128)
17 (140)
18 (105)
19 (114)
20 (213)
b
synthesis rate fold (Log2)
decay rate fold (Log2)
c
d

7.9 Ecdysone regulates genes with specific biological functions in a defined temporal order

We have shown that the functional GO/KEGG annotation of genes with induced and repressed expression levels explains the ecdysone induced phenotypic changes very well (Section 7.5). Having dissected the ecdysone induced gene expression dynamics into multiple distinct kinetics of potentially co-regulated genes, we asked now whether we could assign specific biological annotations to the individual gene clusters (Methods Section 6.3.15.3). While we could not find cluster specific functional enrichment upon separate k-means clustering of nascent mRNA expression/synthesis rate, total mRNA expression or decay rate (Section 7.7), the clusters of the combined clustering are characterized by specific functional enrichment patterns. Eighteen out of twenty clusters show significantly enriched terms (Figure 17b, Supplementary Table 5). These enriched terms can be classified into six generic categories: response to ecdysone, gene expression, signaling, metabolism, cell cycle and differentiation/morphogenesis (Table 1).

The comparison of a cluster's functional enrichment terms with its timing of gene expression changes reveals insights into the temporal order, in which the biological processes are regulated (Figure 17b). Strikingly, this temporal order reflects the timing of the observed phenotypic changes (Figure 6). Clusters characterized by early, strong and sustained induction of gene expression are enriched for the category "response to ecdysone". Clusters with middle and late timing of gene expression induction or repression are enriched for the category "signaling" and "gene expression". The category "signaling" comprises multiple signaling pathways, which are important for regulation of metabolism, cell cycle and development (Table 12). The category "gene expression" comprises rather heterogeneous terms from early to late steps of gene expression. Clusters with mostly middle to late timing of repressed gene expression are involved in diverse metabolic and cell cycle related processes. Interestingly, metabolic changes slightly precede cell cycle related changes. Finally, genes involved in differentiation and morphogenesis are predominantly found in clusters showing late changes in gene expression. Despite some overlap in timing, the temporal order of the functional annotation terms, which are related to the observed phenotype (exit from the cell cycle to enter differentiation), is: "ecdysone signaling" - "metabolism" - "cell cycle" - "differentiation/morphogenesis".

To validate our functional enrichment analysis we used random sampling (Methods Section 6.3.15.3). Except for "ubiquitin mediated proteolysis" and "mitotic cell cycle", which occurred six out of fifty times, none of the other terms was enriched more than five times. The low reoccurrence of specific terms emphasizes the reliability of the functional annotation. Moreover, we repeated the functional annotation using a different enrichment algorithm (*topGO* [1]) and obtained identical results (data not shown).

Taken together, the functional annotation of the clusters of co-regulated genes is unique, reliable and in agreement with the ecdysone induced phenotypic changes. Our analysis reveals the timing and strength at which ecdysone signaling regulates these cellular processes. Therefore, the distinct gene expression kinetics describe how ecdysone signaling directs the cell from a proliferating state into a differentiated state. The question arising from these results is: What are the transcriptional and post-transcriptional regulatory mechanisms that underlie these gene expression kinetics?

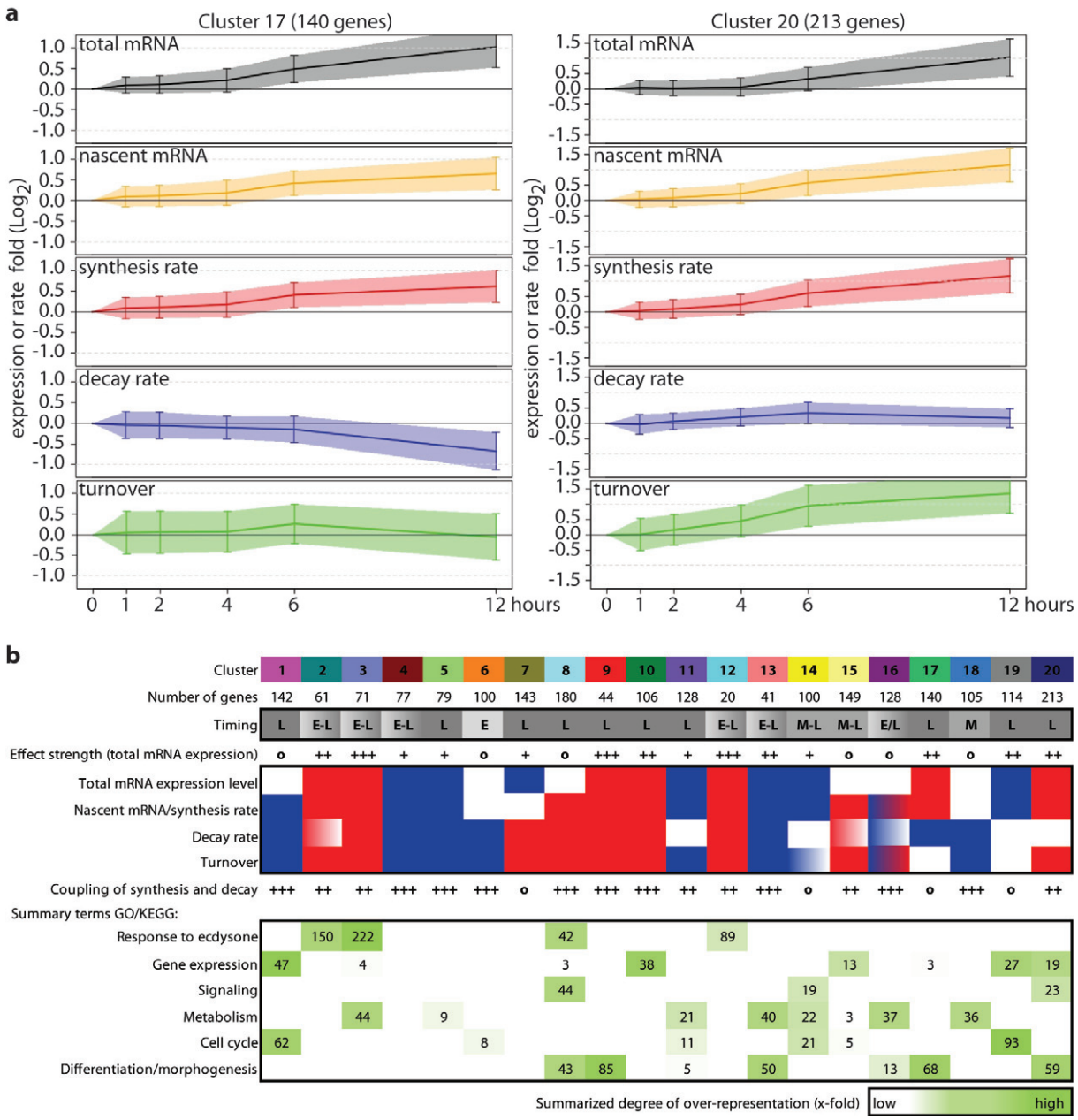

Figure 17: Groups of potentially co-regulated genes are characterized by individual kinetic features and functional annotation. (a) Time course progression of $\log_2$ fold change (y-axis) in total mRNA (grey), nascent mRNA (yellow), synthesis rate (red), decay rate (blue) and turnover (green). Solid line represents mean fold change and shading between error bars the standard deviation. Cluster 17 (left panels) and Cluster 20 (right panels) are representatively shown. All clusters in Supplementary Figure 2. (b) Each cluster is characterized by a specific combination of kinetic features and functional annotation. Catalogue of features was compiled based on mean fold change progression of measured and estimated values (Methods Section 6.3.15.1). Timing was classified as being early (E), middle (M), middle to late (M-L), late (L) and early to late (E-L), based on nascent or total mRNA expression. Effect strength was defined as the maximum mean fold change on total mRNA level: <1.5-fold (o), >1.5-fold (+), >2-fold (++) or >4-fold (+++). Increase (red) or decrease (blue) of gene expression or rate was discretized based on mean fold changes. White denotes mean fold change <1.5-fold. Coupling of synthesis and decay rates was assessed by Pearson correlation of mean fold changes: strong +++ (r >0.75), moderate ++ (r >0.50), poor + (r >0.25) and no coupling o (r <0.25). Functional enrichment for GO "Biological Process" and KEGG terms was calculated using Fisher's exact test (p-value <0.01; Methods Section 6.3.15.3). Enriched terms were manually classified in six generic categories and represented by the summarized degree of over-representation (number of expected genes in a term compared to number of observed genes). Individual terms are listed in Table 12 and Supplementary Figure 3.

Ecdysone response	**Gene expression**	**Signaling**
response to ecdysone	Basal transcription factors*	signal transduction
ecdysone-mediated induction of salivary gland autophagic cell death	regulation of transcription, DNA dependent	protein dephosphorylation
salivary gland histolysis	chromatin remodeling	protein phosphorylation
salivary gland cell autophagic cell death	regulation of chromatin silencing	mTOR signaling pathway*
autophagic cell death	mRNA processing	insulin receptor signaling pathway
autophagy	rRNA processing	Jak-STAT signaling pathway*
activation of caspase activity	ribosome biogenesis	p53 signaling pathway*
larval central nervous system remodeling	Ribosome*	JNK signaling pathway*
molting cycle, chitin-based cuticle	Ubiquitin mediated proteolysis*	ErbB signaling pathway*
ecdysis, chitin-based cuticle	protein ubiquitination	MAPK signaling pathway*
		Wnt signaling pathway*
Metabolism	**Cell cycle**	**Differentiation/Morphogenesis**
response to starvation	Cell cycle*	regulation of developmental process
Glycolysis / Gluconeogenesis*	cell cycle phase	metamorphosis
glycolysis	chromosome condensation	central nervous system development
Citrate cycle (TCA cycle)*	M phase	multicellular organismal development
Glycerolipid metabolism*	mitotic spindle organization	tissue development
glycerol-3-phosphate metabolic process	mitotic cell cycle	tissue morphogenesis
lipid storage	Purine metabolism*	regulation of cell shape
mitochondrion organization	Base excision repair*	cell adhesion
Oxidative phosphorylation*	Nucleotide excision repair*	establishment or maintenance of cell polarity
	DNA replication	actin filament organization
	DNA-dependent DNA replication	actin cable formation
	DNA-dependent DNA replication initiation	regulation of tube size/length, open tracheal system
	Nicotinate and nicotinamide metabolism*	synaptic vesicle docking involved in exocytosis
		axon guidance
		neurotransmitter secretion
		cell projection organization
		vesicle-mediated transport
		septate junction assembly
		Tight junction*

Table 12: Individual functional enrichment terms of the twenty kinetically distinct gene groups. Functional enrichment for GO "Biological Process" and KEGG terms (*) was calculated using Fisher's exact test (p-value <0.01; Methods Section 6.3.15.3). Table lists the individually significantly enriched terms, which were manually classified into six generic categories (bold).

7.10 Establishing miRNA profiling in ecdysone treated S2 cells

To date, the role of post-transcriptional regulation in ecdysone signaling has not been examined. Since we generated, for the first time, genome-wide estimations of ecdysone regulated decay rates (Section 7.6), we now can ask questions about the underlying regulatory mechanisms. We decided to quantify the most accessible mechanistic regulator of mRNA decay, namely miRNAs. Specifically, we sought to identify ecdysone regulated miRNAs and investigate their role in the ecdysone response as a whole and in particular in the early time interval of the ecdysone response.
Before we addressed these questions genome-wide, we determined the time scale on which ecdysone regulates miRNAs in S2 cells, using two known ecdysone responsive miRNAs let-7 [176, 37] and miR-

8 [95, 100]. We treated S2 cells with 10 µM ecdysone for 1-72 hours, quantified let-7 using Northern blotting and pri-mir-8, as well as miR-8 expression using RT-PCT (Methods Sections 6.4.1 - 6.4.3). For both miRNAs we can reproduce the published regulation and timing of regulation. let-7 is induced after 24 hours (Figure 18a) and pri-mir-8, as well as miR-8 are progressively repressed from 4 hours onwards (Figure 18b).
These results show that S2 cells are a good *in vitro* model for studying ecdysone regulated miRNAs. Given the rather late regulation of let-7 and miR-8, we decided to profile the first 12 hours to complement our DTA analysis, but to extend the time series up to 72 hours to identify ecdysone regulated miRNAs in general.

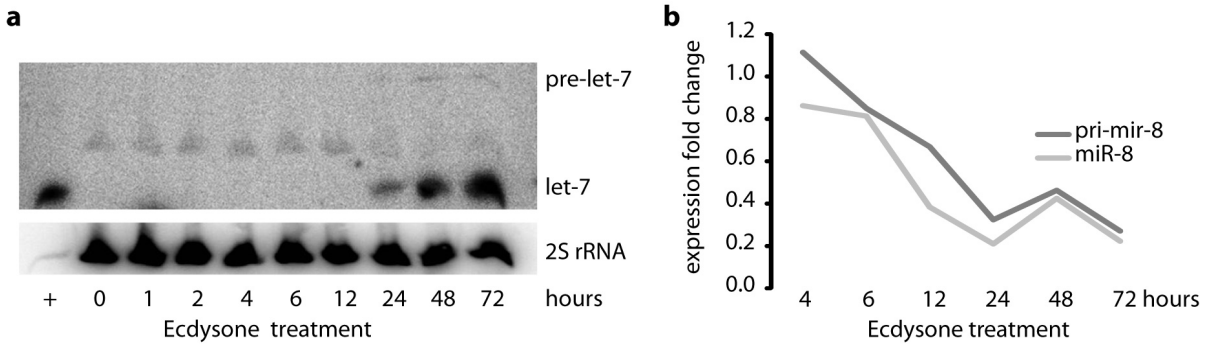

Figure 18: Establishing miRNA profiling in ecdysone treated S2 cells. (a) let-7 expression is induced by ecdysone treatment. S2 cells were treated with 10 µM ecdysone for 1-72 hours or left untreated. Cells were harvested at indicated time points and total RNA was used for Northern blotting (Methods Section 6.4.2). A let-7 DNA oligo was used as positive control (+) and 30 nt long 2S rRNA served as loading control. (b) pri-mir-8 and mature miR-8 expression are progressively repressed by ecdysone treatment. Depicted is the normalized fold change in miRNA expression as analyzed by RT-PCR (Methods Section 6.4.3). pri-mir-8 and miR-8 levels were normalized against housekeeping genes CG30159 and rp49, respectively.

7.11 nCounter expression profiling identifies known and novel ecdysone regulated miRNAs

Recently, a new analysis platform for medium-throughput mRNA and miRNA expression profiling has been introduced, the nanoString nCounter Expression System [69]. The system uses molecular "barcodes" and single molecule imaging. It provides a large dynamic range and offers significantly higher levels of precision and sensitivity compared to microarray gene expression profiling [119]. Using a candidate mRNA pilot screen, we confirmed the reproducibility and sensitivity of the system (data not shown) and then applied it to profile the expression of 184 miRNAs during ecdysone treatment (Methods Section 6.4.4).
Two biological replicates of S2 cells were treated with 10 µM ecdysone for 2-72 hours (Figure 6) and purified total RNA was sent to nCounter expression analysis (Methods Section 6.4.4). A total of 82 miRNAs are expressed in our S2 cells before or after ecdysone treatment (Methods Section 6.4.5). Of these, ecdysone differentially regulates 17 and 38 miRNAs in the time intervals 2-12 hours and 2-72 hours, respectively (Figure 19). Notably, within the early time course miRNAs are mostly repressed, while the late time course is dominated by progressive and pronounced induction of miRNAs. We evaluated the reliability of our data set by two approaches: (i) comparison to published miRNA expression S2 cell data and (ii) evaluation of known ecdysone regulated miRNAs.
First, we compared the 15 highest expressed miRNAs in resting S2 cells with smallRNA-Sequencing data generated in the modENCODE project [20]. Although we used our own S2 cell clone, which is different from the one used by modENCODE, the two data sets agree in more than 70% (considering only miRNAs queried by the nCounter assay; Supplementary Figure 4).

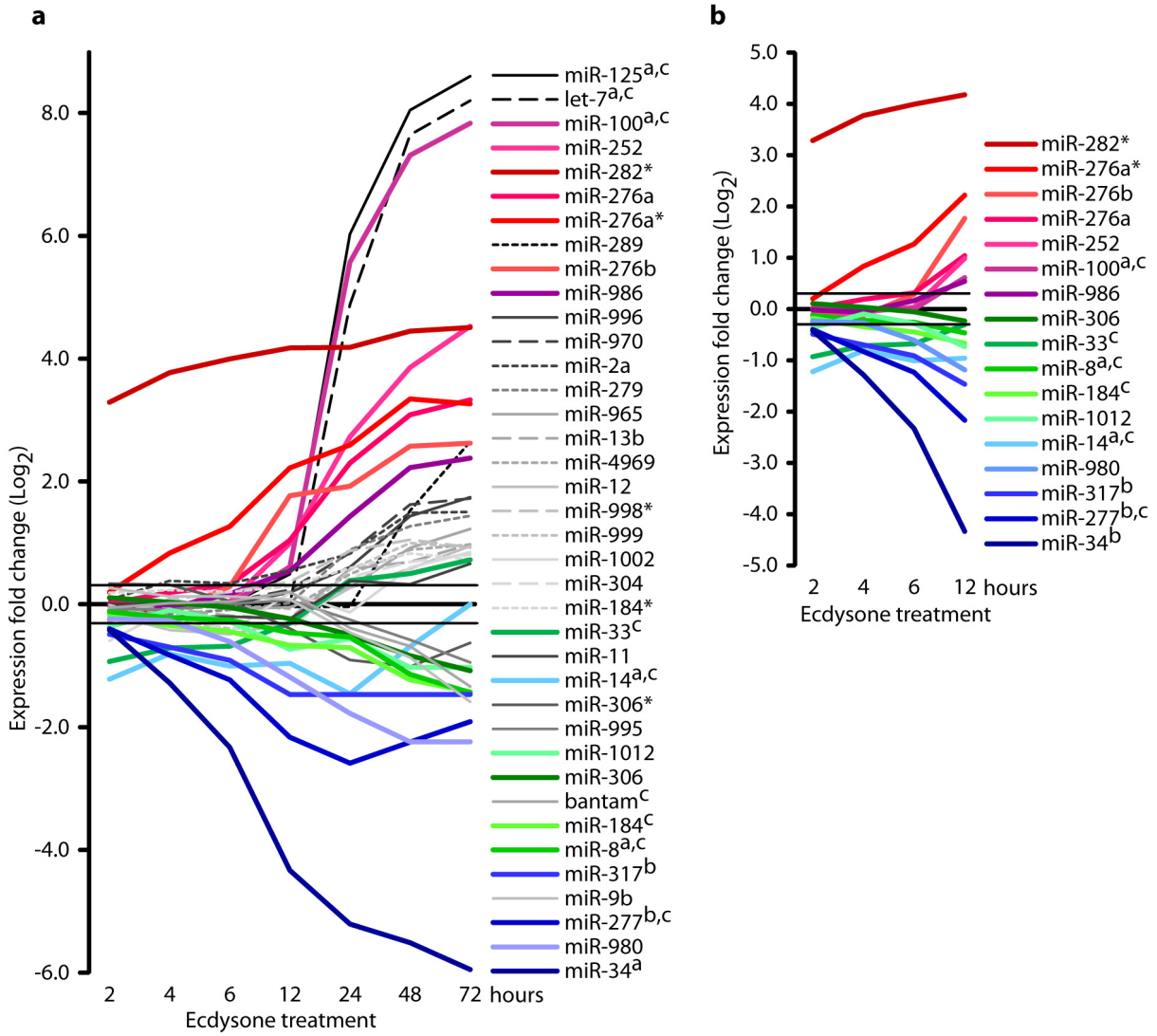

Figure 19: nCounter expression profiling identifies known and novel ecdysone regulated miRNAs. Expression of 184 miRNA was quantified using the nCounter® nanoString system (Methods Section 6.4.4). Significantly regulated miRNAs were identified using Bayesian Estimation of Temporal Regulation (*betr*) (Score >0.99), combined with >1.2-fold change in expression compared to untreated control cells (Methods Section 6.4.5). (a) Ecdysone leads to rapid repression and progressive induction of miRNAs. Probability of differential expression was calculated for 2-72 hours. Diagram depicts the $\log_2$ expression fold change progression of significantly regulated miRNAs over time. Black horizontal lines illustrate $\log_2(1.2)$-fold difference. Order of miRNAs in the legend corresponds to their magnitude in fold change after 72 hours. miRNAs colored from red to blue were regulated in the first 12 hours (see Figure 19b). "^{a}" miRNA has established or "^{b}" potential relationship to ecdysone signaling. "^{c}" miRNA is implicated in the observed phenotypes, namely cell cycle, metabolism or differentiation/morphogenesis. (b) Candidate miRNAs for regulation of differentially expressed mRNAs during the early ecdysone response. Probability of differential miRNA expression was calculated for 2-12 hours. Induced miRNAs colored in red to violet, repressed in green to blue. References for "^{a,b,c}" [177, 193, 35, 95, 97, 102, 108, 194, 37, 42, 100, 130, 27, 58, 146, 159].

Next, we searched for known ecdysone regulated miRNAs in our data set (2-72 hours). As expected, let-7 is not expressed in untreated cells or within the first 12 hours of ecdysone treatment, but is strongly induced later on (Figure 19a). miR-100 and miR-125, which are processed from the same precursor as let-7 (Let-7-C) and are also known to be induced by ecdysone [177], accompany the let-7 induction in timing and strength. miR-14 and its validated target EcR compose a auto-regulatory feedback loop, in which miR-14 modulates EcR expression and EcR limits miR-14 expression [193]. Not surprisingly, miR-14's repression fluctuates around two-fold and recoveres to basal levels at 72 hours, which coincides with decreased EcR protein levels (Figures 19a, 8d). Finally, we also find miR-8 to be down-regulated (Figure 19a).
Thus, by treating S2 cells with ecdysone, we recovered all known ecdysone regulated miRNAs (Figure 19a "*a*"). In addition, we identified six miRNAs, which have a potential relation to ecdysone signaling (Figure 19a "*b*") or one of the phenotypic processes regulated by ecdysone, namely cell cycle, metabolism or differentiation/morphogenesis (Figure 19a "*c*"). All other ecdysone regulated miRNAs (26) have no established function in these processes or are even missing any functional characterization in *Drosophila*. Therefore, our dataset represents an excellent resource to reveal the function of these miRNAs in ecdysone signaling, proliferation, cell cycle, metabolism or differentiation/morphogenesis.

7.12 Potential roles of miRNAs in the ecdysone response of S2 cells

Our data set on miRNA expression demonstrates a great difference in the miRNA transcriptome of proliferating compared to differentiated cells. To evaluate potential roles of ecdysone regulated miRNAs in the ecdysone response we compared the miRNA expression dynamics (Figure 19a) with the temporal order of both the phenotypic changes (Figure 6) and functional annotations of the kinetic clusters (Figure 17b).
The earliest and strongest repressed miRNAs are miR-34, miR-277 and miR-317 (Figure 19b), which are encoded by the same genomic locus [102]. Given that the earliest functional annotation categories are "ecdysone signaling" and "metabolism" (Figure 6) and the earliest observed phenotype is the decline in proliferation rate (Figure 7a), these miRNAs might be important for these processes. This assumption finds support in the literature. miR-34 is known to regulate Eip74EF [130], one of the key regulators of the ecdysone cascade, miR-277 has a well-established role in metabolism [58] and miR-317 targets CycB [159], a crucial regulator of mitosis. The early and strong induction of the so far uncharacterized miR-282* and miR-276a* (Figure 19b) suggests a potential role of these miRNAs in the early biological processes as well. While the rather late kinetics of the induced miRNAs of the let-7 locus (Figure 19a) indicates a role in the later phenotypic changes related to cell cycle exit or differentiation. These miRNAs have been reported to be important for the appropriate stage specific morphologies during the larval-to-pupal transition and genetic elimination of let-7 and miR-125 leads to a delay in cell-cycle exit [35]. Based on the coinciding kinetics of miRNAs and ecdysone phenotypic changes as well as the known functions of some miRNAs, the differentially regulated miRNAs may be important for different aspects of the ecdysone response.
These correlations are corroborated by a preliminary validation experiment using RNAi mediated expression knockdown of Ago1. During the knockdown S2 cells cease proliferation, but recover after a few days and resume proliferation when RNAi knockdown efficiency has declined (data not shown). In contrast, ecdysone treated Ago1 knockdown cells do not resume proliferation, but exhibit decreased viability and undergo cell death. This result demonstrates the crucial role of miRNAs in the ecdysone response. The severe decrease in proliferation of untreated cells in Ago1 knockdown condition mimics the ecdysone induced stop in proliferation. Hence, the miRNAs that are repressed by ecdysone may indeed be essential for proliferation, and their repression crucial for the ecdysone induced stop in proliferation. Moreover, as S2 cells undergo cell death in Ago1 knockdown conditions, miRNAs might be crucial for the specification of the ecdysone response, namely differentiation or

cell death.

7.13 Novel decay rate-based approach for miRNA-mRNA network analysis

To investigate the role of miRNAs in the ecdysone response, we used computational network analysis to identify target genes of those miRNAs. Specifically, we sought to identify the role of miRNAs as regulators of the mRNA kinetics within the first 12 hours of the ecdysone response (Figure 6). To this end, we took advantage of the estimated mRNA decay rates and developed a novel approach for network analysis based on correlation of miRNA expression and mRNA decay rates.
miRNA-mRNA interaction networks are typically based on candidate lists of computationally predicted miRNA targets, which can be reduced to the most promising candidates by correlating miRNA and mRNA expression [150]. Most studies assume that changes in miRNA expression cause inverse changes in mRNA expression, i.e. increased miRNA expression leads to decreased mRNA expression due to miRNA mediated mRNA degradation (or decreased miRNA expression leads to increased mRNA expression). However, this "expression-based" approach evaluates the activity of miRNAs based on a composite effect, since changes of mRNA expression levels underlie the contribution of both mRNA synthesis and decay. Although miRNAs can directly impact the decay rate of their targets, it is unknown to which extent this particular increase or decrease in decay rate affects mRNA expression levels. Furthermore, we and others [144] found that differential mRNA expression levels strongly correlate with mRNA synthesis (Pearson correlation 0.9, data not shown) and not with mRNA decay rates (Pearson correlation -0.13, data not shown). Since most expression-based approaches demand the inverse correlation of miRNA and mRNA expression levels based on miRNA-mediated decay, they ignore the impact of mRNA synthesis on mRNA expression. Consequently, expression-based miRNA-mRNA networks may suffer from a high false-positive rate. To overcome this limitation, we established a novel approach to infer miRNA-mRNA networks using three sources of information, namely miRNA expression, mRNA decay rates and mRNA expression levels (Figure 20a). We first retrieved mRNA target predictions for the significantly regulated miRNAs of the early time course using the miRanda algorithm [22](Methods Section 6.4.6). The miRanda algorithm is a widely used and comprehensive target prediction algorithm. Importantly, it tolerates mismatches in the seed sequence and takes the binding energy of the miRNA-target duplex into account. Of the miRanda predicted targets we considered only targets which show significantly regulated decay rates at any time point within 2-12 hours (fold change >1.5, p-value <0.01; Methods Section 6.3.12).
To correlate miRNA expression kinetics to the mRNA decay rates, we used a simple, but strict matching criterion based on discrete time series patterns of miRNA expression and mRNA decay rate fold changes. Since we investigated a narrow time interval, we reasoned, if a miRNA regulates an mRNA the miRNA expression pattern correlates with the mRNA decay pattern over time, i.e. increased miRNA expression leads to increased mRNA decay rates (or decreased miRNA expression leads to decreased mRNA decay rates). In other words, we took advantage of information that was "encoded" in the expression/decay pattern over time. In addition, we allowed one time shift to account for both a probable time lag between miRNA expression and its effect on decay rates, as well as for lower sensitivity of microarray measurements compared to nCounter measurements [119]. Target interactions with correlated miRNA expression and mRNA decay were called "valid" interactions. Finally, we used mRNA expression data to filter for miRNA-mRNA interactions in which mRNA expression levels were significantly changed, i.e. "reliable" interactions (mRNA expression change >1.5-fold, p-value <0.01; Methods Section 6.3.12).
We called this approach "decay rate-based" network analysis (Figure 20a, Methods Section 6.4.7). The advantage of our novel decay rate-based approach as opposed to expression-based approaches is that mRNA decay rates represent a more direct readout of miRNA activity compared to mRNA expression levels which are a composite readout.

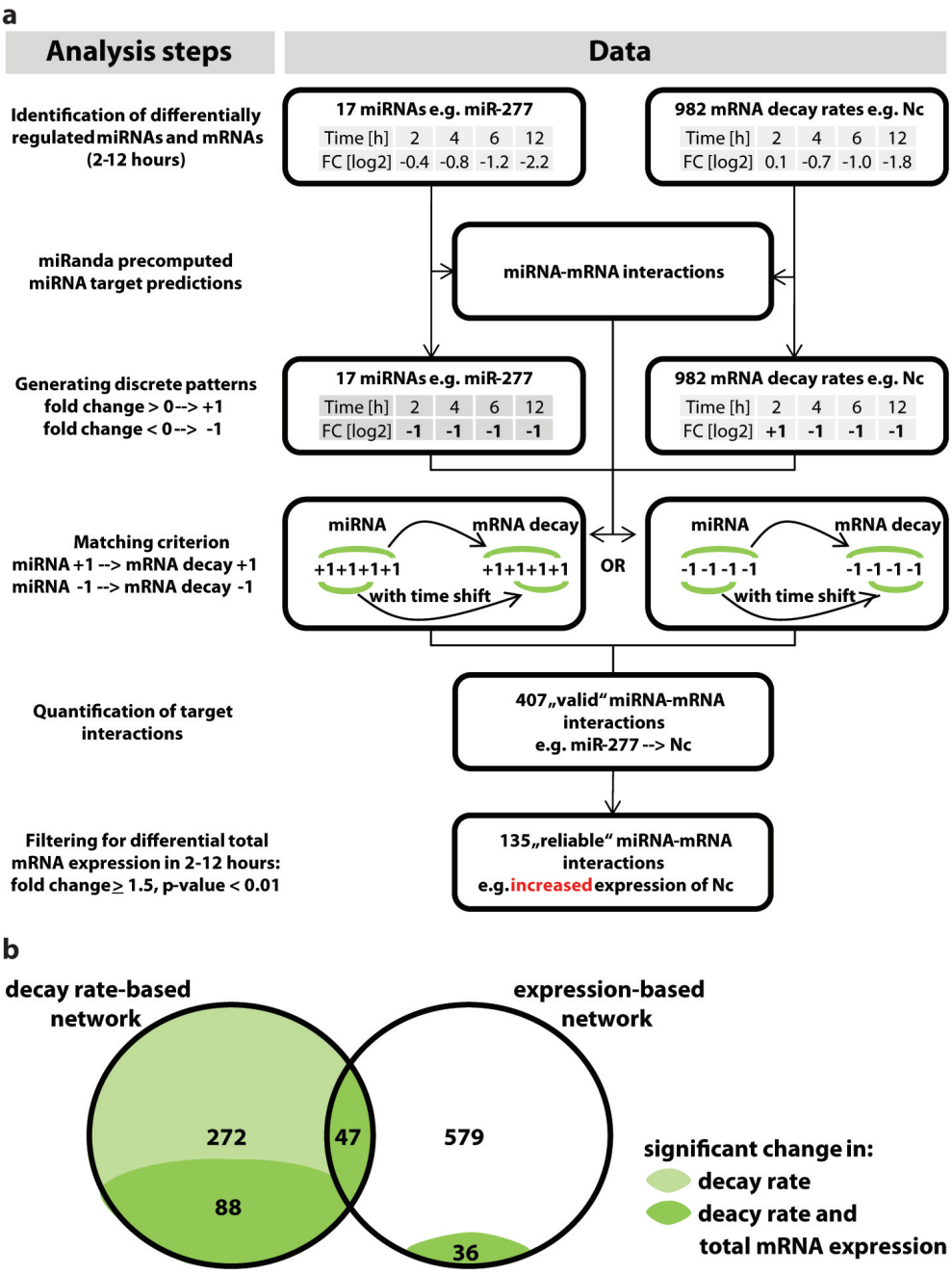

Figure 20: Novel decay rate-based approach for miRNA-mRNA network analysis. (a) Work flow for decay rate-based miRNA-mRNA network analysis. Figure illustrates analysis steps (left) and data (right) which was used or created within individual steps (Methods Section 6.4.7). In brief, significantly differentially regulated miRNAs and mRNAs within 2-12 hours are identified (fold change >1.5, p-value <0.01; Methods Section 6.3.12, 6.4.5). miRNA and mRNA interaction pairs were assigned using computational target predictions taken from miRanda [22]. Next, fold changes in expression or decay rate were discretized to 1 and -1 for positive and negative fold changes, respectively. Discrete fold change patterns of predicted miRNA-mRNA pairs are then match over the entire time course or shifted by one time point ("valid" interaction). "Valid" interactions are filtered for miRNA-mRNAs pairs, in which mRNAs show a significant change in total mRNA expression ("reliable" interaction, fold change >1.5, p-value <0.01). Network of "valid" and "reliable" interactions is shown in Supplementary Figure 5 and Figure 21, respectively. Exemplarily, target interaction of miR-277 and Dronc (Nc) is shown. (b) Number of target interactions in miRNA-mRNA networks. Networks were constructed by matching fold change patterns of miRNA expression to fold change patterns of mRNA decay rates (left) or expression (right). Sections colored in dark green illustrate interactions in which both the mRNA decay rate and the total expression level were significantly regulated. Light green illustrates interactions with only significant differential decay rates.

7.14 The miRNA-mRNA networks during the ecdysone response

The network analysis using our decay rate-based miRNA-mRNA matching approach identified 135 "reliable" interactions (Figure 21; for the 407 "valid" interactions see Supplementary Figure 5).

To compare our novel approach to the conventional expression-based approach, we constructed a miRNA-mRNA network based on matching discrete miRNA and mRNA expression fold change patterns (Methods Section 6.4.7). This expression-based network is 40% larger compared to our decay rate-based network (data not shown). However, in only 12% of all expression-based interactions mRNAs show significantly altered decay rates (fold change >1.5, p-value <0.01; Methods Section 6.3.12). Thus, 88% of differential mRNA expression could not be associated with mRNA decay, and is due to transcriptional regulation. Consequently, the overlap between these networks is rather poor (Figure 20b, Figure 21). These results show the advantage of our decay rate-based network as direct readout of miRNA activity compared to the expression-based network, which represents a composite readout.

The network of repressed miRNAs (Figure 21a) comprises more target interactions compared to the network of induced miRNAs (Figure 21b). This is reasonable, since the number of repressed miRNAs showing an early and pronounced fold change in expression is larger compared to induced miRNAs (Figure 19b). The largest fraction of genes within the network of repressed miRNAs is regulated by miR-8, miR-277, miR-317 and miR-34 (Figure 21a, Table 13). Importantly, multiple genes are co-regulated by these miRNAs. This result is supported by the known cell growth promoting functions of miR-8 and miR-277. miR-8 promotes insulin signaling, which antagonizes ecdysone signaling [100] and miR-277 has been reported to control branched-chain amino acid (BCAA) catabolism and consequently can modulate the activity of the TOR kinase, a central growth regulator [58].

Interestingly, the target genes of repressed miRNAs fall into two classes. While all of their target genes have decreased decay rates, 36% show an induced and 64% a repressed expression level during ecdysone treatment (Table 13). Many genes with induced expression levels are important for processes related to differentiation (e.g. pck, lama and bif [157, 167, 19]), while genes with repressed expression levels are for instance implicated in metabolism (e.g. Got2, Zw and Adk2 [34, 153, 143]). Obviously, target genes with induced expression are implicated in processes that are up-regulated by ecdysone, e.g. differentiation. The same holds true for repressed gene expression levels and down-regulated processes, e.g. metabolism.

Within the network of induced miRNAs the largest fraction of genes was regulated by miR-276a*, miR-276a, miR-282* and miR-252 (Figure 21b, Table 13). Except for mir-252, which is the most highly expressed miRNA in the adult fly and required for proper muscle development [139], none of these miRNAs has an established function. Furthermore, none has been shown to be regulated by ecdysone. Interestingly, miR-282* targets tai, which is a known co-factor for EcR [13]. For target genes of induced miRNAs we observed the same subdivision as for target genes of repressed miRNAs (Table 13). 44% of genes with increased decay rates show increased expression levels, while 56% have repressed expression levels. In the cases of increased expression levels many of these genes regulate processes important for differentiation (e.g. NijA, mbc, Ama and tai [13, 205, 202, 83]), while repressed genes mainly regulate metabolism or cell cycle (e.g. Alr, mei-38, Nmnat, r-l, Cdk7 [121, 133, 204, 197, 78]).

These results emphasize a second advantage of our decay rate-based network approach as it can recover two classes of miRNA-mRNA target interactions. In one class, miRNA-mediated decay has a determining impact on the mRNA expression level. In the other, miRNAs modulate the mRNA expression level that is determined by mRNA synthesis. The specific outcome depends on the biological context of the mRNA target. The function of miRNAs in these interactions is a combination of several accepted mechanistic principles (Section 1.2.2.3), including reinforcing the ecdysone induced transcriptional program, attenuating transcripts that were specific

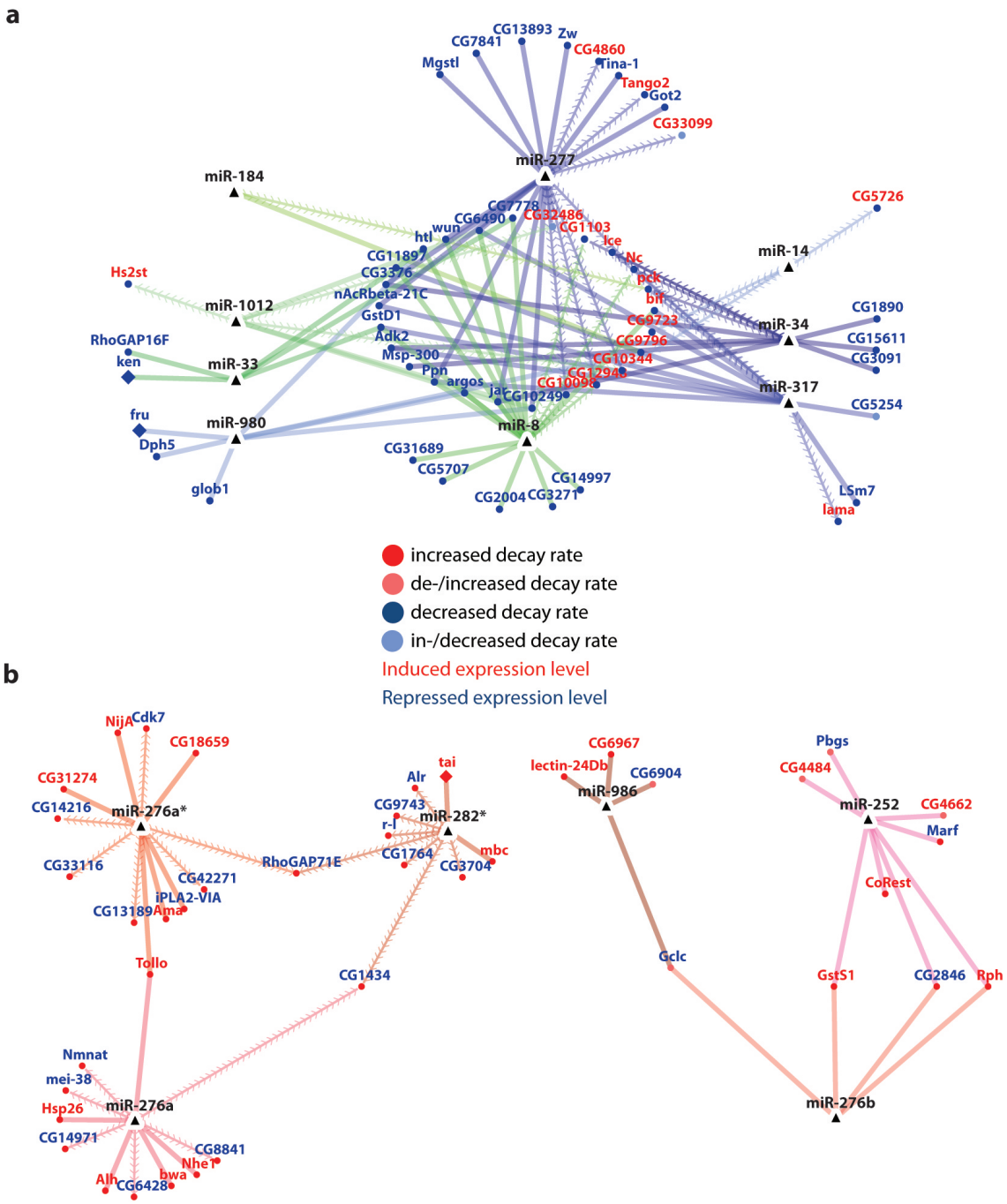

Figure 21: The miRNA-mRNA networks during the ecdysone response. Network was generated as described in Figure 20a, Methods Section 6.4.7 and visualized using Cytoscape v3.1.1 [45]. Network illustrates "reliable" target interactions between repressed (a) or induced (b) miRNAs (triangle) and their predicted targets (circles). Diamonds represent TFs. Circle color denotes significant increased (red) or decreased (blue) decay rates at any time point in the 2-12 hours interval. Lighter-colored circles indicate that decay rate was either first decreased and then increased (light red) or first increased then decreased (light blue). Label color denotes significant total mRNA expression change during ecdysone treatment: red (induction) and blue (repression). Edges are colored according to the respective miRNAs (Figure 19b). Edges with contiguous arrows represent target interactions, which were identified in both the decay rate- and expression-based network.

Repressed miRNAs	Number of target genes	Induced expression	Repressed expression
miR-277	**21**	8	13
miR-8	**19**	5	14
miR-317	**13**	5	8
miR-34	**11**	4	7
miR-980	**7**	1	6
miR-1012	**6**	3	3
miR-33	**5**	-	5
miR-14	**3**	3	-
miR-184	**2**	2	-
miR-306	-	-	-
Sum	**87**	**31**	**56**
[%]	**100**	**36**	**64**

Induced miRNAs	Number of target genes	Induced expression	Repressed expression
miR-276a*	**12**	5	7
miR-276a	**11**	5	6
miR-282*	**9**	2	7
miR-252	**8**	5	3
miR-276b	**4**	2	2
miR-986	**4**	2	2
miR-100	-	-	-
Sum	**48**	**21**	**27**
[%]	**100**	**44**	**56**

Table 13: Summary of miRNA-mRNA networks during the ecdysone response. Listed are repressed (left) and induced (right) miRNAs and number of their targets based on matching miRNA expression and mRNA decay rates (Methods Section 6.4.7). Total number of targets includes only targets, whose expression level was either significantly induced or repressed at any time point in the 2-12 hours interval ("reliable" network).

to the proliferative cell state, stabilizing the new/differentiated cell state or having stabilized the old/proliferative state.

Overall, the obtained miRNA-mRNA network comprises known ecdysone regulated miRNAs and the functions of a large fraction of target genes agree with the ecdysone induced phenotypic changes. Thus, our network presents a promising candidate list for both the validation of our decay rate-based network approach and for unraveling the role of these miRNA-mRNA interactions in ecdysone signaling and its regulated biological processes.

7.15 TFs, miRNA-mRNA interactions and RBPs indicate underlying regulatory mechanisms of ecdysone induced gene expression kinetics

We have shown that ecdysone and its early signaling cascade induce distinct gene expression kinetics in a wide range of functionally diverse genes (Figure 17b). We sought to identify the transcriptional and post-transcriptional regulatory mechanisms that govern these distinct kinetics. To gain first insights we used network analysis to investigate the impact of miRNAs. To associate the obtained miRNA-mRNA interactions with the specific cluster kinetics, we quantified the number of miRNA-mRNA interactions that occurred in each cluster. Although miRNAs target only a minor fraction of genes in the clusters, we identified specific clusters that are targeted by multiple miRNAs (Figure 22). Clusters 4, 13 and 17 are targeted by repressed miRNAs (Figure 23a), while Clusters 7, 9 and 19 are targeted by induced miRNAs (Figure 23b). This result indicates that during the ecdysone response gene expression regulation by miRNA mediated decay seems to be a rather gene specific than a global regulatory mechanism. However, the specific regulation of key regulatory gene might be crucial as for instance miR-282* targets the EcR cofactor tai [13].

To further investigate the post-transcriptional regulation of these kinetics we evaluated the 5´ and 3´ UTR of the cluster genes. Longer UTR have a higher probability to contain structural or sequence motifs that are recognized by miRNAs or RBPs. Several clusters have significantly different UTR lengths compared to the average of all clusters (Figure 22, Supplementary Figure 3, Methods Section 6.3.15.2). In this fairly unspecific analysis the length distribution is not associated with the number of miRNA-mRNA target interactions.

Given the poor availability of experimentally identified RBP targets in *Drosophila*, we were unable to

investigate the regulatory impact of RBPs on a global scale. Nevertheless, we used available data on two ecdysone induced RBPs. Pumilio shows an increased expression level at 12 hours and is known for its role in translational repression and mRNA degradation [71]. Pumilio regulates a significantly enriched number of targets in the Cluster 7 (Methods Section 6.3.15.3), which is characterized by late increase of decay rates and down-regulated expression levels (Figure 22). The second RBP is the translational repressor brat [132], which is strongly induced throughout the entire time course and targets genes with similar induction kinetic in Cluster 3 (Figure 22). Encouraged from these results we used the RBP Database (v3.1 Sep 2012, [47]) to identify further ecdysone regulated RBPs and found 23 induced and 16 repressed RBPs. According to their expression kinetics most RBPs affiliate with late clusters (Figure 22) indicating that during the ecdysone response gene expression regulation by RBPs is a mechanism to regulate the late response genes of the ecdysone cascade.
To gain first insights into the transcriptional regulation, we evaluated the distribution of the 39 ecdysone regulated TFs, for which experimentally determined PWMs were available [206]. We found a specific distribution in early and late clusters, which agrees with the well-established function of these TFs either in ecdysone signaling or the biological processes of the observed phenotype. For instance, the key TFs of the early ecdysone cascade (EcR, br, Eip74EF, Eip75B, Hr39) belong to early and strongly induced clusters such as Clusters 2, 3 or 12 (Figure 22). TFs that are involved in metabolism or differentiation/morphogenesis are found in "late" clusters.
These results have significant impact. It is expected from developmental studies that the early key TFs of the ecdysone cascade have early and similar kinetics [8, 93]. Since in our clustering these TFs accumulate in clusters that are characterized by early, strong and sustained gene expression induction, this result validates the reliability of our clustering approach. Thus, DTA reliably dissects genes expression dynamics during ecdysone signaling. Second, the early, strong and sustained induction strongly suggests that these TFs are the key regulators of the gene expression kinetics in later cluster. Importantly, as other TFs and also RBPs exhibit the same kinetics as those key regulators, the clustering provides evidence that the TFs foxo, Sox14 and schlank as well as the RBPs lin-28 and brat are novel key regulators of ecdysone induced genes expression kinetics. Finally, since the translational repressor Brat targets the TFs Eip74EF and Eip75B our results indicate how translational regulation is generally integrated into the ecdysone response and in particular during this early stage.
In summary, the analysis of ecdysone regulated TFs, RBPs and miRNAs provides first insights into the transcriptional and post-transcriptional regulation of ecdysone induced gene expression kinetics.

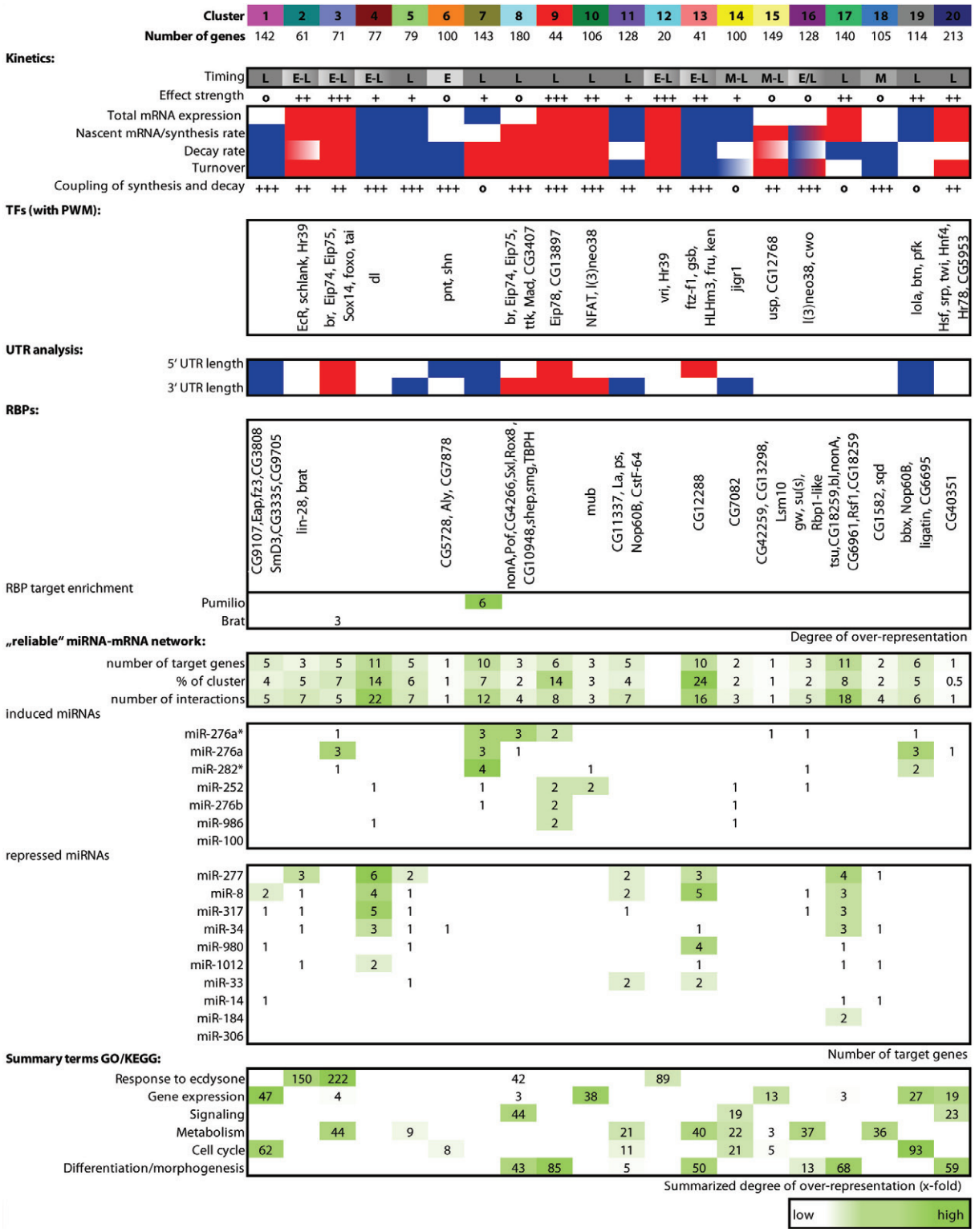

Figure 22: Transcriptional and post-transcriptional regulators of ecdysone induced gene expression kinetics. Catalogue of kinetic features and functional annotation was compiled as in Figure 17b. TFs and RBPs are shown in the cluster they were assigned to by k-means clustering (Section 7.8). Individual microarray probe sets are shown. Average 5′ or 3′ UTR length of each cluster was compared to average 5‘ and 3‘ UTR length of all clusters (Methods Section 6.3.15.2). Red and blue denote significant 25% longer or shorter UTR, respectively (Wilcoxon Rank Sum test; p-value <0.01). Degree of significant over-presentation for RBP targets was calculated: number of expected genes compared to number of observed genes (Fisher's exact test; p-value <0.01), (Methods Section 6.3.15.3). miRNA-mRNA target interactions are taken from Section 7.14. Data sources: Pumilio [71] and Brat (G. Meister unpublished data).

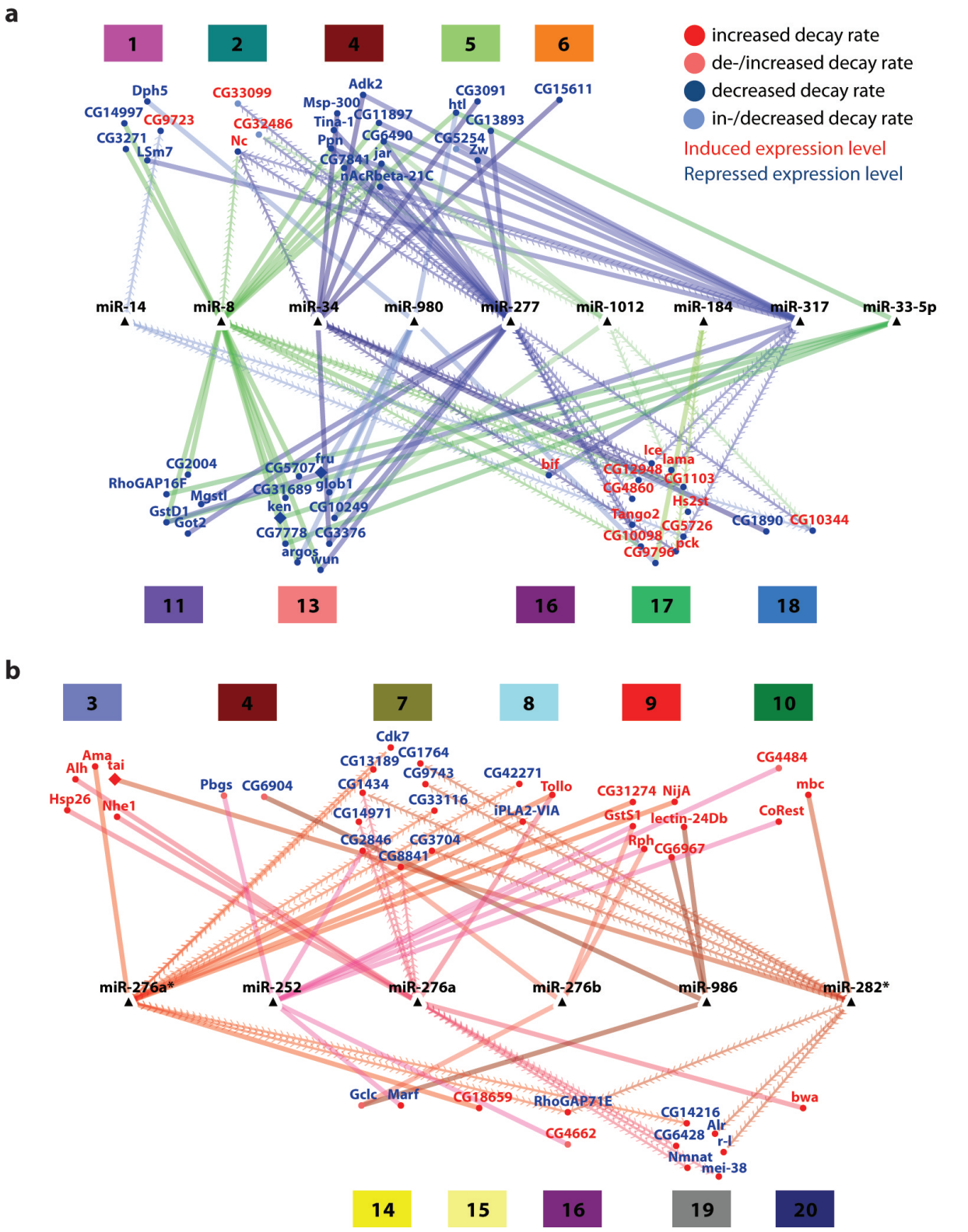

Figure 23: miRNAs regulate individual genes in specific kinetic clusters. Identical network of miRNA-mRNA interactions as in Figure 21, but genes are grouped accoding their affiliation to the 20 kinetic clusters (Section 7.8). (a) Repressed miRNAs; (b) induced miRNAs.

8 Summary and Discussion

Regulation of gene expression is the fundamental process governing both the development and adult homeostasis of all organisms. In this thesis, I applied Dynamic Transcriptome Analysis (DTA) to dissect the regulation of gene expression during ecdysone signaling at the level of mRNA synthesis and decay. By combining the improved temporal resolution of DTA and its simultaneous assessment of mRNA synthesis rates, mRNA decay rates and mRNA expression levels with kinetic clustering analysis, we provide compelling evidence that ecdysone signaling induces a rich and previously unknown diversity of gene expression dynamics. Furthermore, our kinetic analysis leads to a reliable functional description of ecdysone regulated genes and reveals how ecdysone coordinates a wide array of functionally diverse genes to direct the cell from its proliferating state into the differentiated state. In addition, based on mRNA decay rates we developed a novel approach for miRNA-mRNA network analysis and offer insights into the post-transcriptional regulation of these gene expression dynamics by miRNAs. Importantly, our comprehensive description of the ecdysone induced gene expression dynamics and phenotype establishes ecdysone stimulation in *Drosophila* S2 cells as an experimental paradigm for studying mechanistic details of gene expression regulation.

Improvement over existing studies on the genomic and phenotypic response to ecdysone. Although several studies have examined the genomic response to ecdysone [129, 18, 66, 75] as well as the phenotypic behavior of ecdysone stimulated cells [21, 185, 164, 32, 40], our study represents the most comprehensive and detailed description of the ecdysone induced gene expression dynamics and phenotypic changes. By using DTA we present the first genome-wide and simultaneous assessment of mRNA synthesis rates, mRNA decay rates and total mRNA expression levels throughout an early time interval of ecdysone stimulation in *Drosophila* S2 cells. We show that using nascent mRNA for expression profiling improves the sensitivity of time series gene expression measurements for early changes in gene expression and in particular for repressed genes. Compared to a similar time course study of ecdysone treated Kc167 cells [66], which found that within the first 12 hours most genes are induced, we identified four times more differentially regulated genes in general and a predominantly large fraction of repressed genes. Thus, our study measured the genomic response to ecdysone with higher sensitivity and improved temporal resolution compared to existing studies. Furthermore, using DTA we were not limited to study changes of the total expression level of ecdysone regulated genes, but were able to additionally assess ecdysone induced changes of mRNA synthesis rates and decay rates. Therefore, we present the first genome-wide assessment of decay regulation during the ecdysone response.
Using a cell analyzer system, flow cytometry and light microscopy we provide the first systematic and accurate characterization of the ecdysone induced phenotypic changes in S2 cells as well as their timing. We show that upon ecdysone treatment, S2 cells cease proliferation due to cell cycle arrest in the G2 phase. Subsequently the cells acquire a differentiated morphology, characterized by increase in cell size and granularity along with outgrowth of filopodia. The comprehensive and detailed phenotypic characterization was crucial since it enabled us to validate our genomic results and to link the ecdysone induced changes in gene expression to specific biological processes.

Ecdysone induces major changes in the transcriptome that presage the final biological outcome. By taking advantage of the higher sensitivity of DTA, we demonstrate that ecdysone immediately regulates the synthesis rate (nascent mRNA expression) of an initial set of genes and then progressively regulates hundreds of genes, most of them in a sustained fashion. Importantly, the regulated synthesis rates translate into a progressively increasing number of genes that exhibit mostly sustained changes of their total expression level. These progressive changes reflect the architecture of the ecdysone signaling cascade: a small set of early regulators controls the expression of a larger set of regulators, to ultimately control gene expression of a wide array of

functionally diverse genes. We confirmed the functional diversity of ecdysone regulated genes by Gene Ontology [9] and KEGG Pathway [103] enrichment analysis. Importantly, the functional annotation of these genes correlates very well with the ecdysone induced phenotypic changes. The cell cycle arrest is reflected by repressed genes, which are enriched for multiple processes related to DNA replication, cell cycle and proliferation. The extensive remodeling of cell size and shape is reflected by induced genes, which are enriched for morphogenesis and differentiation terms. Furthermore, we found repressed genes to be enriched in multiple terms related to energy and biomolecule production, suggesting a metabolic rearrangement as the cell leaves the proliferating state to enter a resting, differentiated state. Thus, our DTA analysis reveals that the early time interval of ecdysone treatment comprises not only the regulatory key players of the ecdysone cascade, but also the genes presaging the final biological outcome.

First genome-wide assessment of ecdysone regulated decay rates. Owing to the customized statistical approach [173] for the estimation of mRNA decay rates, we were for the first time able to show that ecdysone differentially regulates the decay rates of a large fraction of genes. Strikingly, changes in decay rates are characterized by a less sustained progression compared to changes in synthesis rates, indicating that decay rates are controlled in a temporally more restricted (dynamic) fashion. Although we currently do not fully understand the functional or mechanistic principle of this observation, it suggests that the dynamic regulation of decay rates may facilitate the progression from the proliferating cell state to the differentiated state, while the decay rates in the respective cell states are again similar. Differential regulation of decay rates upon cellular stimulation has been observed by others [166, 163, 162, 149, 160]. It is thought that the dynamic regulation of decay rates is an efficient mechanism for the cell to rapidly respond to environmental challenges and is particularly important for shaping sharp 'peaked' gene expression responses [162, 160].

Ecdysone induces a rich and previously unknown diversity of gene expression dynamics. By complementing the DTA gathered gene expression data with kinetic analysis we arrive at a detailed dissection of ecdysone induced gene expression dynamics, their functional implications and underlying regulatory principles. Specifically, we identified twenty kinetically distinct groups of ecdysone regulated genes. Each group is characterized by a unique combination of effect type, strength and timing of changes in mRNA synthesis and decay rates as well as total expression level. Furthermore, the functional annotation of these groups is specific, reliable and agrees well with the ecdysone induced phenotype. Importantly, only by simultaneously considering the changes in nascent transcription, total mRNA expression, decay and turnover rates as well as their time-dependency, we were able to encompass the entire complexity of ecdysone induced gene expression dynamics.
The twenty distinct gene expression dynamics immediately reveal several significant and novel insights into the genomic response to ecdysone. First, we can both link the distinct gene expression dynamics to specific biological processes and assign a temporal order in which ecdysone regulates these biological processes to direct the cell from its proliferating state into the differentiated state. We show that the earliest regulated gene groups are enriched for functional annotations related to ecdysone signaling. Among the later kinetics we observe that regulation of genes implicated in several aspects of metabolism slightly precede genes important for cell cycle and proliferation. Genes involved in morphology and differentiation show a predominantly late gene expression response. Since the timing of the late processes, namely metabolism, cell cycle and differentiation, overlap, our data demonstrate that the ecdysone cascade regulates a wide variety of functionally diverse genes at the same time.
Many of our observations are consistent with current knowledge of the ecdysone response. For instance the earliest regulated gene groups comprise the early and early-late regulators of the ecdysone response as defined in the Ashburner model [8]. The early and sustained differential expression of these TFs indicates their importance as regulators of the ecdysone induced gene

expression dynamics. Further data analysis will be able to explicitly address this question by modeling the underlying TFs network and its motifs using the nascent transcription data. Importantly, as other TFs and also RBPs exhibit the same kinetics as those key regulators, we provide evidence to extend the set of early regulators. Within this extended set, we find both general regulators of gene expression, such as the translation repressor brat, and regulators of specific cellular processes such as the growth regulator foxo. Since Brat targets the key TFs Eip74EF and Eip75B our results are the first indication how translational regulation is integrated into the ecdysone response.

Another intriguing finding of our study is that we can discriminate the contribution of transcript synthesis and decay to the observed gene expression patterns. We identified several genes, whose changes in total expression level are dependent on either altered synthesis or decay rates. However, the largest fraction of genes is characterized by a correlated (coupled) change in synthesis and decay rates, i.e. simultaneous increase or decrease in synthesis and decay rates. There are several lines of evidence in the current literature that despite the spatial separation of mRNA synthesis and decay, these processes can be coordinated in general and in particular upon environmental perturbation [57, 179, 84, 144, 53, 180, 192, 52, 156, 186, 187]. Coupling is thought to enable an organism to quickly react to a signal and to quickly attain new mRNA steady state levels [80]. One important coupling mechanism involves imprinting of the mRNA with general and/or class specific coordinators, yet, not much is known about how imprinting specifically occurs. Our data suggest that the underlying functional and mechanistic principles of combined or opposing action of synthesis and decay rates seems to be complex and not of global nature. The molecular details and regulation underlying the observed coupling remains to be explored.

The role of miRNAs in the ecdysone response. Our results suggest that miRNAs constitute a crucial additional layer of regulation during the ecdysone response. Upon ecdysone treatment, we observe a rapid repression of several miRNAs and a progressive induction of multiple other miRNAs. The rapid repression indicates that ecdysone induced differentiation requires the coordinated down-regulation of those miRNAs that are probably involved in maintaining the proliferating state. This conclusion is corroborated by our finding that upon abrogation of miRNA activity S2 cells cease proliferation. Furthermore, since ecdysone treated S2 cells undergo cell death in Ago1 knockdown conditions, this suggests a crucial role of miRNAs in the specification of the ecdysone response. The miRNAs of the miR-2 family and bantam have a well-established anti-apoptotic function [122] and inhibition of their function could be one possible explanation for the observed cell death.

The important role of the ecdysone regulated miRNAs in the differentiation of S2 cells is supported by the identified miRNAs which have established functions in ecdysone signaling, cell growth regulation or differentiation (miR-14, miR-8, miR-277 and let-7-C locus [193, 35, 100, 58]). Strikingly, the largest fraction of identified miRNAs and especially the early induced miRNAs have not been implicated in ecdysone signaling or in any of the phenotypic changes. Therefore, our data set represents an excellent resource to reveal the function of these miRNAs in ecdysone signaling, proliferation, cell cycle, metabolism or differentiation/morphogenesis.

By developing a novel decay rate-based approach for miRNA target identification, we already provide a fundamental step for the functional analysis of these miRNAs. Our miRNA-mRNA network approach matches discretized fold change patterns of miRNA expression to discretized fold change patterns of estimated mRNA decay rates. We then used the mRNA expression level as additional information to judge the "reliability" of identified miRNA-mRNA interactions. One advantage of our decay rate-based network approach as opposed to expression-based networks is that mRNA decay rates represent a more direct readout of miRNA activity compared to mRNA expression levels, which represent a composite readout. Consequently, we find that in the expression-based networks only 12% of the mRNAs identified as miRNA targets show differential decay rates. The second advantage of our decay rate-based network approach is that we do not assume an inverse correlation of miRNA and mRNA expression levels. Thus, we can also reliably identify miRNA-mRNA interactions in

which miRNAs only modulate mRNA expression levels, which are determined by mRNA synthesis. Therefore, the decay rate-based network of the ecdysone response is superior to previous approaches and comprises several mechanistic functions of miRNAs, including reinforcing the ecdysone induced transcriptional program, attenuating transcripts that are specific to the proliferative cell state, stabilizing the new/differentiated cell state or having stabilized the old/proliferative state.
We acknowledge the fact that changes in mRNA decay can be due to RBP mediated decay and/or mechanistic coupling of transcription and decay. However, our approach reduces computationally predicted miRNA-mRNA target interactions to an experimentally supported candidate list. The obtained miRNA-mRNA network comprises known ecdysone regulated miRNAs and a large fraction of the inferred target interactions agree with the ecdysone induced phenotypic changes. Thus, our network represents a promising candidate list for both the validation of our decay rate-based network approach and for unraveling the role of these miRNA-mRNA interactions in ecdysone signaling and/or its regulated biological processes.
Finally, owing to the unprecedented and rich diversity of ecdysone induced gene expression dynamics, this thesis establishes ecdysone stimulation in *Drosophila* S2 cells as an excellent experimental paradigm for studying mechanistic details of gene expression regulation.

9 Outlook

Quantitative mechanistic understanding of transcriptional and post-transcriptional regulation of gene expression upon environmental perturbation is fundamental to life science and medicine. This thesis used the genomic response to the steroid hormone ecdysone in the *Drosophila* S2 cell line as an experimental model to study various aspects of gene regulation. To this end, we combined quantitative data of mRNA synthesis and decay with microRNA expression profiling as well as with phenotypic readouts of proliferation, cell cycle and cell morphology. Some of the immediate and long-term future challenges arising from results presented here are discussed in the following paragraphs.

Mapping the transcriptional and post-transcriptional network governing the ecdysone response
Realistic reconstruction of transcriptional and post-transcriptional regulatory networks that control gene expression is one of the current key challenges in systems biology. Although gene expression dynamics are ultimately encoded by constellations of cis-regulatory binding sites recognized by trans-acting regulators such as TFs, RBPs and miRNAs, our understanding of this regulatory code and its context-dependent readout is very fragmentary. Several recent studies prove that computational modeling of genome-wide gene expression dynamics is a powerful approach to reconstruct regulatory networks [36, 154, 15, 178, 14]. To this end, several types of quantitative and genome-wide biological data are integrated, including gene expression data, mapping of cis-regulatory sequences and their occupancy with TFs or the general Pol II transcription machinery, as well as miRNA and RBP expression and binding data. Ideally, these data are evaluated in a time-series fashion upon environmental perturbation to sample dynamics and coordination of transcriptional and post-transcriptional regulatory networks.
Our DTA data provide such quantitative data for modeling complex gene-regulatory systems including transcriptional and post-transcriptional networks, their dynamics and coordination. We identified multiple distinct patterns of coordinated gene expression activity whose underlying regulatory mechanisms remain to be fully explored.
The ecdysone induced gene expression cascade represents one of the best-studied transcriptional cascades in *Drosophila*. However, a global description of the underling regulatory network and its motifs is still missing. The nascent transcription data, together with the identified ecdysone regulated TFs, will enable modeling of this network. To this end, one first needs to identify TF

binding sites in enhancers of ecdysone regulated genes, which can be addressed computationally using a binding site prediction algorithm such as MotEvo [6]. The challenge ahead is to generate accurate genome-wide maps of active enhancers during the ecdysone response to reduce the search space for computational prediction of the binding sites. One method that not only allows for identification of enhancers, but also has the unique advantage to uncover TF binding sites, if coupled to extremely deep next-generation sequencing, is DNase I hypersensitive site (DHS) sequencing [191, 151].
Until now, the role of post-transcriptional regulation in the ecdysone response has not been studied. Based on our genome-wide estimated decay rates our study evaluates miRNAs as one mechanistic regulator of the post-transcriptional network governing the ecdysone response. For a comprehensive description of this network the target interactions of ecdysone regulated RBPs have to be integrated. However, availability of experimentally determined target interactions are limited for *Drosophila* and computational prediction of targets is hampered by the fact that RBPs have much more scope to achieve specificity through secondary structure than though sequence [10]. One experimental technique that could be used to map RNA binding sites of RBPs on a genome-wide scale is PAR-CLIP.
Importantly, by integrating the networks governed by TF, miRNA and RBPs we would arrive at a quantitative description of gene expression as function of transcriptional and post-transcriptional interactions.

Using the ecdysone paradigm to study coupling of mRNA transcription and decay
Eukaryotic gene expression is traditionally divided into several stages, including mRNA synthesis, processing, export, translation and decay. A growing body of evidence argues that regulation of gene expression is circular, by elucidating more and more mechanistic aspect of the coupling between RNA transcription and decay [57, 114, 84, 29, 53, 52, 180, 192, 156, 186, 80, 81, 187]. Importantly, coupling most often accompanies cellular processes that involve transitions in gene expression patterns, for example during mitotic division, cellular differentiation or in response to cellular stress. Several coupling mechanisms have been studied on the molecular level including imprinting of coupling coordinators onto the nascent mRNA, which then interact with the cytoplasmic decay machinery (see references in [80]) or mechanisms involving feedback regulation between the decay and transcription machinery. The latter was recently studied in yeast using synthesis and decay rates obtained by cDTA (comparativeDTA) [186, 187]. Since the kinetic analysis of ecdysone induced gene expression dynamics shows a widespread coupling, the ecdysone paradigm is a perfect model system to study mechanistic aspects of coupling. As we observe different extent of coupling in distinct groups of genes, it will be interesting to investigate, if the respective coupling underlies specific or global mechanisms. Experimentally this could be addressed by impairing factors of mRNA synthesis or degradation coupled to DTA. Given that most mechanistic studies were conducted in yeast, studying coupling in *Drosophila* would generalize these findings to metazoan or identify novel and metazoan specific mechanisms.

Validation of the decay rate-based network approach and the role of miRNA in the ecdysone response
Using single molecule imaging we identified multiple ecdysone regulated miRNAs. To date most of these miRNAs have no established function in ecdysone signaling, proliferation, cell cycle, metabolism or differentiation/morphogenesis. Furthermore, some miRNAs are even missing any functional characterization in *Drosophila*. Therefore, our dataset represents an excellent resource to study the function of these miRNAs.
A crucial step in understanding the role of miRNAs is to determine their authentic miRNA targets. We established an improved miRNA-mRNA network approach to reduce computationally predicted target interactions to an experimentally supported candidate list. We acknowledge one drawback of our current approach that is the matching criterion we used for the correlation of miRNA

expression and mRNA decay rates. Since we demanded a complete match of the discretized expression/decay rate fold change patterns, we increased the number of false negative results, thus rendering our approach rather conservative. An improved strategy would be to use Pearson or Spearman correlation or regression based analyses [150]. Although this improvement should be made to extent the list of candidate interactions, we are confident that our strict matching criterion identified some of the most promising miRNA-mRNA target interactions.
A validation strategy for these target interactions is be to insert the 3´ UTR of the identified targets downstream of a luciferase gene and test the degree of target down regulation during ecdysone treatment using a luciferase reporter assay. In order to use the ecdysone induced differential of endogenous miRNA levels the sensitivity of the luciferase assay has to be optimized by using rapid response luciferases [3].
Furthermore, individual or combined knockdown of the involved miRNAs in untreated and ecdysone treated cells could help to determine the role of these miRNAs in ecdysone signaling and/or the ecdysone regulated biological processes. The most interesting candidates are the early and strongly repressed miRNAs miR-34, miR-277 and miR-317 as well as the so far unstudied and relatively early induced miRNAs miR-282*, miR-276a*, miR-276a, miR-276b and miR-252.

Relevance for cell biology and medicine
The results presented in this thesis can provide novel insights into cell biology and medicine. Both, our detailed characterization of ecdysone induced phenotypic changes and the functional annotation of differential expressed genes demonstrate the major impact ecdysone has on cell proliferation, cell cycle, growth, metabolism, morphology and differentiation. One of many possible future applications arising from our data set could be to study the possible mechanistic link between metabolism and cell cycle exit. The functional annotation of the kinetically distinct gene groups suggests that gene expression changes in metabolic genes slightly precede the ones in cell cycle related genes. This raises the question, if the rearrangement of metabolism may be causative for the cell cycle exit. This hypothesis is supported by a recent publication that studied stem cell proliferation and terminal differentiation in *Drosophila* neural stem cells [90]. The authors demonstrate that ecdysone induced changes in energy metabolism initiate an irreversible cascade of events leading to cell cycle exit. Therefore, analysis of metabolism and cell cycle related genes in our data could provide further mechanistic insight into the pivotal role of metabolic rearrangement for cell cycle exit.
Finally, since mammalian steroid hormone signaling is also involved in proliferation control, our results extend beyond insect development and homeostasis. In fact, most of the established prostate and breast cancer treatments are designed to modulate steroid hormone production or response [90]. The presented mechanistic connections between steroid hormone signaling, energy metabolism, and cell proliferation regulation could for instance provide novel insights into cancer therapy.

Part IV

Establishing an improved DTA-RNA-Sequencing protocol for dissecting the *Drosophila* core promoter

10 Results and Discussion

The core promoter project seeks to arrive at a quantitative understanding of the contributions core promoters make to the gene expression level. To this end, genome-wide binding profiles of key protein components, namely nucleosomes and the general transcription machinery (Pol II, TBP, TFIID), as well as the output transcript steady state and nascent transcription rates were measured in S2 cells (Figure 24). My contribution to the project was the measurement of transcript steady state and nascent transcription rates using DTA-RNA-Sequencing. To this end, I first adapted the DTA microarray protocol to next-generation sequencing and established a novel procedure for data normalization using artificial Spike-In transcripts (Section 10.1), as well as a novel strategy for rRNA depletion during sequencing library preparation, employing rRNA specific oligo probes (Section 10.2).

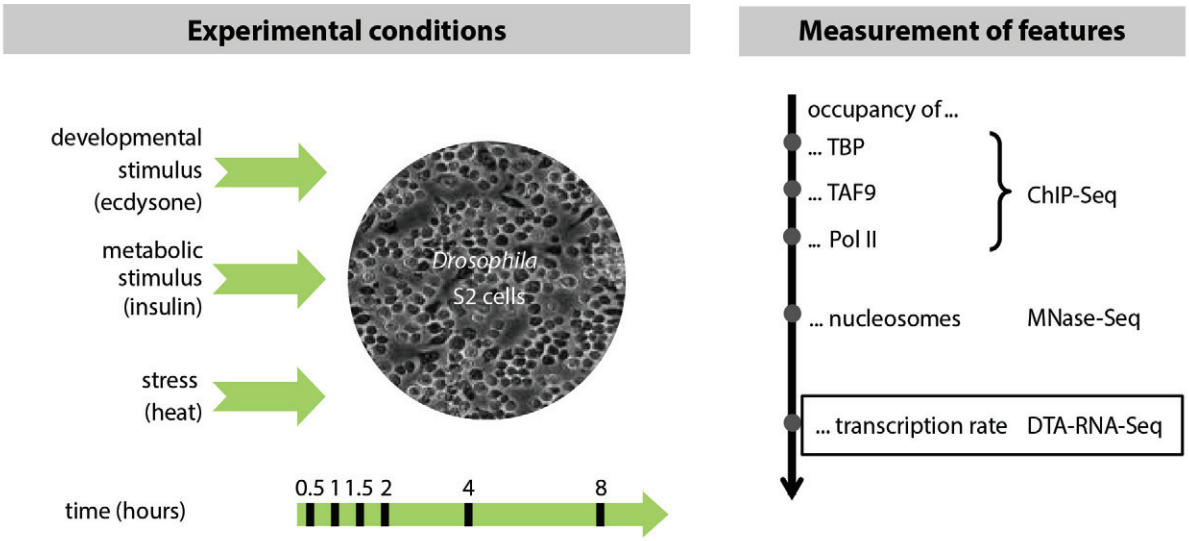

Figure 24: Outline of the genome-wide experiments for dissecting the *Drosophila* core promoter. In the core promoter project we measured genome-wide protein-DNA binding and expression profiles in S2 cells. The cells were stimulated in a time series fashion with well-defined stimuli that are known to trigger different (transcriptional) responses.

10.1 4sU labeled and unlabeled Spike-In transcripts enable DTA-RNA-Sequencing data normalization

The integration of diverse genome-wide data sets is fundamental to the core promoter project, and therefore all data sets have to be measured in a highly quantitative manner and with best accuracy. Transcriptome analysis using DTA fulfills these criteria, as it provides a highly sensitive and direct readout of transcription [144]. However, one of the major drawbacks in transcriptomics is the unknown normalization factor between samples. Variations in RNA extraction efficiencies,

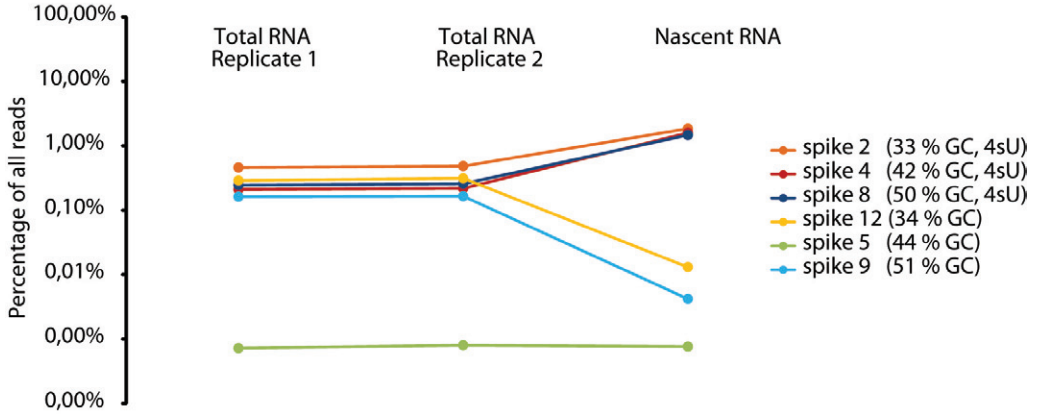

Figure 25: Spike-In procedure is highly reproducible and controls for nascent RNA extraction efficiency. Equal amounts of six Spike-In transcripts, three 4sU labeled and three unlabeled, were added to all samples after cell lysis (Methods Section 6.5.1). Diagram presents sequencing results of an experiment used for establishing the appropriate Spike-In amount. In this particular experiment Spike-In 5 was not added to the cell lysate in order to determine the background level. The reads per Spike-In are expressed as the percentage of all reads derived from libraries prepared using either total or nascent RNA. Total RNA libraries were prepared in two technical replicates.

purification and amplification steps in the protocol and sequencing bias introduce differences in global abundance levels. The estimation of the normalization factors limits the precision of DTA. To largely overcome this limitation, I adapted a novel procedure for data normalization using artificial RNA Spike-In transcripts for the DTA protocol. The main achievement was to create 4sU labeled Spike-Ins to enable normalization of both the total and the nascent RNA fraction. The Spike-In sequences were derived from the ERCC RNA Spike-In Mix (Ambion), which contains 92 well-characterized transcripts from random unique sequences with no homology to mouse, rat, human, drosophila or bacteria. Six of these sequences were chosen based on defined criteria: (i) approximate length of 1000 nt, (ii) almost equal number of uridines and (iii) either 30%, 40% or 50% GC content. The different GC contents are represented by two Spike-Ins; one 4sU labeled, one unlabeled. Besides normalization of the sequencing data, using 4sU labeled and unlabeled Spike-Ins allows estimating the extraction efficiency of nascent RNA by the presence of unlabeled Spike-Ins in the nascent RNA fraction. Spike-Ins were generated by *in vitro* transcription (Methods Section 6.5.1) and added to all samples after cell lysis. The amount of added Spike-Ins is first calculated as 1% of all total RNA library reads, further refined by two sequencing test runs and finally determined as 1.44×10^6 molecules per Spike-In. The Spike-In procedure was highly reproducible between technical replicates (Figure 25). We observed a slight contamination of the nascent RNA fraction with total RNA. In the nascent RNA fraction, unlabeled Spike-Ins yielded one order of magnitude more reads compared to a Spike-In that was not present in the sample.

10.2 InDA-C technology efficiently depletes *Drosophila* rRNA during sequencing library preparation

The major determinants for the choice of sequencing strategies are whether sequencing libraries are prepared strand specific and how rRNA transcripts, if not explicitly under study, are depleted. The strategy for strand specificity inherently depends on the purchased library preparation kit and is often a corporate secret. rRNA transcripts typically represent 70-80% of all transcripts. Therefore, several strategies for rRNA depletion were developed: (i) hybridization-mediated pull down of rRNA, (ii) hybridization-mediated enrichment of poly-A transcripts, or (iii) rRNA disfavoring primers for

cDNA generation. We could not employ the first two strategies, since these require more starting RNA material than we can isolate in our DTA protocol. Furthermore, we seek to minimize the handling steps on RNA to confer best RNA quality. The strategy of using rRNA disfavoring primers did not prove as efficient, since the primers are not optimized to disfavor *Drosophila* rRNA transcripts (Figure 26b). To overcome these limitations, I employed the novel Insert Dependent Adaptor Cleavage (InDA-C) technology that selectively targets and eliminates unwanted transcripts from sequencing libraries (Figure 26a). In collaboration with the company NuGEN, which established this technology, we designed 124 *Drosophila* rRNA specific oligo probes (Methods Section 6.5.2) and successfully depleted rRNA fragments down to 20% and 2% of total reads, derived from total and nascent RNA libraries, respectively (Figure 26b,c). Moreover, the InDA-C technology was high reproducible and did not show unwanted off-target effects (data not shown).

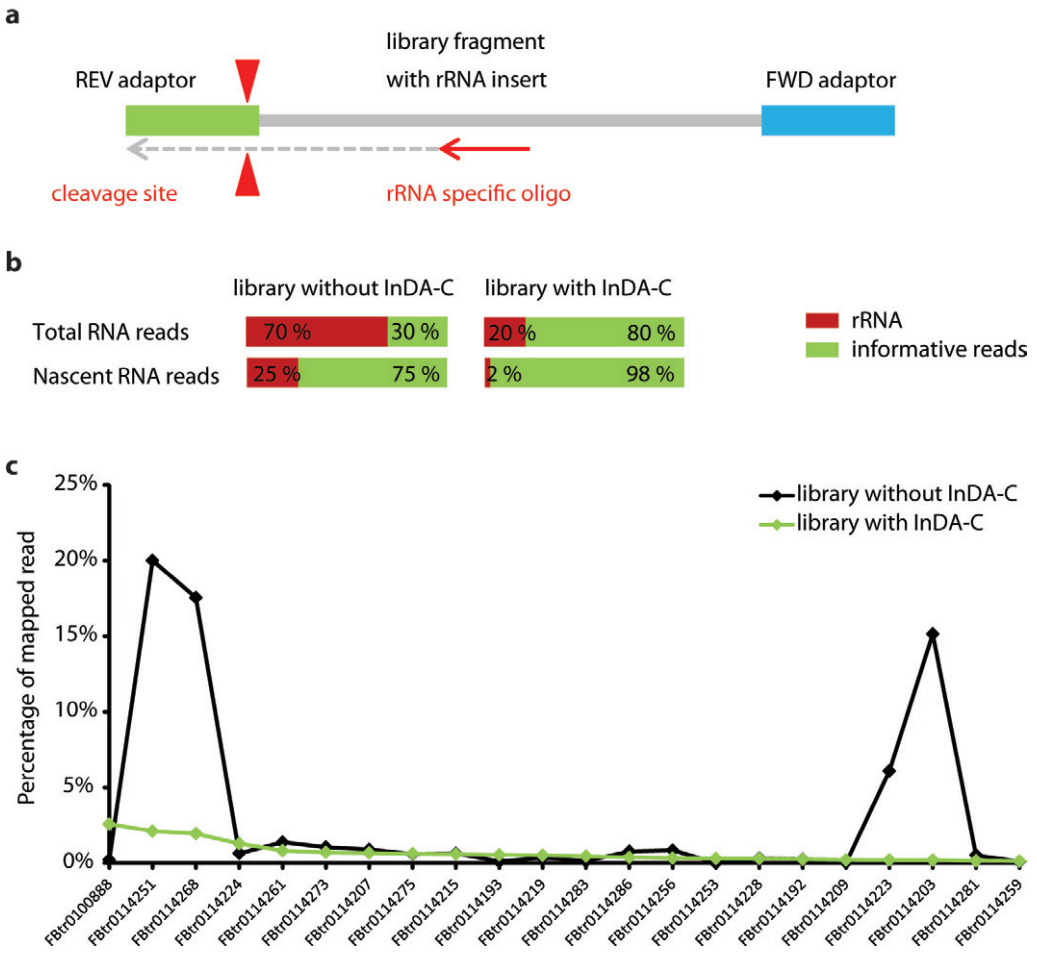

Figure 26: InDA-C technology efficiently depletes rRNA. (a) Insert Dependent Adaptor Cleavage (InDA-C) technology enables depletion of unwanted transcripts, e.g. rRNA transcripts, through sequence-specific targeting. After library preparation and strand selection the single stranded library is incubated with customized oligo probes targeting e.g. *Drosophila* rRNA. The oligo probe is extended towards the reverse sequencing adaptor, where it complements a restriction site for adaptor cleavage. In the subsequent library amplification only library fragments with both intact adaptors are amplified exponentially. (b) Effective depletion of *Drosophila* rRNA library fragments using the InDA-C technology with 124 *Drosophila* specific rRNA oligo probes. Oligos were designed as described in Methods Section 6.5.2. Illustrated is the distribution of rRNA and informative reads (non rRNA) in total (top) or nascent RNA (bottom) libraries prepared without (left) and with (right) the InDA-C technology. (c) Efficient depletion of abundant rRNA transcripts. Diagram depicts the percentage of mapped reads from a sequenced library that mapped to rRNA transcripts. Shown are the Top 22 rRNAs based on libraries prepared without the InDA-C technology.

10.3 Genome-wide measurement of transcript steady state and nascent transcription rates

To describe and quantify the rules underlying variability and degree of plasticity in the transcriptional output between genes, it is crucial to measure transcript abundance and transcription rate in an activity depended manner. We triggered different transcriptional programs by stimulating S2 cells in a time series with ecdysone as developmental stimulus, insulin as metabolic stimulus and heat shock to induce a stress response (Figure 24). The stimulation time intervals were individually determined for each stimulus based on previous experiments using nascent mRNA profiling (data not shown). Heat-shock stimulation is limited to 2 hours, since afterwards cells undergo cell death. Insulin and ecdysone treatment were monitored in frequently sampled early time points and extended to 8 hours, to measure not only primary but also secondary response genes. In the final experiment, all treatments were conducted simultaneously and the DTA protocol as well as sequencing library preparation (38 libraries) were carried out as described in Methods Sections 6.1.3, 6.3.1 - 6.3.4, 6.3.6, 6.5.3. All libraries yielded high quality sequencing data (data not shown) and were in the initial phase of data analysis at the time this thesis was written (Methods Section 6.5.4).

Taken together, I successfully established a standardized, strand-specific RNA-sequencing protocol and carried out genome-wide measurement of transcript steady state and nascent transcription rates. The established Spike-In controls will enable bias corrections for all experimental steps, after RNA extraction to data generation. This will improve comparisons of DTA-RNA-Sequencing samples both within the core promoter project and future projects. Furthermore, Spike-In normalization will facilitate identification of global changes in transcription. The adaption of the InDA-C technology to *Drosophila* rRNA depletion was highly efficient and cost-effective. Due to the higher fraction of informative reads in the sequencing libraries, I could decrease the costs for sequencing and was able to conduct paired-end, instead of single-end sequencing, within the project budget. The obtained transcription rates will be correlated with computationally identified promoter sequence motifs (XX-motif), Pol II and GTF binding profiles (ChIP-Seq) as well as nucleosome positioning data (MNase-Seq) in order to classify core promoters and generate quantitative models for their activity. Furthermore, the DTA-RNA-Seq data set of S2 cells under various stimulation conditions represents a crucial data resource beyond the core promoter project.

Part V

Appendix

11 Supplementary Figures

Supplementary Figure 1: Cluster trajectories
Ecdysone regulated genes were clustered as described in Methods Section 6.3.14.2. Shown are the individual cluster trajectories in decay and synthesis rate (left) and nascent (labeled) and total RNA (right). Trajectories delineate mean fold change at one time point (1 hour to trajectory end at 12 hours).

Supplementary Figure 2: Cluster fold change progression
Ecdysone regulated genes were clustered as described in Methods Section 6.3.14.2. Time course progression of individual cluster $\log_2$ fold changes (y-axis) in nascent RNA (yellow), total RNA (grey), decay rate (blue), synthesis rate (red) and turnover (green) are shown. Solid line represents mean fold change and shading between error bars the standard deviation.

Supplementary Figure 3: All cluster features and GO/KEGG enrichment terms
Kinetic features according to Methods Section 6.3.15.1. Average 5´ or 3´ UTR length of each cluster was compared to average 5´ or 3´ UTR length of all clusters (Methods Section 6.3.15.2). Green denotes 25% longer or shorter UTR. Functional enrichment for GO "Biological Process" and KEGG terms (*) was calculated using Fisher's exact test (p-value <0.01; Methods Section 6.3.15). Table lists the individual significantly enriched terms. Summarized degree of over-representation: number of expected genes in a term, compared to number of observed genes.

Supplementary Figure 4: The 15 highest expressed miRNAs
The 15 highest expressed miRNAs from smallRNA-Seq data of Berezikov et al. 2011 (modENCODE) were compared to miRNAs profilied in this study (Methods Section 6.4.5) for untreated and ecdysone treated cells (12 and 72 hours).

Supplementary Figure 5: "Valid" interaction networks of miRNA-mRNAs
Network was generated as described in Figure 20and Methods Section 6.4.7. Networks illustrates "valid" interactions between induced **(a)** and repressed **(b)** miRNAs (triangle) and their predicted targets (circles). Diamonds represent TFs. Circle color denotes significantly increased (red) or decreased (blue) decay rates at any time point in the 2-12 hours interval (fold change >1.5, p-value <0.01). Lighter-colored circles indicate that decay rate was either first decreased and then increased (light red) or first increased then decreased (light blue). Label color denotes significant total mRNA expression change during ecdysone treatment (fold change >1.5, p-value <0.01): red (induction), blue (repression) or no change significant change (black). Edges are colored according to regulated miRNAs (Figure 19b). Edges with contiguous arrows represent target interactions, which were identified in both the decay rate-based and expression-based network.

Supplementary Figure 1: Cluster trajectories (Cl 1-5)

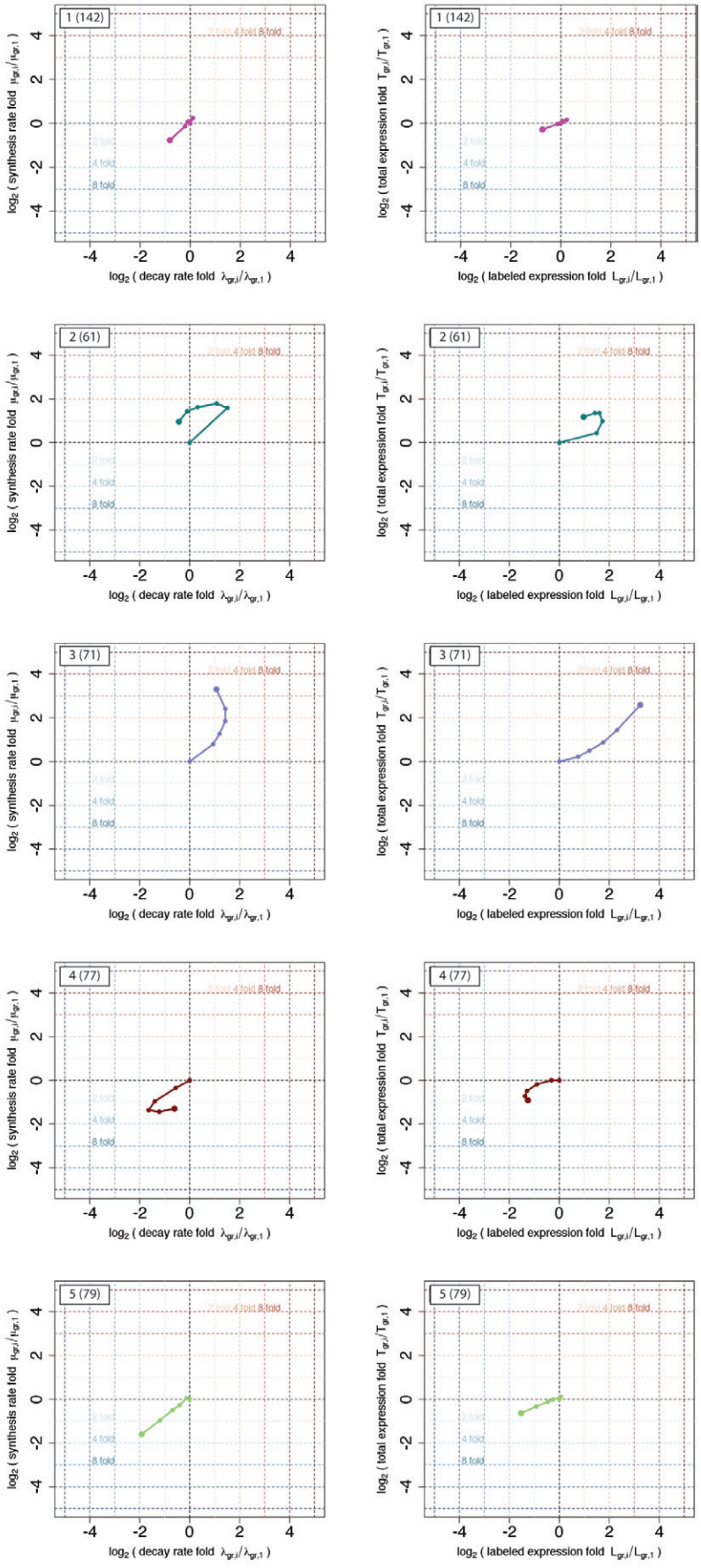

Supplementary Figure 1: Cluster trajectories (Cl 6-10)

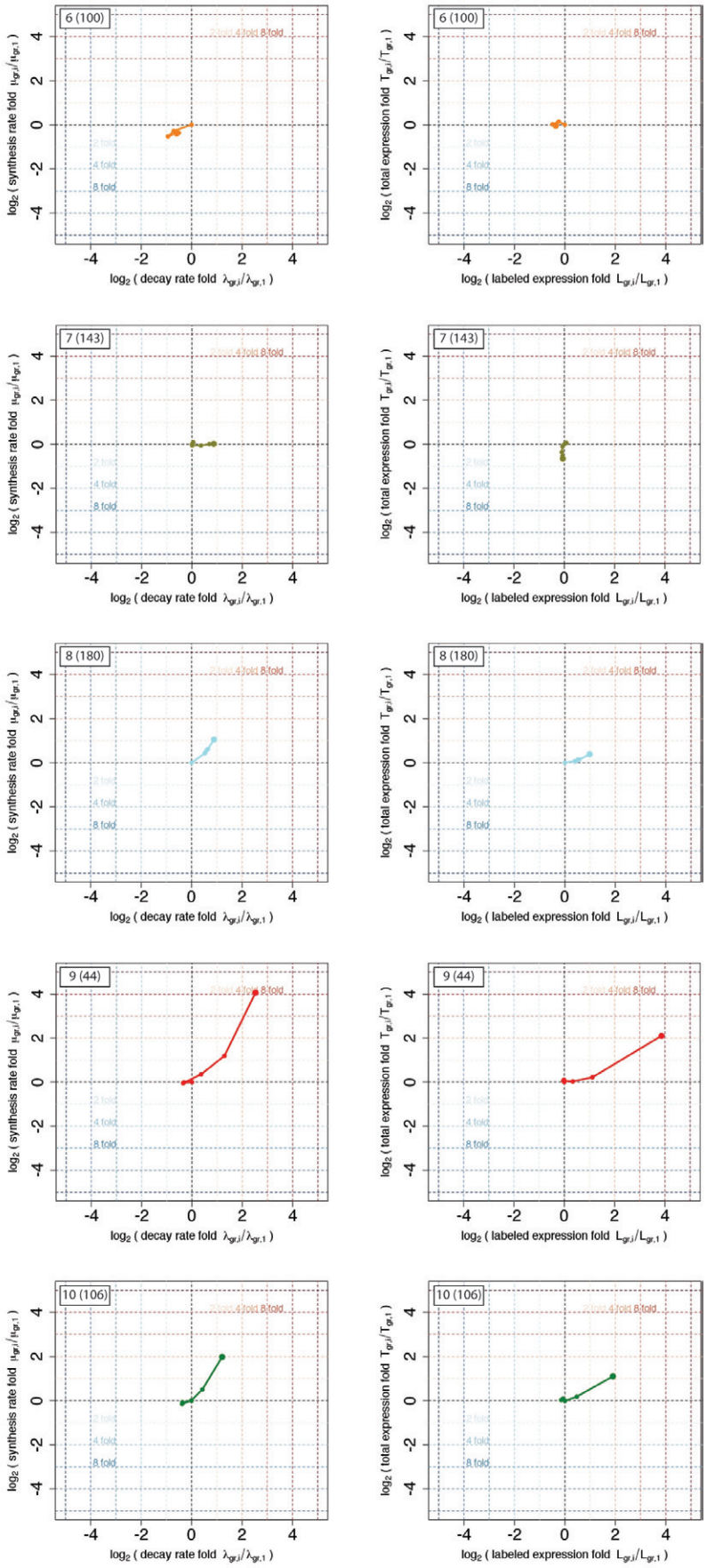

Supplementary Figure 1: Cluster trajectories (Cl 11-15)

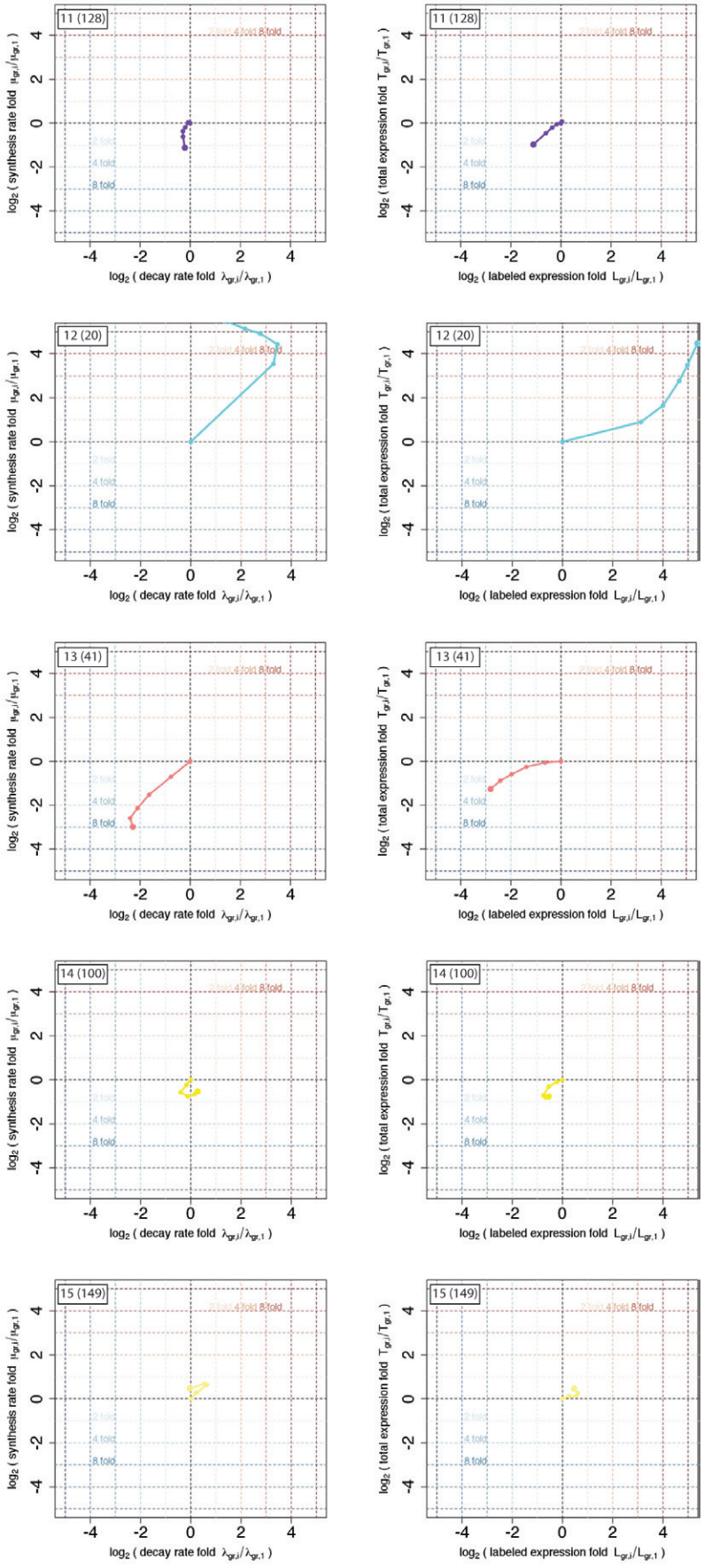

Supplementary Figure 1: Cluster trajectories (Cl 16-20)

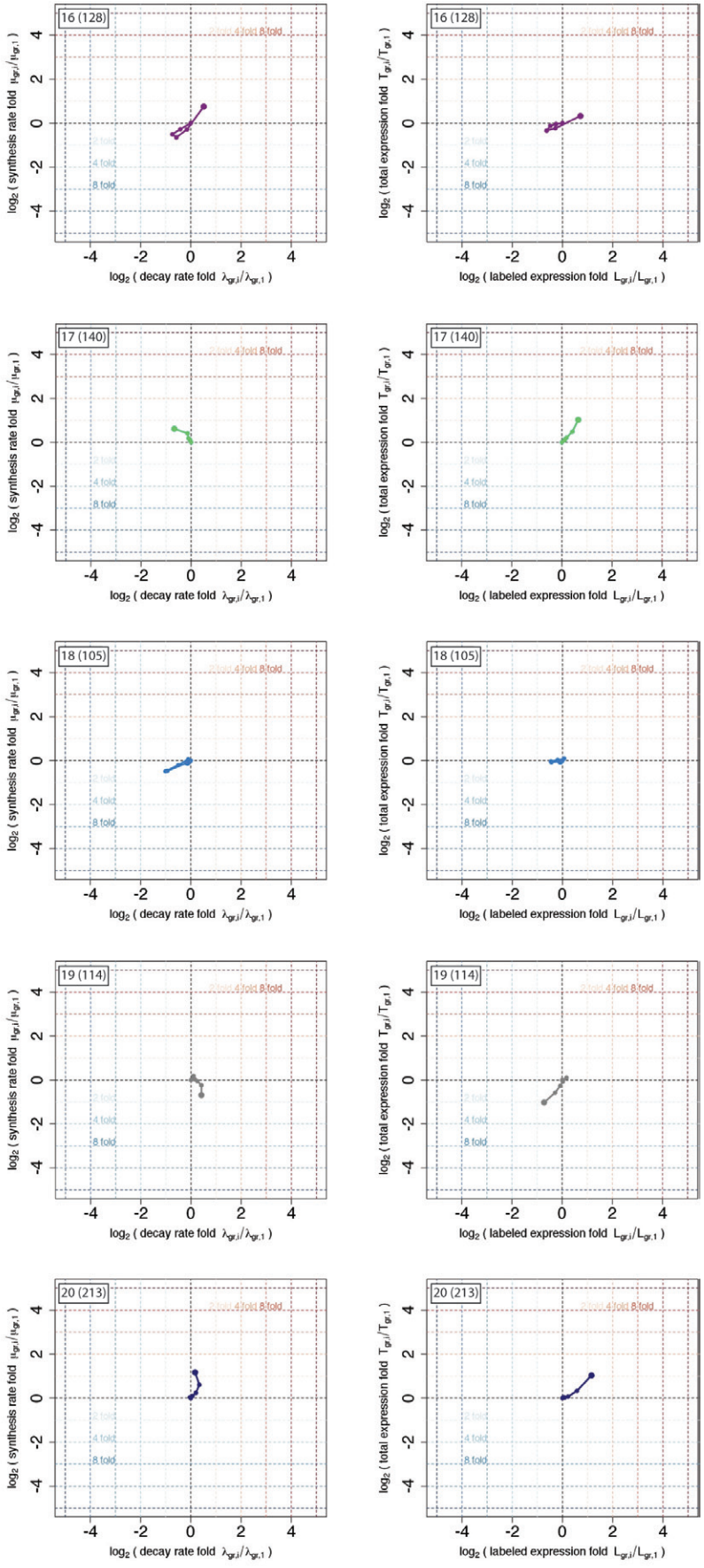

Supplementary Figure 2: Cluster fold change progression (Cl 1-4)

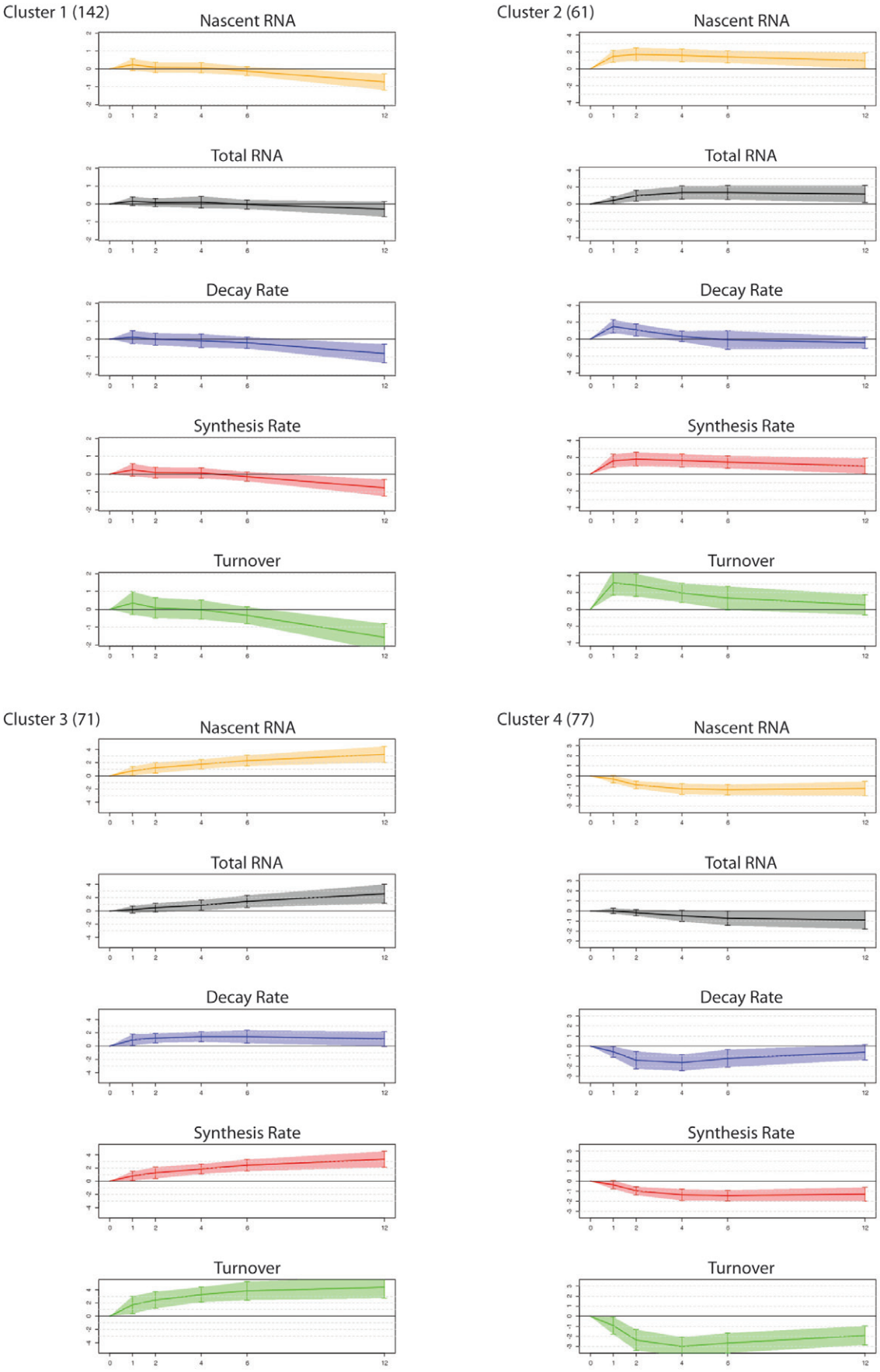

Supplementary Figure 2: Cluster fold change progression (Cl 5-8)

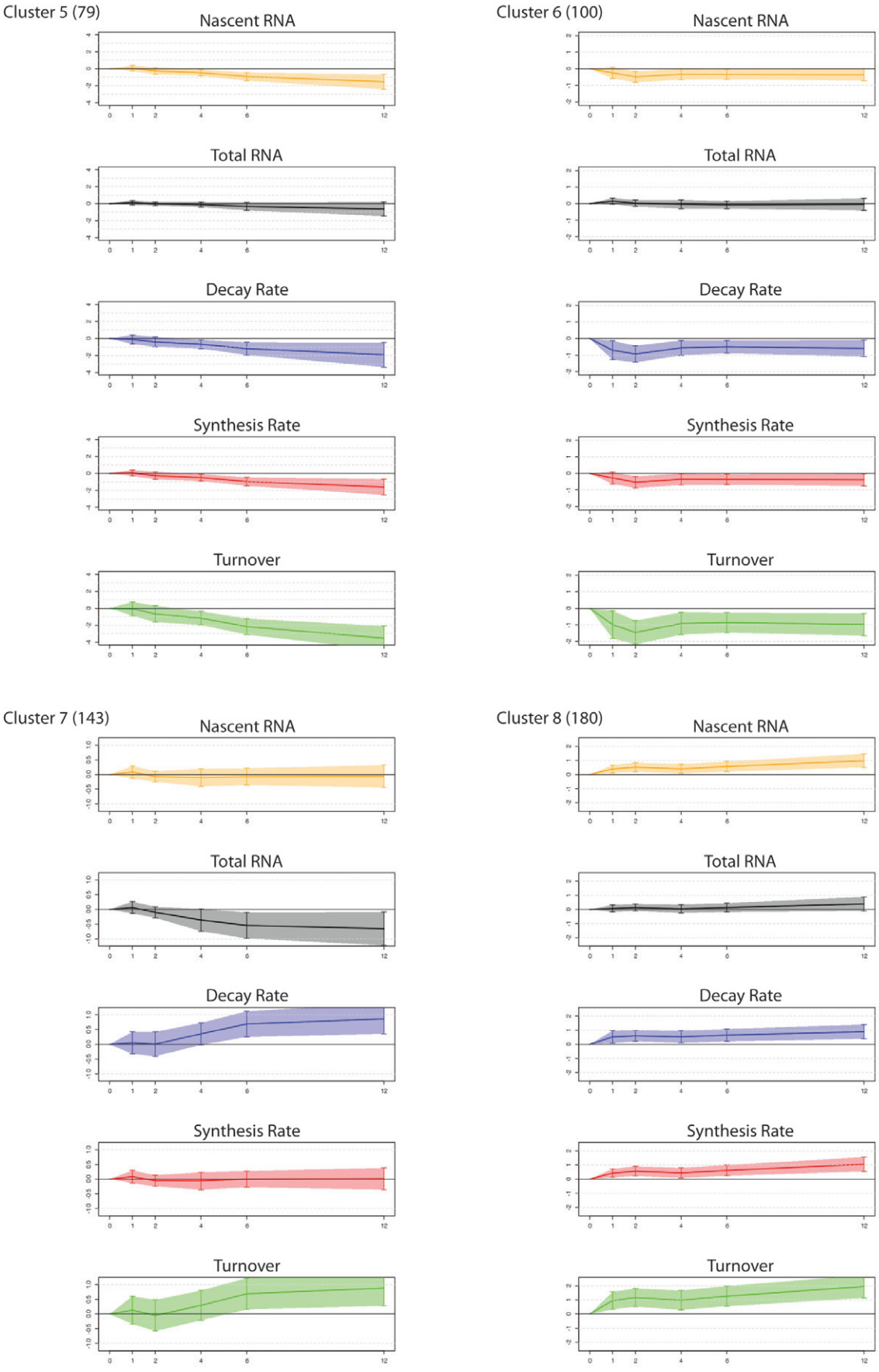

Supplementary Figure 2: Cluster fold change progression (Cl 9-12)

Cluster 9 (44)

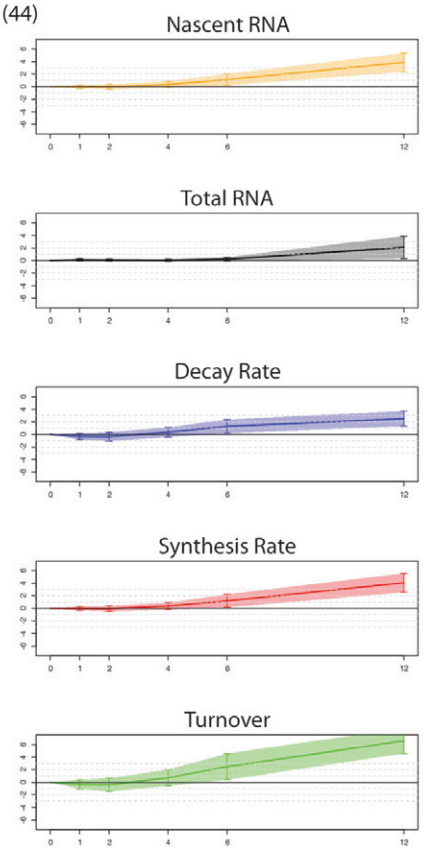

Cluster 10 (106)

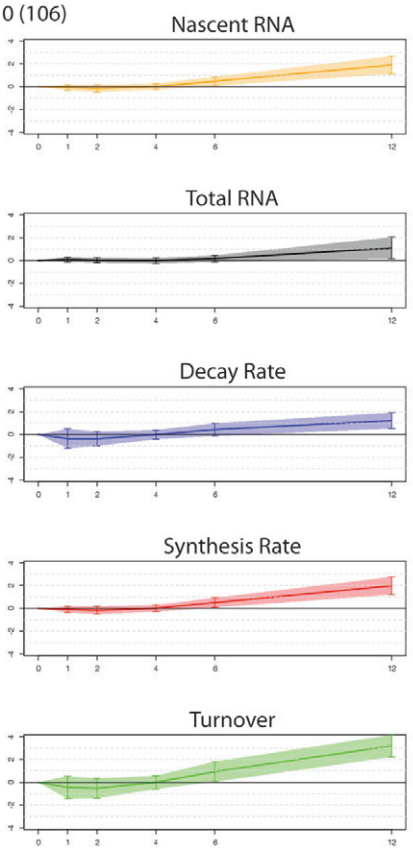

Cluster 11 (128)

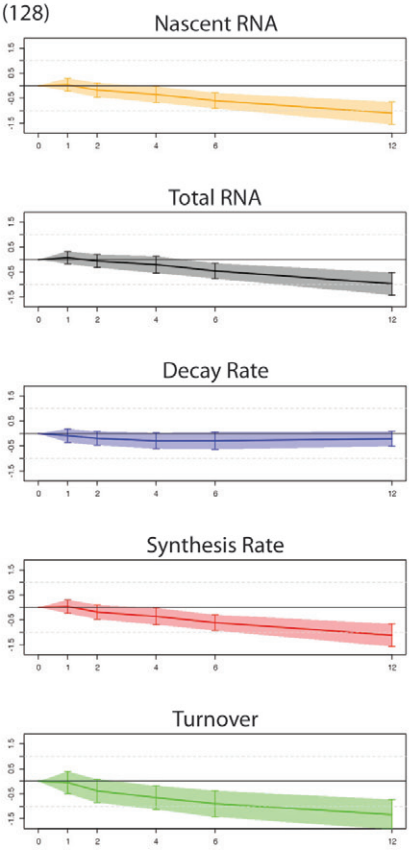

Cluster 12 (20)

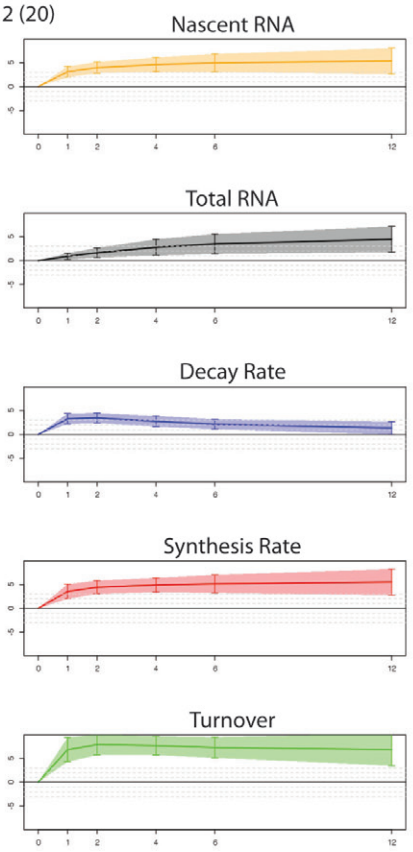

Supplementary Figure 2: Cluster fold change progression (Cl 13-16)

Cluster 13 (41)

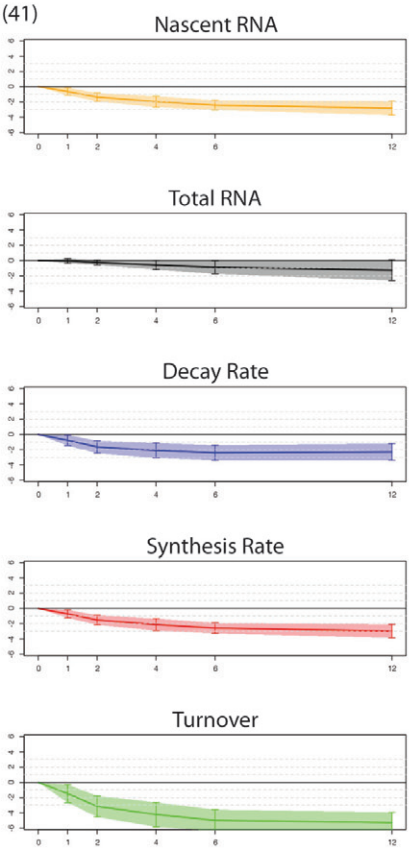

Cluster 14 (100)

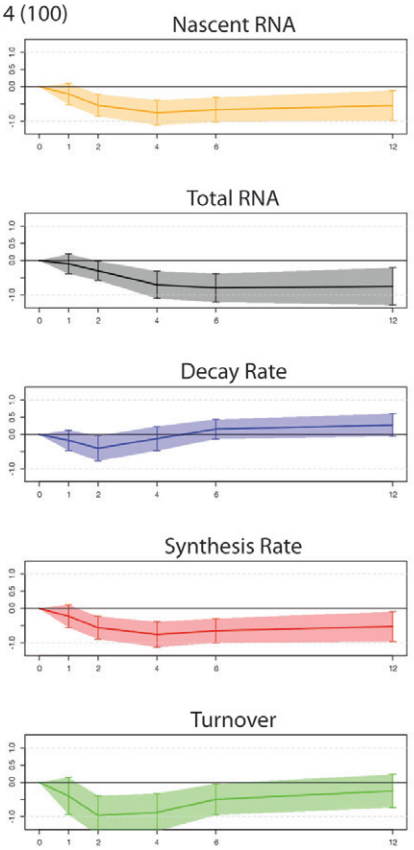

Cluster 15 (149)

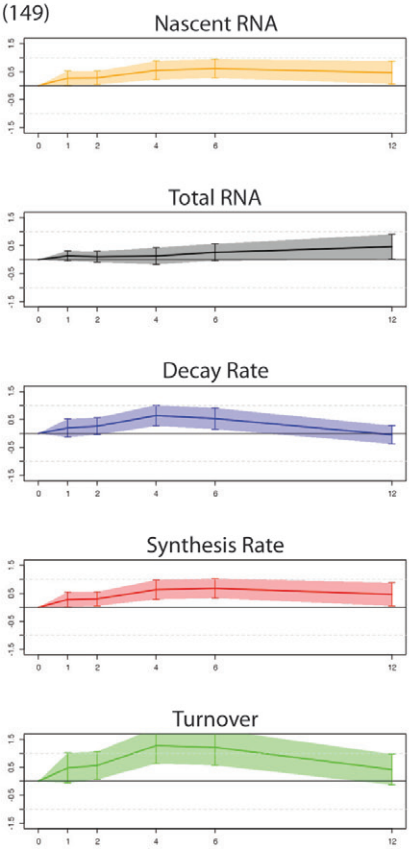

Cluster 16 (128)

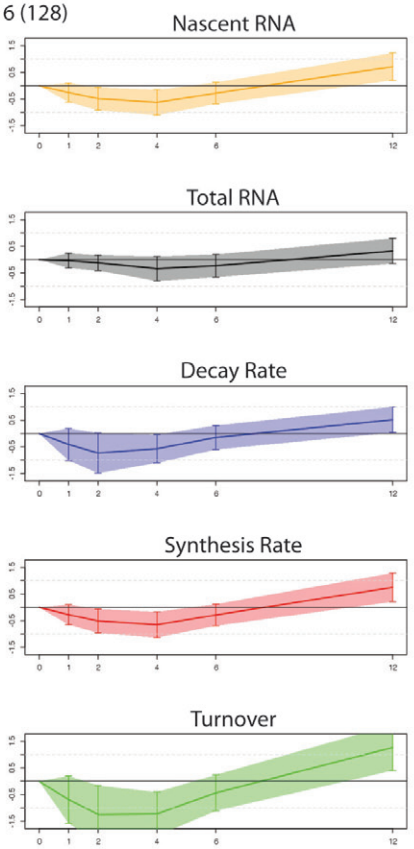

Supplementary Figure 2: Cluster fold change progression (Cl 17-20)

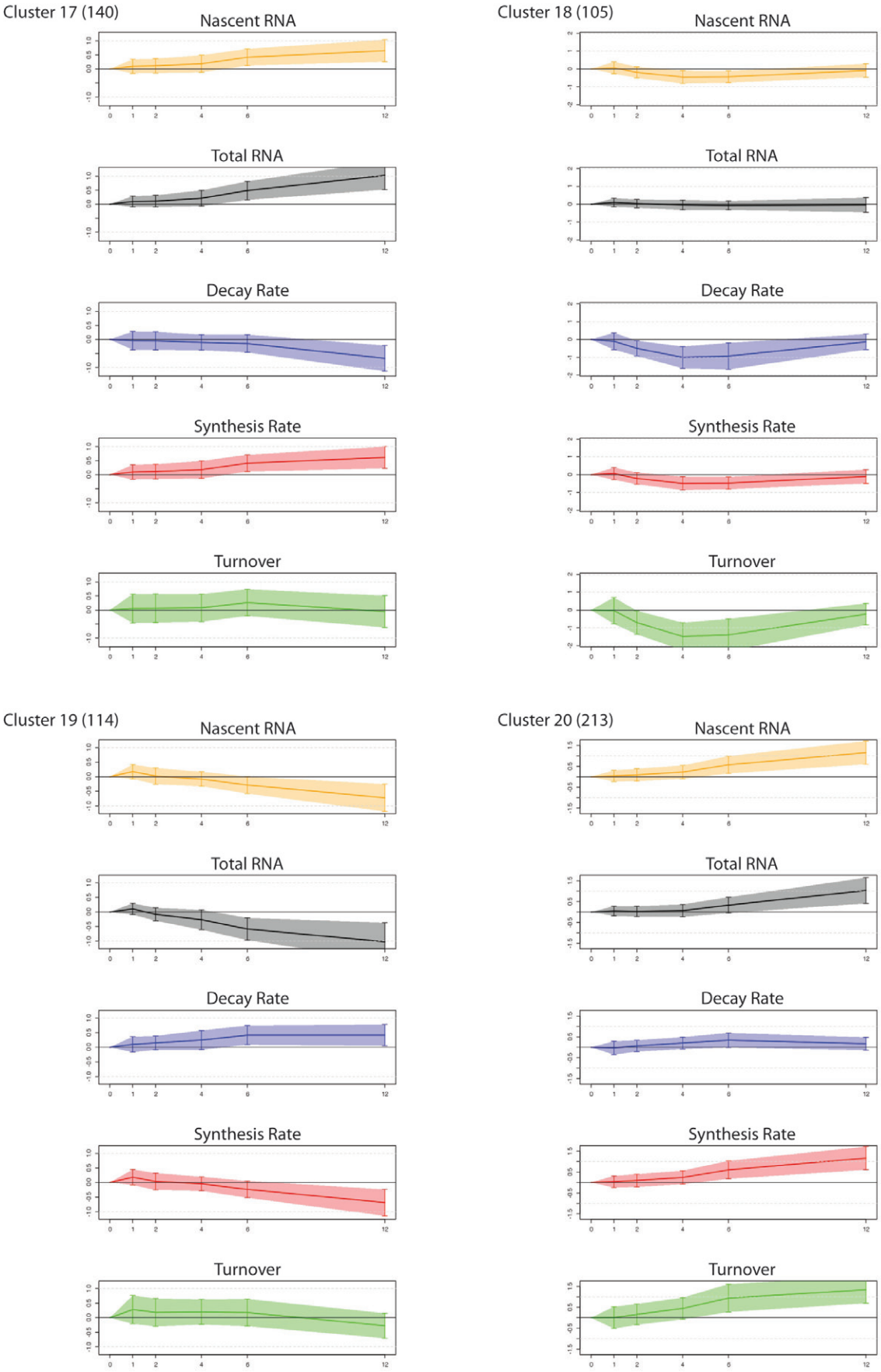

Supplementary Figure 3: All cluster features and GO/KEGG enrichment terms.

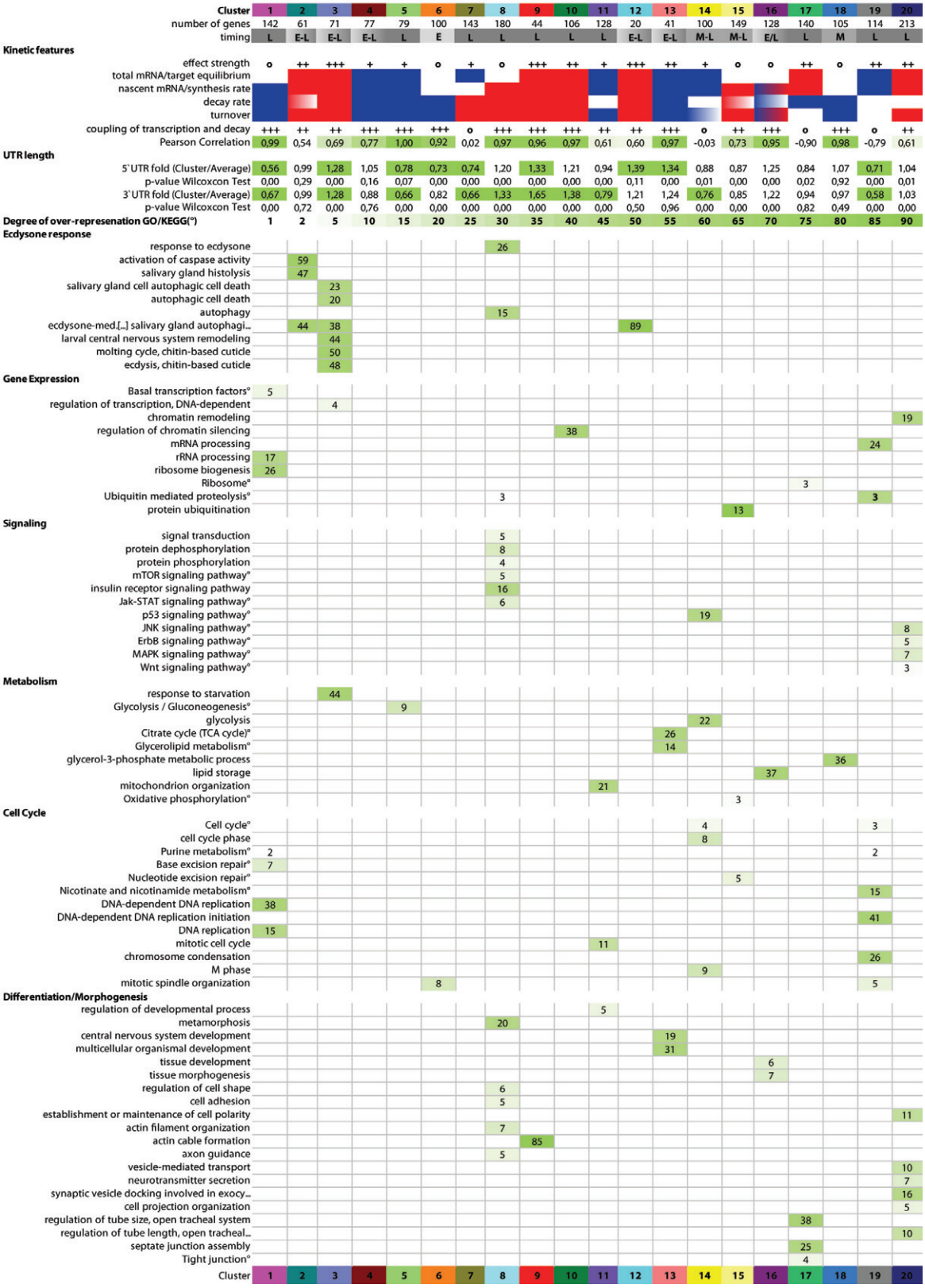

Supplementary Figure 4: 15 most expressed miRNAs.

Berezikov et al. 2011 (modENCODE)		This study untreated	
miRNA	read counts	miRNA	counts
bantam-3p	**14.081.371**	miR-8-3p	14.892
mir-184-3p	**2.730.062**	miR-184-3p	11.925
mir-2a-2	1.437.869	bantam-3p	11.583
mir-14-3p	1.297.615	miR-276a-3p	5.687
mir-2a-1	1.112.467	miR-279-3p	5.523
mir-2b-1	752.158	miR-275-3p	4.042
mir-2b-2	727.359	miR-995-3p	2.321
mir-996-3p	**711.140**	miR-996-3p	2.144
mir-8-3p	**624.874**	miR-277-3p	2.103
mir-13b-2	606.944	miR-306-5p	1.628
mir-282-5p	594.335	miR-13b-3p	1.287
mir-11-3p	**357.425**	miR-34-5p	1.169
mir-13b-1	**319.060**	miR-304-5p	989
mir-34-5p	**280.892**	miR-11-3p	989
mir-276a-3p	**272.952**	miR-9c-5p	969

This study 12 hours ecdysone		This study 72 hours ecdysone	
miRNA	Rank gain	miRNA	Rank gain
bantam-3p	2	miR-276a-3p	3
miR-276a-3p	2	miR-279-3p	3
miR-8-3p	-2	miR-996-3p	5
miR-184-3p	-2	miR-282-3p	21
miR-275-3p	1	miR-125-5p	60
miR-279-3p	-1	miR-8-3p	-5
miR-282-3p	18	bantam-3p	-4
miR-996-3p	0	let-7-5p	58
miR-995-3p	-2	miR-184-3p	-7
miR-306-5p	0	miR-100-5p	57
miR-13b-3p	0	miR-275-3p	-5
miR-11-3p	2	miR-13b-3p	-1
miR-304-5p	0	miR-304-5p	0
miR-9c-5p	1	miR-11-3p	0
miR-988-3p	1	miR-970-3p	3
		miR-995-3p	-10
		miR-277-3p	-16
		miR-306-5p	-11
		miR-34-5p	-41

mir-2b-1	**Rank 17**
miR-2a-1	**Rank 19**
mir-14-3p	**Rank 36**
mir-282-5p	not expressed
mir-13b-2	not queried
miR-2a-2	not queried
mir-2b-1	not queried

up, down in 2-72 hours

BOLD found in Berezikov 2011

Supplementary Figure 5: *Valid* **miRNA-mRNA network**

a

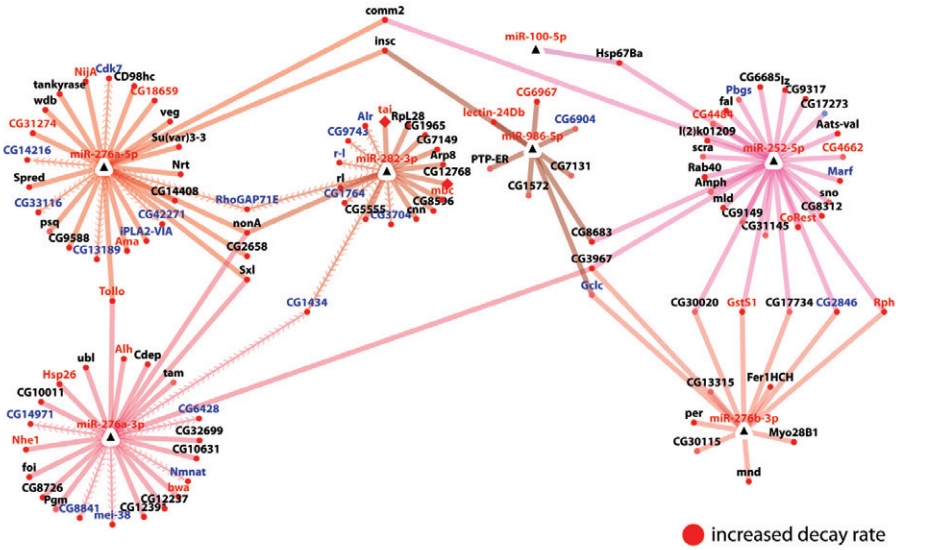

b

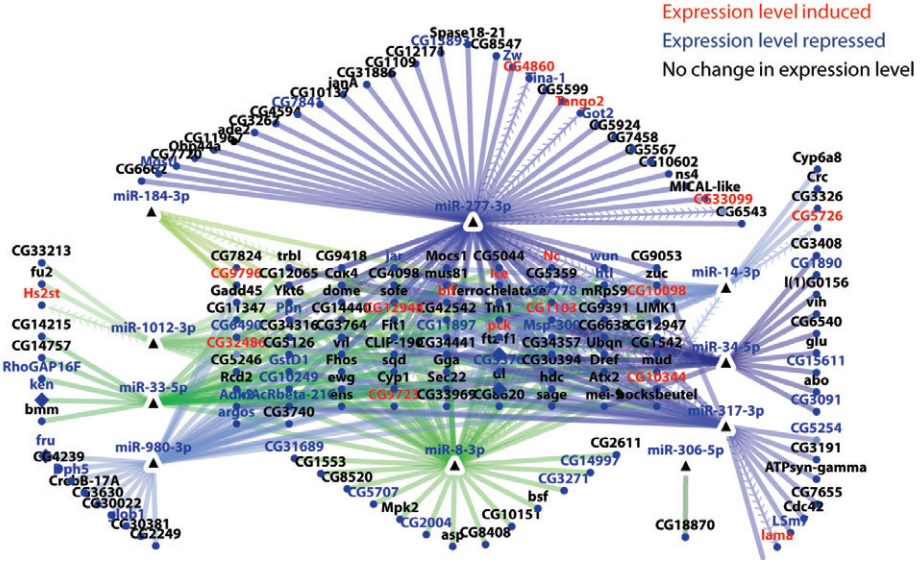

12 Supplementary Tables (CD-ROM)

All Supplementary Tables are provided as data files on the attached CD-ROM.

Supplementary Table 1: Expressed and differential genes
Table contains all genes queried by the Affymetrix *Drosophila* Genome 2.0 microarray that are expressed in S2 cells (Methods Section 6.3.10). For all genes ecdysone induced fold change and p-value (Student's t-test) compared to untreated cells for Nascent (N) RNA, Total RNA (T), Synthesis (S) rate and Decay (D) rate data sets are shown. Significant induction or repression as well as time series hit (*betr*) is stated (Methods Section 6.3.12).

Supplementary Table 2: *top*GO functional enrichment of ecdysone regulated genes
Ecdysone regulated genes were tested for functional enrichment in GO terms of "Biological Process", "Cellular Component" and "Molecular Function" using *top*GO (Method Section 6.3.13.1). Enrichment was calculated for (i) all regulated genes), (ii) induced genes and (iii) repressed genes. The *elim* algorithm was used to sort the enriched GO categories according to their p-value.

Supplementary Table 3: ClueGO functional enrichment of ecdysone regulated genes
All regulated genes were tested for functional enrichment in terms related to Cell Cycle, Metabolism, Differentiation/Morphogenesis using the Cytoscape plugin ClueGO (Methods Section 6.3.13.2).

Supplementary Table 4: ClueGO functional enrichment of differentially regulated synthesis and decay rates
Genes with altered synthesis and decay rates were tested for functional enrichment in in GO and KEGG terms of "Biological Process" using the Cytoscape plugin ClueGO (Methods Section 6.3.13.2).

Supplementary Table 5: Functional enrichment of k-means clusters
The functional annotation enrichment of each cluster was calculated using Fisher's exact test against all genes present on the Affymetrix *Drosophila* genome 2.0 array (Methods Section 6.3.15.3).

Supplementary Table 6: Spike-In sequences used for DTA-RNA-Sequencing
Methods Section 6.5.1 and Table 4.

Supplementary Table 7: InDA-C oligo sequences used for DTA-RNA-Sequencing
Methods Section 6.5.2.

13 Supplementary File (CD-ROM)

Supplementary File: DTA output files and *betr* time series hits
DTA package output lists for labeled (nascent) expression, total expression, synthesis rate and decay rate (Methods Section 6.3.10, 6.3.11). *Betr* time series hits for labeled and total RNA (Methods Section 6.3.12).

References

[1] Adrian Alexa, Jörg Rahnenführer, and Thomas Lengauer. Improved scoring of functional groups from gene expression data by decorrelating GO graph structure. *Bioinformatics*, 22(13):1600–7, July 2006. 6.3.13.1, 7.5, 7.9

[2] Panagiotis Alexiou, Manolis Maragkakis, Giorgos L Papadopoulos, Martin Reczko, and Artemis G Hatzigeorgiou. Lost in translation: an assessment and perspective for computational microRNA target identification. *Bioinformatics (Oxford, England)*, 25(23):3049–55, December 2009. 1.2.2.4

[3] Brian D Almond, Alex Zdanovsky, Marina Zdanovskaia, Dongping Ma, Pete Stecha, Aileen Paguio, Denise Garvin, Keith Wood, and Promega Corporation. Promega Notes 87: Introducing the Rapid Response(TM) Reporter Vector. 9

[4] Stefan Ludwig Ameres, Javier Martinez, and Renée Schroeder. Molecular basis for target RNA recognition and cleavage by human RISC. *Cell*, 130(1):101–12, July 2007. 1.2.2.2

[5] Simon Anders and Wolfgang Huber. Differential expression analysis for sequence count data. *Genome biology*, 11(10):R106, January 2010. 6.5.4

[6] Phil Arnold, Ionas Erb, Mikhail Pachkov, Nacho Molina, and Erik van Nimwegen. MotEvo: integrated Bayesian probabilistic methods for inferring regulatory sites and motifs on multiple alignments of DNA sequences. *Bioinformatics*, 28(4):487–94, February 2012. 9

[7] Martin J Aryee, José a Gutiérrez-Pabello, Igor Kramnik, Tapabrata Maiti, and John Quackenbush. An improved empirical bayes approach to estimating differential gene expression in microarray time-course data: BETR (Bayesian Estimation of Temporal Regulation). *BMC bioinformatics*, 10(409):409, January 2009. 6.3.12.2, 7.4

[8] Michael Ashburner. Sequential gene activation by ecdysone in polytene chromosomes of Drosophila melanogaster. *Developmental Biology*, 39(1):141–157, July 1974. 2.2, 7.15, 8

[9] Michael Ashburner. Gene Ontology : tool for the unification of biology. *Nature genetics*, 25:25–29, 2000. 7.5, 8

[10] Naomi Attar. The RBPome: where the brains meet the brawn. *Genome Biol*, 15(1):402, 2014. 9

[11] Paul Badenhorst, Hua Xiao, Lucy Cherbas, So Yeon Kwon, Matt Voas, Ilaria Rebay, Peter Cherbas, and Carl Wu. The Drosophila nucleosome remodeling factor NURF is required for Ecdysteroid signaling and metamorphosis. *Genes & development*, 19(21):2540–5, November 2005. 2.2

[12] Eric H Baehrecke. Ecdysone signaling cascade and regulation of Drosophila metamorphosis. *Archives of insect biochemistry and physiology*, 33(3-4):231–44, January 1996. 2, 2.1

[13] Jianwu Bai, Yoshihiko Uehara, and Denise J Montell. Regulation of invasive cell behavior by taiman, a Drosophila protein related to AIB1, a steroid receptor coactivator amplified in breast cancer. *Cell*, 103(7):1047–58, December 2000. 2.2, 7.14, 7.15

[14] Piotr J Balwierz, Mikhail Pachkov, Phil Arnold, Andreas J Gruber, Mihaela Zavolan, and Erik van Nimwegen. ISMARA: automated modeling of genomic signals as a democracy of regulatory motifs. *Genome research*, 24(5):869–84, March 2014. 9

[15] Ziv Bar-Joseph, Anthony Gitter, and Itamar Simon. Studying and modelling dynamic biological processes using time-series gene expression data. *Nature reviews. Genetics*, 13(8):552–64, August 2012. 9

[16] David P. Bartel. MicroRNAs: target recognition and regulatory functions. *Cell*, 136(2):215–233, Jan 2009. 1.2.2.1

[17] Arash Bashirullah, Amy E. Pasquinelli, Amy a. Kiger, Norbert Perrimon, Gary Ruvkun, and Carl S. Thummel. Coordinate regulation of small temporal RNAs at the onset of Drosophila metamorphosis. *Developmental biology*, 259(1):1–8, July 2003. 2.3

[18] Robert B Beckstead, Geanette Lam, and Carl S Thummel. The genomic response to 20-hydroxyecdysone at the onset of Drosophila metamorphosis. *Genome biology*, 6(12):R99, January 2005. 4, 8

[19] Matthias Behr, Dietmar Riedel, and Reinhard Schuh. The claudin-like megatrachea is essential in septate junctions for the epithelial barrier function in Drosophila. *Development Cell*, 5(4):611–620, Oct 2003. 7.14

[20] Eugene Berezikov, Nicolas Robine, Anastasia Samsonova, Jakub O Westholm, Ammar Naqvi, Jui-Hung Hung, Katsutomo Okamura, Qi Dai, Diane Bortolamiol-Becet, Raquel Martin, Yongjun Zhao, Phillip D Zamore, Gregory J Hannon, Marco a Marra, Zhiping Weng, Norbert Perrimon, and Eric C Lai. Deep annotation of Drosophila melanogaster microRNAs yields insights into their processing, modification, and emergence. *Genome research*, 21(2):203–15, February 2011. 7.11

[21] Edward Berger, Robert Ringler, Stamatis Alahiotis, and Mark Frank. Ecdysone-Induced Changes in Morphology and Protein Drosophila Cell Cultures Synthesis in. *Developmental biology*, 62:498–511, 1978. 8

[22] Doron Betel, Anjali Koppal, Phaedra Agius, Chris Sander, and Christina Leslie. Comprehensive modeling of microRNA targets predicts functional non-conserved and non-canonical sites. *Genome biology*, 11(8):R90, January 2010. 1.2.2.4, 6.4.6, 7.13, 20

[23] M Bettencourt-Dias, R Giet, R Sinka, a Mazumdar, W G Lock, F Balloux, P J Zafiropoulos, S Yamaguchi, S Winter, R W Carthew, M Cooper, D Jones, L Frenz, and D M Glover. Genome-wide survey of protein kinases required for cell cycle progression. *Nature*, 432(7020):980–7, December 2004. 6.1.4, 7.1

[24] Gabriela Bindea, Bernhard Mlecnik, Hubert Hackl, Pornpimol Charoentong, Marie Tosolini, Amos Kirilovsky, Wolf-Herman Fridman, Franck Pagès, Zlatko Trajanoski, and Jérôme Galon. ClueGO: a Cytoscape plug-in to decipher functionally grouped gene ontology and pathway annotation networks. *Bioinformatics*, 25(8):1091–3, April 2009. 6.3.13.2, 7.5, 11

[25] Mikael Björklund, Minna Taipale, Markku Varjosalo, Juha Saharinen, Juhani Lahdenperä, and Jussi Taipale. Identification of pathways regulating cell size and cell-cycle progression by RNAi. *Nature*, 439(7079):1009–13, February 2006. 6.1.4, 7.1

[26] Daniel Blankenberg, Assaf Gordon, Gregory Von Kuster, Nathan Coraor, James Taylor, and Anton Nekrutenko. Manipulation of FASTQ data with Galaxy. *Bioinformatics*, 26(14):1783–5, July 2010. 6.5.4

[27] Laura Boulan, David Martín, and Marco Milán. bantam miRNA promotes systemic growth by connecting insulin signaling and ecdysone production. *Current biology : CB*, 23(6):473–8, March 2013. 19

[28] Joerg E Braun, Eric Huntzinger, and Elisa Izaurralde. A molecular link between miRISCs and deadenylases provides new insight into the mechanism of gene silencing by microRNAs. *Cold Spring Harbor perspectives in biology*, 4(12), December 2012. 1.2.1, 1.2.2.2

[29] Almog Bregman, Moran Avraham-Kelbert, Oren Barkai, Lea Duek, Adi Guterman, and Mordechai Choder. Promoter Elements Regulate Cytoplasmic mRNA Decay. *Cell*, 147(7):1473–1483, December 2011. 9

[30] Alberts Bruce, Dennis Bray, Karen Hopkin, Alexander D Johnson, Julian Lewis, Martin Raff, Keith Roberts, and Peter Walter. Control of Gene Expression. In *Essentail Cell Biology*, volume 2, chapter 8, pages 269–299. 3rd edition, October 2009. 1

[31] Adolf Butenandt and Peter Karlson. Über die Isolierung eines Metamorphose-Hormons der Insekten in kristallisierter Form. *Zeitschrift für Naturforschung*, 9b(6):389–391, 1954. 2

[32] Dimitrios Cakouros, Tasman Daish, Damali Martin, Eric H Baehrecke, and Sharad Kumar. Ecdysone-induced expression of the caspase DRONC during hormone-dependent programmed cell death in Drosophila is regulated by Broad-Complex. *Cell*, 157(6):985–995, 2002. 7.1, 7.5, 8

[33] Marc Carlson. Affymetrix Drosophila Genome 2.0 Array annotation data (chip drosophila2). *R package version 2.14.0*. 6.3.13.1, 6.3.15.3

[34] D. R. Cavener and M. T. Clegg. The genetics of glutamate oxaloacetate transaminase in Drosophila melanogaster. *J Hered*, 67(5):313–314, 1976. 7.14

[35] Elizabeth E Caygill and Laura A Johnston. Temporal regulation of metamorphic processes in Drosophila by the let-7 and miR-125 heterochronic microRNAs. *Current biology : CB*, 18(13):943–50, July 2008. 2.3, 19, 7.12, 8

[36] The FANTOM Consortium & Riken Omics Science Center. The transcriptional network that controls growth arrest and differentiation in a human myeloid leukemia cell line. *Nature genetics*, 41(5):553–62, May 2009. 9

[37] Geetanjali Chawla and Nicholas S Sokol. Hormonal activation of let-7-C microRNAs via EcR is required for adult Drosophila melanogaster morphology and function. *Development*, 139(10):1788–97, May 2012. 2.3, 7.10, 19

[38] Lucy Cherbas. EcR isoforms in Drosophila: testing tissue-specific requirements by targeted blockade and rescue. *Development*, 130(2):271–284, January 2003. 2.2

[39] Lucy Cherbas, Aarron Willingham, Dayu Zhang, Li Yang, Yi Zou, Brian D Eads, Joseph W Carlson, Jane M Landolin, Philipp Kapranov, Jacqueline Dumais, Anastasia Samsonova, Jeong-Hyeon Choi, Johnny Roberts, Carrie A Davis, Haixu Tang, Marijke J van Baren, Srinka Ghosh, Alexander Dobin, Kim Bell, Wei Lin, Laura Langton, Michael O Duff, Aaron E Tenney, Chris Zaleski, Michael R Brent, Roger A Hoskins, Thomas C Kaufman, Justen Andrews, Brenton R Graveley, Norbert Perrimon, Susan E Celniker, Thomas R Gingeras, and Peter Cherbas. The transcriptional diversity of 25 Drosophila cell lines. *Genome research*, 21(2):301–14, February 2011. 6.3.10

[40] Suganthi Chittaranjan, Melissa McConechy, Ying-chen Claire Hou, J Douglas Freeman, and Sharon M Gorski. Steroid Hormone Control of Cell Death and Cell Survival : Molecular Insights Using RNAi. *PLoS Genetics*, 5(2):18–22, 2009. 7.1, 7.5, 8

[41] Piotr Chomczynski and Kevin Mackey. Short technical reports. Modification of the TRI reagent procedure for isolation of RNA from polysaccharide- and proteoglycan-rich sources. *BioTechniques*, 19(6):942–5, December 1995. 6.3.2

[42] Daniel Cirera-Salinas, Montse Pauta, Ryan M Allen, Alessandro G Salerno, Cristina M Ramírez, Aránzazu Chamorro-jorganes, Amarylis C Wanschel, Miguel A Lasunción, Manuel Morales-ruiz, Yajaira Suárez, Ángel Baldán, Enric Esplugues, and Carlos Fernández-hernando. Mir-33 regulates cell proliferation and cell cycle progression. *Cell Cycle*, 11(5):922–933, 2012. 19

[43] Michael D Cleary. Cell Type Specific Analysis of mRNA Synthesis and Decay In Vivo with Uracil Phosphoribosyltransferase and 4-thiouracil. *Methods*, 448(08):379–406, 2008. 3

[44] Michael D Cleary, Christopher D Meiering, Eric Jan, Rebecca Guymon, and John C Boothroyd. Biosynthetic labeling of RNA with uracil phosphoribosyltransferase allows cell-specific microarray analysis of mRNA synthesis and decay. *Nature Biotechnology*, 23(2):232–237, 2005. 3

[45] Melissa S Cline, Michael Smoot, Ethan Cerami, Allan Kuchinsky, Nerius Landys, Chris Workman, Rowan Christmas, Iliana Avila-Campilo, Michael Creech, Benjamin Gross, Kristina Hanspers, Ruth Isserlin, Ryan Kelley, Sarah Killcoyne, Samad Lotia, Steven Maere, John Morris, Keiichiro Ono, Vuk Pavlovic, Alexander R Pico, Aditya Vailaya, Peng-Liang Wang, Annette Adler, Bruce R Conklin, Leroy Hood, Martin Kuiper, Chris Sander, Ilya Schmulevich, Benno Schwikowski, Guy J Warner, Trey Ideker, and Gary D Bader. Integration of biological networks and gene expression data using Cytoscape. *Nature protocols*, 2(10):2366–82, January 2007. 6.3.13.2, 6.4.7, 21

[46] Jeff Coller and Roy Parker. Eukaryotic mRNA decapping. *Annu Rev Biochem*, 73:861–890, 2004. 1.2.1

[47] Kate B Cook, Hilal Kazan, Khalid Zuberi, Quaid Morris, and Timothy R Hughes. RBPDB: a database of RNA-binding specificities. *Nucleic acids research*, 39(Database issue):D301–8, January 2011. 7.15

[48] Ahmet M Denli, Bastiaan B J Tops, Ronald H a Plasterk, René F Ketting, and Gregory J Hannon. Processing of primary microRNAs by the Microprocessor complex. *Nature*, 432(7014):231–5, November 2004. 1.2.2.1

[49] Development Core Team. R: A language and environment for statistical computing. R Foundation for Statistical Computing, Vienna, Austria. ISBN 3-900051-07-0, 2011. 6.3.10

[50] Sergej Djuranovic, Ali Nahvi, and Rachel Green. miRNA-mediated gene silencing by translational repression followed by mRNA deadenylation and decay. *Science*, 336(6078):237–40, April 2012. 1.2.2.2

[51] Lars Dölken, Zsolt Ruzsics, Bernd Rädle, Caroline C Friedel, Ralf Zimmer, Jörg Mages, Reinhard Hoffmann, Paul Dickinson, Thorsten Forster, Peter Ghazal, and Ulrich H Koszinowski. High-resolution gene expression profiling for simultaneous kinetic parameter analysis of RNA synthesis and decay. *RNA*, 14(9):1959–72, September 2008. 3, 4, 6.3, 6.3.7, 7.2

[52] Mally Dori-Bachash, Ophir Shalem, Yair S Manor, Yitzhak Pilpel, and Itay Tirosh. Widespread promoter-mediated coordination of transcription and mRNA degradation. *Genome biology*, 13(12):R114, December 2012. 8, 9

[53] Mally Dori-Bachash, Efrat Shema, and Itay Tirosh. Coupled evolution of transcription and mRNA degradation. *PLoS biology*, 9(7):e1001106, July 2011. 8, 9

[54] Margaret S Ebert and Phillip A Sharp. Roles for microRNAs in conferring robustness to biological processes. *Cell*, 149(3):515–24, April 2012. 1.2.2.3

[55] Ivette F Emery, Vahe Bedian, and Gregory M Guild. Differential expression of Broad-Complex transcription factors may forecast tissue-specific developmental fates during Drosophila metamorphosis. *Development (Cambridge, England)*, 120(11):3275–87, November 1994. 7.2, 8

[56] Anton J Enright, Bino John, Ulrike Gaul, Thomas Tuschl, Chris Sander, and Debora S Marks. MicroRNA targets in Drosophila. *Genome biology*, 5(1):R1, January 2003. 6.4.6

[57] Jörg Enssle, Wilfried Kugler, Matthias W Hentze, and Andreas E Kulozik. Determination of mRNA fate by different RNA polymerase II promoters. *Proceedings of the National Academy of Sciences of the United States of America*, 90(21):10091–5, November 1993. 8, 9

[58] Stephanie Maria Esslinger, Björn Schwalb, Stephanie Helfer, Katharina Maria Michalik, Heidi Witte, Kerstin C Maier, Dietmar Martin, Bernhard Michalke, Achim Tresch, Patrick Cramer, and Klaus Förstemann. Drosophila miR-277 controls branched-chain amino acid catabolism and affects lifespan. *RNA biology*, 10(6):1–15, April 2013. 4, 19, 7.12, 7.14, 8

[59] Marc R Fabian and Nahum Sonenberg. The mechanics of miRNA-mediated gene silencing: a look under the hood of miRISC. *Nature structural & molecular biology*, 19(6):586–93, June 2012. 1.2.2.2

[60] Joshua J Forman, Aster Legesse-Miller, and Hilary A Coller. A search for conserved sequences in coding regions reveals that the let-7 microRNA targets Dicer within its coding sequence. *Proceedings of the National Academy of Sciences of the United States of America*, 105(39):14879–84, September 2008. 1.2.2.2

[61] Klaus Förstemann, Yukihide Tomari, Tingting Du, Vasily V Vagin, Ahmet M Denli, Diana P Bratu, Carla Klattenhoff, William E Theurkauf, and Phillip D Zamore. Normal microRNA maturation and germ-line stem cell maintenance requires Loquacious, a double-stranded RNA-binding domain protein. *PLoS biology*, 3(7):e236, July 2005. 6.4.2

[62] Víctor A Francis, Antonio Zorzano, and Aurelio A Teleman. dDOR is an EcR coactivator that forms a feed-forward loop connecting insulin and ecdysone signaling. *Current biology : CB*, 20(20):1799–808, October 2010. 2.2

[63] Josè Garcìa-Martìnez, Agustìn Aranda, and Josè E Pèrez-Ortìn. Genomic Run-On Evaluates Transcription Rates for All Yeast Genes and Identifies Gene Regulatory Mechanisms. *Molecular cell*, 15:303–313, 2004. 3

[64] Nicole L Garneau, Jeffrey Wilusz, and Carol J Wilusz. The highways and byways of mRNA decay. *Nature reviews. Molecular cell biology*, 8(2):113–26, February 2007. 1.2.1

[65] Julie Gates, Geanette Lam, José A Ortiz, Régine Losson, and Carl S Thummel. rigor mortis encodes a novel nuclear receptor interacting protein required for ecdysone signaling during Drosophila larval development. *Development*, 131(1):25–36, January 2004. 2.2

[66] Zareen Gauhar, Ling V Sun, Sujun Hua, Christopher E Mason, Florian Fuchs, Tong-Ruei Li, Michael Boutros, and Kevin P White. Genomic mapping of binding regions for the Ecdysone receptor protein complex. *Genome research*, 19(6):1006–13, June 2009. 2.2, 4, 8

[67] Leslie Gay, Kate V Karfilis, Michael R Miller, Chris Q Doe, and Kryn Stankunas. Applying thiouracil tagging to mouse transcriptome analysis. *Nature protocols*, 9(2):410–20, February 2014. 3

[68] Fátima Gebauer and Matthias W Hentze. Molecular mechanisms of translational control. *Nature reviews. Molecular cell biology*, 5(10):827–35, October 2004. 1.2.1

[69] Gary K Geiss, Roger E Bumgarner, Brian Birditt, Timothy Dahl, Naeem Dowidar, Dwayne L Dunaway, H Perry Fell, Sean Ferree, Renee D George, Tammy Grogan, Jeffrey J James, Malini Maysuria, Jeffrey D Mitton, Paola Oliveri, Jennifer L Osborn, Tao Peng, Amber L Ratcliffe, Philippa J Webster, Eric H Davidson, Leroy Hood, and Krassen Dimitrov. Direct multiplexed measurement of gene expression with color-coded probe pairs. *Nature biotechnology*, 26(3):317–25, March 2008. 7.11

[70] Robert C Gentleman, Vincent J Carey, Douglas M Bates, Ben Bolstad, Marcel Dettling, Sandrine Dudoit, Byron Ellis, Laurent Gautier, Yongchao Ge, Jeff Gentry, Kurt Hornik, Torsten Hothorn, Wolfgang Huber, Stefano Iacus, Rafael Irizarry, Friedrich Leisch, Cheng Li, Martin Maechler, Anthony J Rossini, Gunther Sawitzki, Colin Smith, Gordon Smyth, Luke Tierney, Jean Y H Yang, and Jianhua Zhang. Bioconductor: open software development for computational biology and bioinformatics. *Genome biology*, 5(10):R80, January 2004. 6.3.10

[71] André P Gerber, Stefan Luschnig, Mark A Krasnow, Patrick O Brown, and Daniel Herschlag. Genome-wide identification of mRNAs associated with the translational regulator PUMILIO in Drosophila melanogaster. *Proceedings of the National Academy of Sciences of the United States of America*, 103(12):4487–92, March 2006. 6.3.15.3, 7.15, 22

[72] Belinda Giardine, Cathy Riemer, Ross C Hardison, Richard Burhans, Laura Elnitski, Prachi Shah, Yi Zhang, Daniel Blankenberg, Istvan Albert, James Taylor, Webb Miller, W James Kent, and Anton Nekrutenko. Galaxy: a platform for interactive large-scale genome analysis. *Genome research*, 15(10):1451–5, October 2005. 6.5.4

[73] Jeremy Goecks, Anton Nekrutenko, and James Taylor. Galaxy: a comprehensive approach for supporting accessible, reproducible, and transparent computational research in the life sciences. *Genome biology*, 11(8):R86, January 2010. 6.5.4

[74] Aaron C Goldstrohm and Marvin Wickens. Multifunctional deadenylase complexes diversify mRNA control. *Nature reviews. Molecular cell biology*, 9(4):337–344, April 2008. 1.2.1

[75] Sarah E Gonsalves, Scott J Neal, Amy S Kehoe, and J Timothy Westwood. Genome-wide examination of the transcriptional response to ecdysteroids 20-hydroxyecdysone and ponasterone A in Drosophila melanogaster. *BMC genomics*, 12(475), January 2011. 4, 8

[76] Brenton R Graveley, Angela N Brooks, Joseph W Carlson, Michael O Duff, Jane M Landolin, Li Yang, Carlo G Artieri, Marijke J van Baren, Nathan Boley, Benjamin W Booth, James B Brown, Lucy Cherbas, Carrie A Davis, Alex Dobin, Renhua Li, Wei Lin, John H Malone, Nicolas R Mattiuzzo, David Miller, David Sturgill, Brian B Tuch, Chris Zaleski, Dayu Zhang, Marco Blanchette, Sandrine Dudoit, Brian Eads, Richard E Green, Ann Hammonds, Lichun Jiang, Phil Kapranov, Laura Langton, Norbert Perrimon, Jeremy E Sandler, Kenneth H Wan, Aarron Willingham, Yu Zhang, Yi Zou, Justen Andrews, Peter J Bickel, Steven E Brenner, Michael R Brent, Peter Cherbas, Thomas R Gingeras, Roger A Hoskins, Thomas C

Kaufman, Brian Oliver, and Susan E Celniker. The developmental transcriptome of Drosophila melanogaster. *Nature*, 471(7339):473–9, March 2011. 6.3.10

[77] Andrew Grimson, Kyle Kai-How Farh, Wendy K Johnston, Philip Garrett-Engele, Lee P Lim, and David P Bartel. MicroRNA targeting specificity in mammals: determinants beyond seed pairing. *Molecular cell*, 27(1):91–105, July 2007. 1.2.2.2

[78] Stephen T Guest, Jingkai Yu, Dongmei Liu, Julie A Hines, Maria A Kashat, and Russell L Finley. A protein network-guided screen for cell cycle regulators in Drosophila. *BMC Systems Biology*, 5(1):65, 2011. 7.14

[79] Markus Hafner, Markus Landthaler, Lukas Burger, Mohsen Khorshid, Jean Hausser, Philipp Berninger, Andrea Rothballer, Manuel Ascano, Anna-carina Jungkamp, Mathias Munschauer, Alexander Ulrich, Greg S Wardle, Scott Dewell, Mihaela Zavolan, and Thomas Tuschl. Resource Transcriptome-wide Identification of RNA-Binding Protein and MicroRNA Target Sites by PAR-CLIP. *Cell*, 141(1):129–141, 2010. 1.2.2.4

[80] Gal Haimovich, Mordechai Choder, Robert H Singer, and Tatjana Trcek. The fate of the messenger is pre-determined: a new model for regulation of gene expression. *Biochimica et biophysica acta*, 1829(6-7):643–53, 2013. 1.2.1, 8, 9

[81] Gal Haimovich, Daniel A. Medina, Sebastien Z. Causse, Manuel Garber, Gonzalo Millán-Zambrano, Oren Barkai, Sebastián Chávez, José E. Pérez-Ortín, Xavier Darzacq, and Mordechai Choder. Gene expression is circular: factors for mRNA degradation also foster mRNA synthesis. *Cell*, 153(5):1000–1011, May 2013. 9

[82] Scott M Hammond, Emily Bernstein, David Beach, and Gregory J Hannon. An RNA-directed nuclease mediates post-transcriptional gene silencing in Drosophila cells. *Nature*, 404(6775):293–6, March 2000. 7.1, 7

[83] Shruti Haralalka, Claude Shelton, Heather N. Cartwright, Erin Katzfey, Evan Janzen, and Susan M. Abmayr. Asymmetric mbc, active rac1 and f-actin foci in the fusion-competent myoblasts during myoblast fusion in drosophila. *Development*, 138(8):1551–1562, Apr 2011. 7.14

[84] Liat Harel-Sharvit, Naama Eldad, Gal Haimovich, Oren Barkai, Lea Duek, and Mordechai Choder. RNA polymerase II subunits link transcription and mRNA decay to translation. *Cell*, 143(4):552–63, November 2010. 8, 9

[85] Jean Hausser, Afzal Pasha Syed, Biter Bilen, and Mihaela Zavolan. Analysis of CDS-located miRNA target sites suggests that they can effectively inhibit translation. *Genome research*, 23(4):604–15, April 2013. 1.2.2.2

[86] David G Hendrickson, Daniel J Hogan, Heather L McCullough, Jason W Myers, Daniel Herschlag, James E Ferrell, and Patrick O Brown. Concordant regulation of translation and mRNA abundance for hundreds of targets of a human microRNA. *PLoS biology*, 7(11):e1000238, November 2009. 1.2.2.2

[87] Héctor Herranz and Stephen M Cohen. MicroRNAs and gene regulatory networks: managing the impact of noise in biological systems. *Genes & development*, 24(13):1339–44, July 2010. 1.2.2.3

[88] John W B Hershey, Nahum Sonenberg, and Michael B Mathews. Principles of translational control: an overview. *Cold Spring Harbor perspectives in biology*, 4(12):a011528, December 2012. 1

[89] Ronald J Hill, Isabelle M L Billas, François Bonneton, Lloyd D Graham, and Michael C Lawrence. Ecdysone receptors: from the Ashburner model to structural biology. *Annual review of entomology*, 58:251–71, January 2013. 4, 7.4

[90] Catarina C.F. Homem, Victoria Steinmann, Thomas R. Burkard, Alexander Jais, Harald Esterbauer, and Juergen A. Knoblich. Ecdysone and Mediator Change Energy Metabolism to Terminate Proliferation in Drosophila Neural Stem Cells. *Cell*, 158(4):874–888, August 2014. 9

[91] Jonathan Houseley and David Tollervey. The many pathways of RNA degradation. *Cell*, 136(4):763–776, Feb 2009. 1.2.1

[92] Xiao Hu, Lucy Cherbas, and Peter Cherbas. Transcription activation by the ecdysone receptor (EcR/USP): identification of activation functions. *Molecular endocrinology (Baltimore, Md.)*, 17(4):716–31, April 2003. 2.2

[93] Francois Huet, Claude Ruiz, and Geoff Richards. Sequential gene activation by ecdysone in Drosophila melanogaster: the hierarchical equivalence of early and early late genes. *Development*, 121(4):1195–204, April 1995. 2.2, 7.15

[94] Eric Huntzinger and Elisa Izaurralde. Gene silencing by microRNAs: contributions of translational repression and mRNA decay. *Nature reviews. Genetics*, 12(2):99–110, February 2011. 1.2.2.2

[95] Seogang Hyun, Jung Hyun Lee, Hua Jin, JinWu Nam, Bumjin Namkoong, Gina Lee, Jongkyeong Chung, and V Narry Kim. Conserved MicroRNA miR-8/miR-200 and its target USH/FOG2 control growth by regulating PI3K. *Cell*, 139(6):1096–108, December 2009. 2.3, 7.10, 19

[96] Masafumi Inui, Graziano Martello, and Stefano Piccolo. MicroRNA control of signal transduction. *Nature reviews. Molecular cell biology*, 11(4):252–63, April 2010. 1.2.2, 1.2.2.1, 1.2.2.3

[97] Nicola Iovino, Attilio Pane, and Ulrike Gaul. miR-184 has multiple roles in Drosophila female germline development. *Developmental cell*, 17(1):123–33, July 2009. 1.2.2.3, 19

[98] Naduparambil Korah Jacob, James V Cooley, Tamara N Yee, Jidhin Jacob, Hansjuerg Alder, Priyankara Wickramasinghe, Kirsteen H Maclean, and Arnab Chakravarti. Identification of Sensitive Serum microRNA Biomarkers for Radiation Biodosimetry. *PloS one*, 8(2):e57603, January 2013. 6.4.5

[99] Changan Jiang, J Lamblin, Hermann Steller, Carl S Thummel, and Howard Hughes. A Steroid-Triggered Transcriptional Hierarchy Controls Salivary Gland Cell Death during Drosophila Metamorphosis. 5:445–455, 2000. 7.5

[100] Hua Jin, V Narry Kim, and Seogang Hyun. Conserved microRNA miR-8 controls body size in response to steroid signaling in Drosophila. *Genes & development*, 26(13):1427–32, July 2012. 2.3, 7.10, 19, 7.14, 8

[101] Tamar Juven-Gershon and James T Kadonaga. Regulation of gene expression via the core promoter and the basal transcriptional machinery. *Developmental biology*, 339(2):225–9, March 2010. 1.1

[102] Sebastian Kadener, Joseph Rodriguez, Katharine Compton Abruzzi, Yevgenia L Khodor, Ken Sugino, Michael T Marr, Sacha Nelson, and Michael Rosbash. Genome-wide identification of targets of the drosha-pasha/DGCR8 complex. *RNA*, 15(4):537–45, April 2009. 19, 7.12

[103] Minoru Kanehisa and Susumu Goto. KEGG: kyoto encyclopedia of genes and genomes. *Nucleic acids research*, 28(1):27–30, January 2000. 6.3.13.2, 7.5, 8

[104] Felix D Karim and Carl S Thummel. Temporal coordination of regulatory gene expression by the steroid hormone ecdysone. *The EMBO journal*, 11(11):4083–93, November 1992. 2.2

[105] M Kenzelmann, S Maertens, M Hergenhahn, S Kueffer, A Hotz-Wagenblatt, L Li, S Wang, C Ittrich, T Lemberger, R Arribas, S Jonnakuty, M C Hollstein, W Schmidt, N Gretz, H J Gröne, and G Schütz. Microarray analysis of newly synthesized RNA in cells and animal. *PNAS*, 104(15):6164–6169, 2007. 3

[106] Michael Kertesz, Nicola Iovino, Ulrich Unnerstall, Ulrike Gaul, and Eran Segal. The role of site accessibility in microRNA target recognition. *Nature genetics*, 39(10):1278–84, October 2007. 1.2.2.4

[107] Daehwan Kim, Geo Pertea, Cole Trapnell, Harold Pimentel, Ryan Kelley, and Steven L Salzberg. TopHat2: accurate alignment of transcriptomes in the presence of insertions, deletions and gene fusions. *Genome biology*, 14(4):R36, April 2013. 6.5.4

[108] Hyeon Ho Kim, Yuki Kuwano, Subramanya Srikantan, Eun Kyung Lee, Jennifer L Martindale, and Myriam Gorospe. HuR recruits let-7/RISC to repress c-Myc expression. *Genes & development*, 23(15):1743–8, August 2009. 1.2.2.1, 19

[109] Shuhei Kimura, Shun Sawatsubashi, Saya Ito, Alexander Kouzmenko, Eriko Suzuki, Yue Zhao, Kaoru Yamagata, Masahiko Tanabe, Takashi Ueda, Sari Fujiyama, Takuya Murata, Hiroyuki Matsukawa, Ken-Ichi Takeyama, Nobuo Yaegashi, and Shigeaki Kato. Drosophila arginine methyltransferase 1 (DART1) is an ecdysone receptor co-repressor. *Biochemical and biophysical research communications*, 371(4):889–93, July 2008. 2.2

[110] Kirst King-Jones and Carl S Thummel. Nuclear receptors–a perspective from Drosophila. *Nature reviews. Genetics*, 6(4):311–23, April 2005. 2, 2.2

[111] Marianthi Kiriakidou, Grace S. Tan, Styliani Lamprinaki, Mariangels De Planell-Saguer, Peter T. Nelson, and Zissimos Mourelatos. An mRNA m7G cap binding-like motif within human Ago2 represses translation. *Cell*, 129(6):1141–51, Jun 2007. 1.2.2.2

[112] Shivendra Kishore, Sandra Luber, and Mihaela Zavolan. Deciphering the role of RNA-binding proteins in the post-transcriptional control of gene expression. *Briefings in functional genomics*, 9(5-6):391–404, December 2010. 1.2.1

[113] M R Koelle, W S Talbot, W a Segraves, M T Bender, P Cherbas, and D S Hogness. The Drosophila EcR gene encodes an ecdysone receptor, a new member of the steroid receptor superfamily. *Cell*, 67(1):59–77, October 1991. 2.2

[114] Suzanne Komili and Pamela A Silver. Coupling and coordination in gene expression processes: a systems biology view. *Nature reviews. Genetics*, 9(1):38–48, January 2008. 1, 1.1, 9

[115] Triinu Koressaar and Maido Remm. Enhancements and modifications of primer design program Primer3. *Bioinformatics*, 23(10):1289–91, May 2007. 3, 6.3.8

[116] Dirk Kostrewa, Mirijam E Zeller, Karim-Jean Armache, Martin Seizl, Kristin Leike, Michael Thomm, and Patrick Cramer. RNA polymerase II-TFIIB structure and mechanism of transcription initiation. *Nature*, 462(7271):323–30, November 2009. 1.1

[117] Jacek Krol, Inga Loedige, and Witold Filipowicz. The widespread regulation of microRNA biogenesis, function and decay. *Nature reviews. Genetics*, 11(9):597–610, September 2010. 1.2.2.3, 2

[118] Mariya M Kucherenko and Halyna R Shcherbata. Steroids as external temporal codes act via microRNAs and cooperate with cytokines in differential neurogenesis. *Fly*, 7(3):173–183, 2013. 2.2

[119] Meghana M Kulkarni. Digital multiplexed gene expression analysis using the NanoString nCounter system. *Current protocols in molecular biology*, Chapter 25(April):Unit25B.10, April 2011. 7.11, 7.13

[120] Ben Langmead, Cole Trapnell, Mihai Pop, and Steven L Salzberg. Ultrafast and memory-efficient alignment of short DNA sequences to the human genome. *Genome biology*, 10(3):R25, January 2009. 6.5.4

[121] D. M. Lastowski and D. R. Falk. Characterization of an autosomal rudimentary-shaped wing mutation in Drosophila melanogaster that affects pyrimidine synthesis. *Genetics*, 96(2):471–478, Oct 1980. 7.14

[122] Dan Leaman, Po Yu Chen, John Fak, Abdullah Yalcin, Michael Pearce, Ulrich Unnerstall, Debora S Marks, Chris Sander, Thomas Tuschl, and Ulrike Gaul. Antisense-Mediated Depletion Reveals Essential and Specific Functions of MicroRNAs in Drosophila Development. *Development*, 121(7):1097–1108, 2005. 1.2.2.3, 8

[123] Alice Lebreton and Bertrand Séraphin. Exosome-mediated quality control: substrate recruitment and molecular activity. *Biochim Biophys Acta*, 1779(9):558–565, Sep 2008. 1.2.1

[124] Cheng-Yu Lee, Emily A Clough, Paula Yellon, Tanya M Teslovich, Dietrich A Stephan, and Eric H Baehrecke. Genome-wide analyses of steroid- and radiation-triggered programmed cell death in Drosophila. *Current biology : CB*, 13(4):350–7, March 2003. 7.5

[125] Rosalind C Lee, Rhonda L Feinbaum, and Victor Ambros. The C . elegans Heterochronic Gene lin-4 Encodes Small RNAs with Antisense Complementarity to lin-14. *Cell*, 75:843–854, 1993. 1.2.2

[126] Tong. I. Lee and Richard A. Young. Transcription of eukaryotic protein-coding genes. *Annual Review of Genetics*, 34:77–137, 2000. 1.1

[127] Yoontae Lee, Chiyoung Ahn, Jinju Han, Hyounjeong Choi, Jaekwang Kim, Jeongbin Yim, Junho Lee, Patrick Provost, Olof Rå dmark, Sunyoung Kim, and V Narry Kim. The nuclear RNase III Drosha initiates microRNA processing. *Nature*, 425(6956):415–9, September 2003. 1.2.2.1

[128] Jingyi Jessica Li, Peter J Bickel, and Mark D Biggin. System wide analyses have underestimated protein abundances and the importance of transcription in mammals. *PeerJ*, 2:e270, January 2014. 4

[129] Tong-Ruei Li and Kevin P White. Tissue-specific gene expression and ecdysone-regulated genomic networks in Drosophila. *Developmental cell*, 5(1):59–72, July 2003. 4, 8

[130] Nan Liu, Michael Landreh, Kajia Cao, Masashi Abe, Gert-Jan Hendriks, Jason R Kennerdell, Yongqing Zhu, Li-San Wang, and Nancy M Bonini. The microRNA miR-34 modulates ageing and neurodegeneration in Drosophila. *Nature*, 482(7386):519–23, February 2012. 19, 7.12

[131] Kenneth J Livak and Thomas D Schmittgen. Analysis of relative gene expression data using real-time quantitative PCR and the 2(-Delta Delta C(T)) Method. *Methods*, 25(4):402–8, December 2001. 6.3.8, 6.4.3

[132] Inga Loedige, Mathias Stotz, Saadia Qamar, Katharina Kramer, Janosch Hennig, Thomas Schubert, Patrick Löffler, Gernot Längst, Rainer Merkl, Henning Urlaub, and Gunter Meister. The NHL domain of BRAT is an RNA-binding domain that directly contacts the hunchback mRNA for regulation. *Genes & development*, 28(7):749–64, April 2014. 7.15

[133] John J. Long, Anne Leresche, Richard W. Kriwacki, and Joel M. Gottesfeld. Repression of TFIIH transcriptional activity and TFIIH-associated cdk7 kinase activity at mitosis. *Mol Cell Biol*, 18(3):1467–1476, Mar 1998. 7.14

[134] Keira Lucas and Alexander S Raikhel. Insect microRNAs: biogenesis, expression profiling and biological functions. *Insect biochemistry and molecular biology*, 43(1):24–38, January 2013. 1.2.2.1, 1.2.2.3

[135] Carol S Lutz and Alexandra Moreira. Alternative mRNA polyadenylation in eukaryotes: an effective regulator of gene expression. *Wiley interdisciplinary reviews. RNA*, 2(1):23–31, 2011. 1.2.1

[136] J Robin Lytle, Therese A Yario, and Joan A Steitz. Target mRNAs are repressed as efficiently by microRNA-binding sites in the 5' UTR as in the 3' UTR. *Proceedings of the National Academy of Sciences of the United States of America*, 104(23):9667–72, June 2007. 1.2.2.2

[137] William H Majoros and Uwe Ohler. Spatial preferences of microRNA targets in 3' untranslated regions. *BMC genomics*, 8(152), January 2007. 1.2.2.2

[138] Lisa Marcinowski, Michael Lidschreiber, Lukas Windhager, Martina Rieder, Jens B Bosse, Bernd Rädle, Thomas Bonfert, Ildiko György, Miranda de Graaf, Olivia Prazeres da Costa, Philip Rosenstiel, Caroline C Friedel, Ralf Zimmer, Zsolt Ruzsics, and Lars Dölken. Real-time Transcriptional Profiling of Cellular and Viral Gene Expression during Lytic Cytomegalovirus Infection. *PLoS pathogens*, 8(9):e1002908, September 2012. 3

[139] April K Marrone, Evgeniia V Edeleva, Mariya M Kucherenko, Nai-Hua Hsiao, and Halyna R Shcherbata. Dg-Dys-Syn1 signaling in Drosophila regulates the microRNA profile. *BMC cell biology*, 13(1):26, January 2012. 7.14

[140] Gunter Meister. Argonaute proteins: functional insights and emerging roles. *Nature reviews. Genetics*, 14(7):447–459, 2013. 1.2.2.1

[141] Gunter Meister, Markus Landthaler, Agnieszka Patkaniowska, Yair Dorsett, Grace Teng, and Thomas Tuschl. Human Argonaute2 mediates RNA cleavage targeted by miRNAs and siRNAs. *Mol Cell*, 15(2):185–197, Jul 2004. 1.2.2.2

[142] William T. Melvin, Helen B. Milne, Alison A. Slater, Hamish J. Allen, and Hamish M. Keir. Incorporation of 6-Thioguanosine and 4-Thiouridine into RNA. Application to Isolation of Newly Synthesised RNA by Affinity Chromatography. *European Journal of Biochemistry*, 92(2):373–379, December 1978. 3

[143] Thomas J. S. Merritt, Caitlin Kuczynski, Efe Sezgin, Chen-Tseh. Zhu, Seiji Kumagai, and Walter F. Eanes. Quantifying Interactions Within the NADP(H) Enzyme Network in Drosophila melanogaster. *Genetics*, 182(2):565–574, Mar 2009. 7.14

[144] Christian Miller, Björn Schwalb, Kerstin Maier, Daniel Schulz, Sebastian Dümcke, Benedikt Zacher, Andreas Mayer, Jasmin Sydow, Lisa Marcinowski, Lars Dölken, Dietmar E Martin, Achim Tresch, and Patrick Cramer. Dynamic transcriptome analysis measures rates of mRNA synthesis and decay in yeast. *Molecular systems biology*, 7(458):458, January 2011. 5, 3, 4, 6.3, 6.3.11, 6.3.11, 6.3.11, 7.3, 7.13, 8, 10.1

[145] Michael R Miller, Kristin J Robinson, Michael D Cleary, and Chris Q Doe. TU-tagging : cell type-specific RNA isolation from intact complex tissues. *Nature Publishing Group*, 6(6):439–441, 2009. 3

[146] Javier Morante, Diana M Vallejo, Claude Desplan, and Maria Dominguez. Conserved miR-8/miR-200 defines a glial niche that controls neuroepithelial expansion and neuroblast transition. *Developmental cell*, 27(2):174–87, October 2013. 19

[147] Francesca Moretti, Constanze Kaiser, Agnieszka Zdanowicz-Specht, and Matthias W. Hentze. PABP and the poly(A) tail augment microRNA repression by facilitated miRISC binding. *Nat Struct Mol Biol*, 19(6):603–608, Jun 2012. 1.2.2.2

[148] Bruno Mugat, Veronique Brodu, Jana Kejzlarova-Lepesant, Christo Antoniewski, Cynthia A Bayer, James W Fristrom, and Jean-Antoine Lepesant. Dynamic expression of broad-complex isoforms mediates temporal control of an ecdysteroid target gene at the onset of Drosophila metamorphosis. *Developmental biology*, 227(1):104–17, November 2000. 2.2

[149] Sarah E Munchel, Ryan K Shultzaberger, Naoki Takizawa, and Karsten Weis. Dynamic profiling of mRNA turnover reveals gene-specific and system-wide regulation of mRNA decay. *Molecular biology of the cell*, 22(15):2787–95, August 2011. 8

[150] Ander Muniategui, Jon Pey, Francisco J Planes, and Angel Rubio. Joint analysis of miRNA and mRNA expression data. *Briefings in bioinformatics*, 14(3):263–78, May 2013. 7.13, 9

[151] Shane Neph, Jeff Vierstra, Andrew B. Stergachis, Alex P. Reynolds, Eric Haugen, Benjamin Vernot, Robert E. Thurman, Sam John, Richard Sandstrom, Audra K. Johnson, and et al. An expansive human regulatory lexicon encoded in transcription factor footprints. *Nature*, 489(7414):83–90, Sep 2012. 9

[152] Tadashi Nishihara, Latifa Zekri, Joerg E Braun, and Elisa Izaurralde. miRISC recruits decapping factors to miRNA targets to enhance their degradation. *Nucleic acids research*, 41(18):8692–705, October 2013. 1.2.2.2

[153] Takafumi Noma, Ryutaro Murakami, Yasuhiro Yamashiro, Koichi Fujisawa, Sachie Inouye, and Atsushi Nakazawa. cDNA cloning and chromosomal mapping of the gene encoding adenylate kinase 2 from Drosophila melanogaster. *Biochimica et Biophysica Acta (BBA) - Gene Structure and Expression*, 1490(1-2):109–114, Jan 2000. 7.14

[154] Noa Novershtern, Aravind Subramanian, Lee N. Lawton, Raymond H. Mak, W Nicholas Haining, Marie E. McConkey, Naomi Habib, Nir Yosef, Cindy Y. Chang, Tal Shay, Garrett M. Frampton, Adam C B. Drake, Ilya Leskov, Bjorn Nilsson, Fred Preffer, David Dombkowski, John W. Evans, Ted Liefeld, John S. Smutko, Jianzhu Chen, Nir Friedman, Richard A. Young, Todd R. Golub, Aviv Regev, and Benjamin L. Ebert. Densely interconnected transcriptional circuits control cell states in human hematopoiesis. *Cell*, 144(2):296–309, Jan 2011. 9

[155] Qiuxiang Ou and Kirst King-Jones. What goes up must come down: transcription factors have their say in making ecdysone pulses. *Current topics in developmental biology*, 103:35–71, January 2013. 2.1, 3, 2.1, 2.2, 4

[156] Athma A Pai, Carolyn E Cain, Orna Mizrahi-Man, Sherryl De Leon, Noah Lewellen, Jean-Baptiste Veyrieras, Jacob F Degner, Daniel J Gaffney, Joseph K Pickrell, Matthew Stephens, Jonathan K Pritchard, and Yoav Gilad. The contribution of RNA decay quantitative trait loci to inter-individual variation in steady-state gene expression levels. *PLoS genetics*, 8(10):e1003000, January 2012. 8, 9

[157] Sharon E. Perez and Hermann Steller. Molecular and genetic analyses of lama, an evolutionarily conserved gene expressed in the precursors of the Drosophila first optic ganglion. *Mechanisms of Development*, 59(1):11–27, Sep 1996. 7.14

[158] Sudhakaran Prabakaran, Guy Lippens, Hanno Steen, and Jeremy Gunawardena. Post-translational modification: nature's escape from genetic imprisonment and the basis for dynamic information encoding. *WIREs Syst Biol Med*, 4(6):565–83, Aug 2012. 1

[159] Sreerangam N C V L Pushpavalli, Arpita Sarkar, Indira Bag, Clayton R Hunt, M Janaki Ramaiah, Tej K Pandita, Utpal Bhadra, and Manika Pal-Bhadra. Argonaute-1 functions as a mitotic regulator by controlling Cyclin B during Drosophila early embryogenesis. *FASEB journal : official publication of the Federation of American Societies for Experimental Biology*, 28(2):655–66, February 2014. 19, 7.12

[160] Michal Rabani, Joshua Z Levin, Lin Fan, Xian Adiconis, Raktima Raychowdhury, Manuel Garber, Andreas Gnirke, Chad Nusbaum, Nir Hacohen, Nir Friedman, Ido Amit, and Aviv Regev. Metabolic labeling of RNA uncovers principles of RNA production and degradation dynamics in mammalian cells. *Nature biotechnology*, 29(5):436–42, May 2011. 1, 3, 4, 4, 8

[161] Marta Radman-Livaja and Oliver J Rando. Nucleosome positioning: how is it established, and why does it matter? *Developmental biology*, 339(2):258–66, March 2010. 1.1

[162] Arvind Raghavan and Paul R Bohjanen. Microarray-based analyses of mRNA decay in the regulation of mammalian gene expression. *Briefings in functional genomics and proteomics*, 3(2):112–124, 2004. 8

[163] Arvind Raghavan, Rachel L Ogilvie, Cavan Reilly, Michelle L Abelson, Jayprakash Vasdewani, Mitchell Krathwohl, and Paul R Bohjanen. Genome-wide analysis of mRNA decay in resting and activated primary human T lymphocytes. *Nucleic Acids Research*, 30(24):5529–38, 2002. 8

[164] C Ress, M Holtmann, U Maas, J Sofsky, and A Dorn. 20-Hydroxyecdysone-induced differentiation and apoptosis in the Drosophila cell line, l(2)mbn. *Tissue and Cell*, 32(6):464–477, 2000. 8

[165] Lynn M Riddiford. Hormones and Drosophila development. In *Bate, N., Martinez-Arias, A. (Eds.), The Development of Drosophila melanogaster, Cold Spring Harbor Laboratory Press, Cold Spring Harbor*, pages 899–939. 1993. 2.1

[166] J Ross. mRNA stability in mammalian cells. *Microbiological reviews*, 59(3):423–50, September 1995. 8

[167] Wenjing Ruan, Hong Long, Dac Hien Vuong, and Yong Rao. Bifocal is a downstream target of the Ste20-like serine/threonine kinase misshapen in regulating photoreceptor growth cone targeting in Drosophila. *Neuron*, 36(5):831–842, Dec 2002. 7.14

[168] Albin Sandelin, Piero Carninci, Boris Lenhard, Jasmina Ponjavic, Yoshihide Hayashizaki, and David A. Hume. Mammalian RNA polymerase II core promoters : insights from genome-wide studies. *Nature Reviews Genetics*, 8(6):424–436, June 2007. 1.2.1

[169] Shun Sawatsubashi, Takuya Murata, Jinseon Lim, Ryoji Fujiki, Saya Ito, Eriko Suzuki, Masahiko Tanabe, Yue Zhao, Shuhei Kimura, Sally Fujiyama, Takashi Ueda, Daiki Umetsu, Takashi Ito, Ken-ichi Takeyama, and Shigeaki Kato. A histone chaperone, DEK, transcriptionally coactivates a nuclear receptor. *Genes & development*, 24(2):159–70, January 2010. 2.2

[170] Klaus Scherrer, Harriet Latham, and James. E. Darnell. Demonstration of an unstable RNA and of a precursor to ribosomal RNA in HeLa cells. *Proc Natl Acad Sci U S A*, 49:240–248, Feb 1963. 3

[171] Michael Schnall-Levin, Yong Zhao, Norbert Perrimon, and Bonnie Berger. Conserved microRNA targeting in Drosophila is as widespread in coding regions as in 3'UTRs. *Proceedings of the National Academy of Sciences of the United States of America*, 107(36):15751–6, September 2010. 1.2.2.2

[172] Björn Schwalb, Daniel Schulz, Mai Sun, Benedikt Zacher, Sebastian Dümcke, Dietmar E Martin, Patrick Cramer, and Achim Tresch. Measurement of genome-wide RNA synthesis and decay rates with Dynamic Transcriptome Analysis (DTA). *Bioinformatics*, 28(6):884–5, March 2012. 3

[173] Björn Schwalb, Benedikt Zacher, Sebastian Duemcke, and Achim Tresch. DTA: Dynamic Transcriptome Analysis. *R package version 2.0.2*, 2011. 6.3.11, 8

[174] Björn Schwanhäusser, Dorothea Busse, Na Li, Gunnar Dittmar, Johannes Schuchhardt, Jana Wolf, Wei Chen, and Matthias Selbach. Global quantification of mammalian gene expression control. *Nature*, 473(7347):337–42, May 2011. 4

[175] Yurii Sedkov, Elizabeth Cho, Svetlana Petruk, Lucy Cherbas, Sheryl T Smith, Richard S Jones, Peter Cherbas, Eli Canaani, James B Jaynes, and Alexander Mazo. Methylation at lysine 4 of histone H3 in ecdysone-dependent development of Drosophila. *Nature*, 426(6962):78–83, 2003. 2.2

[176] Lorenzo F Sempere, Edward B Dubrovsky, Veronica A Dubrovskaya, Edward M Berger, and Victor Ambros. The expression of the let-7 small regulatory RNA is controlled by ecdysone during metamorphosis in Drosophila melanogaster. *Developmental biology*, 244(1):170–9, April 2002. 2.3, 7.10

[177] Lorenzo F Sempere, Nicholas S Sokol, Edward B Dubrovsky, Edward M Berger, and Victor Ambros. Temporal regulation of microRNA expression in Drosophila melanogaster mediated by hormonal signals and Broad-Complex gene activity. *Developmental Biology*, 259(1):9–18, July 2003. 2.3, 19, 7.11

[178] Manu Setty, Karim Helmy, Aly A. Khan, Joachim Silber, Aaron Arvey, Frank Neezen, Phaedra Agius, Jason T. Huse, Eric C. Holland, and Christina S. Leslie. Inferring transcriptional and microRNA-mediated regulatory programs in glioblastoma. *Molecular Systems Biology*, 8:605, 2012. 9

[179] Ophir Shalem, Orna Dahan, Michal Levo, Maria Rodriguez Martinez, Itay Furman, Eran Segal, and Yitzhak Pilpel. Transient transcriptional responses to stress are generated by opposing effects of mRNA production and degradation. *Molecular Systems Biology*, 4(223):223, 2008. 8

[180] Ophir Shalem, Bella Groisman, Mordechai Choder, Orna Dahan, and Yitzhak Pilpel. Transcriptome Kinetics Is Governed by a Genome-Wide Coupling of mRNA Production and Degradation : A Role for RNA Pol II. *PLoS Genetics*, 7(9), 2011. 8, 9

[181] Ann-Bin Shyu, Michael E Greenberg, and Joel G Belasco. The c-fos transcript is targeted for rapid decay by two distinct mRNA degradation pathways. *Genes & Development*, 3(1):60–72, January 1989. 3

[182] Timothy W Sikorski and Stephen Buratowski. The Basal Initiation Machinery: Beyond the General Transcription Factors. *Current Opinion in Cell Biology*, 21(3):344–351, 2009. 1.1

[183] Peter Smibert and Eric C Lai. A view from Drosophila: multiple biological functions for individual microRNAs. *Seminars in Cell & Developmental Biology*, 21(7):745–753, 2010. 1.2.2.3

[184] Gordon K Smyth. Limma : Linear Models for Microarray Data. In *Bioinformatics and Computational Biology Solutions using R and Bioconductor, R. Gentleman, V. Carey, S. Dudoit, R. Irizarry, W. Huber (eds.), Springer, New York*, number 2005, pages 397–420. 2005. 6.3.12.1

[185] Bryn Stevens and O'Conner John D. The acquisition of resistance to ecdysteroids in cultured Drosophila cells. *Developmental biology*, 94(1):176–82, November 1982. 8

[186] Mai Sun, Björn Schwalb, Daniel Schulz, Nicole Pirkl, Stefanie Etzold, Laurent Larivière, Kerstin C Maier, Martin Seizl, Achim Tresch, and Patrick Cramer. Comparative dynamic transcriptome analysis (cDTA) reveals mutual feedback between mRNA synthesis and degradation. *Genome research*, 22(7):1350–9, July 2012. 3, 4, 8, 9

[187] Mai Sun, Björn Schwalb, Nicole Pirkl, Kerstin C. Maier, Arne Schenk, Henrik Failmezger, Achim Tresch, and Patrick Cramer. Global analysis of eukaryotic mRNA degradation reveals Xrn1-dependent buffering of transcript levels. *Molecular Cell*, 52(1):52–62, Oct 2013. 8, 9

[188] Emilia Szostak and Fátima Gebauer. Translational control by 3‘ -UTR-binding proteins. *Briefings in functional genomics*, 12(1):58–65, 2012. 1.2.1

[189] William S Talbot, Elizabeth A Swyryd, and David S Hogness. Drosophila tissues with different metamorphic responses to ecdysone express different ecdysone receptor isoforms. *Cell*, 73(7):1323–37, July 1993. 2.2, 2.2, 7.2

[190] Marshall Thomas, Judy Lieberman, and Ashish Lal. Desperately seeking microRNA targets. *Nature structural & molecular biology*, 17(10):1169–74, October 2010. 1.2.2.4

[191] Sean Thomas, Xiao-Yong Li, Peter J Sabo, Richard Sandstrom, Robert E Thurman, Theresa K Canfield, Erika Giste, William Fisher, Ann Hammonds, Susan E Celniker, Mark D Biggin, and John A Stamatoyannopoulos. Dynamic reprogramming of chromatin accessibility during Drosophila embryo development. *Genome biology*, 12(5):R43, January 2011. 9

[192] Tatjana Trcek, Daniel R Larson, Alberto Moldón, Charles C Query, and Robert H Singer. Single-molecule mRNA decay measurements reveal promoter- regulated mRNA stability in yeast. *Cell*, 147(7):1484–97, December 2011. 8, 9

[193] Jishy Varghese and Stephen M Cohen. microRNA miR-14 acts to modulate a positive autoregulatory loop controlling steroid hormone signaling in Drosophila. *Genes & development*, 21(18):2277–82, September 2007. 2.3, 19, 7.11, 8

[194] Jishy Varghese, Sing Fee Lim, and Stephen M Cohen. Drosophila miR-14 regulates insulin production and metabolism through its target, sugarbabe. *Genes & development*, 24(24):2748–53, December 2010. 19

[195] Daryl Waggott, Kenneth Chu, Shaoming Yin, Bradly G Wouters, Fei-Fei Liu, and Paul C Boutros. NanoStringNorm: an extensible R package for the pre-processing of NanoString mRNA and miRNA data. *Bioinformatics*, 28(11):1546–8, June 2012. 6.4.5

[196] Gabriele Weintz, Jesper V Olsen, Katja Frühauf, Magdalena Niedzielska, Ido Amit, Jonathan Jantsch, Jörg Mages, Cornelie Frech, Lars Dölken, Matthias Mann, and Roland Lang. The phosphoproteome of toll-like receptor-activated macrophages. *Molecular systems biology*, 6(371):371, June 2010. 3

[197] Changjian Wu, Vinod Singaram, and Kim S. McKim. mei-38 is required for chromosome segregation during meiosis in Drosophila females. *Genetics*, 180(1):61–72, Sep 2008. 7.14

[198] Zhijin Wu, Rafael A Irizarry, Robert Gentleman, Francisco Martinez-Murillo, and Forrest Spencer. A Model-Based Background Adjustment for Oligonucleotide Expression Arrays. *Journal of the American Statistical Association*, 99(468):909–917, December 2004. 6.3.10

[199] Han Yan, Kavitha Venkatesan, John E Beaver, Niels Klitgord, Muhammed a Yildirim, Tong Hao, David E Hill, Michael E Cusick, Norbert Perrimon, Frederick P Roth, and Marc Vidal. A genome-wide gene function prediction resource for Drosophila melanogaster. *PloS one*, 5(8):e12139, January 2010. 6.3.15.3

[200] Edward Yang, Erik van Nimwegen, Mihaela Zavolan, Nikolaus Rajewsky, Mark Schroeder, Marcelo Magnasco, and James E Darnell. Decay rates of human mRNAs: correlation with functional characteristics and sequence attributes. *Genome research*, 13(8):1863–72, August 2003. 4

[201] Jian Ye, George Coulouris, Irena Zaretskaya, Ioana Cutcutache, Steve Rozen, and Thomas L Madden. Primer-BLAST: a tool to design target-specific primers for polymerase chain reaction. *BMC bioinformatics*, 13(134):134, January 2012. 3, 6.3.8

[202] Tzviya Zeev-Ben-Mordehai, Efstratios Mylonas, Aviv Paz, Yoav Peleg, Lilly Toker, Israel Silman, Dmitri I. Svergun, and Joel L. Sussman. The quaternary structure of amalgam, a Drosophila neuronal adhesion protein, explains its dual adhesion properties. *Biophys J*, 97(8):2316–2326, Oct 2009. 7.14

[203] Gabriel E Zentner and Steven Henikoff. Regulation of nucleosome dynamics by histone modifications. *Nature structural & molecular biology*, 20(3):259–66, March 2013. 1.1

[204] R Grace Zhai, Yu Cao, P Robin Hiesinger, Yi Zhou, Sunil Q. Mehta, Karen L. Schulze, Patrik Verstreken, and Hugo J. Bellen. Drosophila NMNAT maintains neural integrity independent of its NAD synthesis activity. *PLoS Biol*, 4(12):e416, Nov 2006. 7.14

[205] Shuning Zhang, Gina M. Dailey, Elaine Kwan, Bernadette M. Glasheen, Gyna E. Sroga, and Andrea Page-McCaw. An MMP liberates the Ninjurin A ectodomain to signal a loss of cell adhesion. *Genes Dev*, 20(14):1899–1910, Jul 2006. 7.14

[206] Lihua J. Zhu, Ryan G. Christensen, Majid Kazemian, Christopher J. Hull, Metewo S. Enuameh, Matthew D. Basciotta, Jessi A. Brasefield, Cong Zhu, Yuna Asriyan, David S. Lapointe, Sinha Saurabh, Wolfe Scott A., and Brodsky Michael H. FlyFactorSurvey: a database of Drosophila transcription factor binding specificities determined using the bacterial one-hybrid system. *Nucleic Acids Research*, 39(Database):D111–7, Nov 2010. 7.15

[207] Claudia B Zraly, Frank A Middleton, and Andrew K Dingwall. Hormone-response genes are direct in vivo regulatory targets of Brahma (SWI/SNF) complex function. *The Journal of biological chemistry*, 281(46):35305–15, November 2006. 2.2

List of Figures

List of Tables